Contralateral responses to an inflammatory stimulus in man

Shenker, Nicholas

Award date:
2005

Awarding institution:
University of Bath

Contralateral responses to an inflammatory stimulus in man

Dr Nicholas Shenker MA BM BCh MRCP

A thesis submitted for the degree of Doctor of Philosophy

University of Bath

School for Health

November 2005

Nicke GN Shenker

ProQuest LLC
789 East Eisenhower Parkway
P.O. Box 1346
Ann Arbor, MI 48106-1346

Table of Contents

List of Images

List of Tables

List of Figures

Acknowledgements

With many thanks to Bo, Csilla, Sam and Maya without whose understanding this would have been impossible.
I also thank the support and love of my family

I could not have done this work without the guidance of my supervisors:
Professor David Blake
Dr Nigel Harris
Professor J Christopher Buckland-Wright
Dr Paul Mapp

I have had the luck to have worked with and been helped by very generous co-workers and would like to acknowledge Ms Emma Roberts, Dr Cliff Stevens, Dr Viv Winrow, Mr Gordon Taylor, Dr Elizabeth Messent, Ms Emily Bennett, Mr David Elvins, Dr Richard Haigh, Mrs Jean Hueting, Mrs Jana Stott, Mrs Alison MacKenzie and Mr Stefan Ivanavicius.

Declaration

I declare that this work has been produced by my own endeavour and that no part of this has been carried out by anyone else, except where acknowledged. This work has been carried out whilst registered as a postgraduate student at the University of Bath.

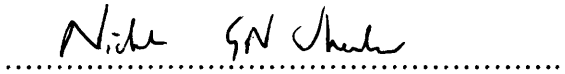

Abstract

Two observations are made. Firstly, many chronic inflammatory diseases manifest a bilateral symmetry far greater than expected by chance. This observation is supported by examining the distribution of erosions in the hands and wrists of 42 patients with rheumatoid arthritis using a microfocal radiographic technique. This demonstrated that particular areas were predisposed to erosions and that these areas contributed most to the symmetry seen in this disease. Secondly, from published literature afferent neural pathways that cross through the spinal cord, or via higher order connections, are anatomically identifiable, physiologically active and implicated in the distant transmission of inflammation in several animal models. The thesis is that local inflammation can be neurally reflected to the topographically precise contralateral region in man. This can then explain the symmetrical phenotype of chronic inflammatory diseases and expose new targets for anti-inflammatory treatments.

The first hypothesis is that the skin blood flow in the area of the contralateral arm, precisely topographical to an active immunisation given 2-4 days prior, will be different to that of control areas in a group of healthy volunteers. Using a laser Doppler imager to semi-quantify the skin blood flow there were no differences seen between the experimental and control contralateral regions.

The second hypothesis is that there is greater expression of endothelial E-selectin in skin biopsies taken from the exact contralateral area to an MMR immunisation (given 1-3 days prior) when compared to the control biopsy taken from a different contralateral dermatomal area. Using a supraoptimal dilutional immunohistochemical technique there were no differences in E-selectin expression between the experimental and control groups contralateral to the MMR immunisation. The null hypothesis is again supported.

Further work should consider a different stimulus or extending the timing of the observations before the thesis can be rejected.

Chapter 1. Symmetry in clinical practice

Summary

There is a recognition that biological patterns can instruct underlying mechanisms. The observation of bilateral symmetrical patterns occurring in mainly chronic inflammatory diseases is made. Possible explanations for this symmetry are explored. These include neurogenic, genetic, anatomical and biomechanical reasons. These influences may not be mutually exclusive. A neurogenic hypothesis to explain the symmetrical nature of chronic inflammatory disease is preferred.

1.1.1 Introduction

Biological patterns are the result of overlapping combinations of underlying complex processes. Understanding some of these underlying processes can reveal the generation of the biological pattern. Recognising the presence of a pattern for which an underlying mechanism has been previously described may also shed light onto other hitherto undiscovered processes. These 'higher' organisational operations necessary for the structure of life are constrained by physico-chemical laws and may influence biological processes well after the genome has spawned proteins.

D'Arcy Wentworth Thompson's 'On Growth and Form', first published in 1917, provides many examples of the value of studying form and physical properties outside of the Darwinian constraints of function and utility. One such famous example is the observation of the Fibonacci sequence and the Golden Angle (about 137°) in the number of, and spatial relationship between, the petals of plants such as daisies and sunflowers, or the leaves on their stalks. The Fibonacci sequence (1,1,2,3,5,8,13 etc...) is related to the Golden Angle mathematically. The ratio of consecutive Fibonacci numbers later in the sequence is defined as ϕ (about 1.6), which happens to be the square root of the number required to divide into 360 degrees to obtain the Golden Angle. This somewhat tortuous link is in fact mathematically robust. The plant phenotype is understood better as the underlying developmental processes were discovered, and is guided by the principle that the distribution of a new structure, i.e. petal or leaf, should be as far away from previous

structures in order to allow more colour to radiate from the petal or sunlight to reach the leaf. Structures that are nascent every 137° around a circumference support the surrounding space more efficiently than at any other angle. By recognising the pattern and understanding the evolutionary pressures, the underlying process, namely the build up of chemokines and growth factors spatially and temporally along the developing bud, makes more sense and explains why this property exists across many plant species. That this is governed ultimately by genetic transcription and translation is remarkable and it is this that has yet to be satisfactorily explained.

1.1.2 Phenotypical patterns demonstrate insight into developmental biology

Causal biological systems imply that a pattern observed in the adult has embryological implications. These were enlighteningly explored by the famous computing pioneer Turing (1952). His proposal, a reaction-diffusion system, consisted of two homogeneously distributed substances each of which has differing consequences for the differentiation of cells under their influence. The two substances' properties are such that one would auto-catalyse and affect the concentration of the other. Furthermore, their diffusion rates would be different. These properties dictate a programmed interaction that produces stable patterns, such as stripes on the skin, during morphogenesis. The phenotypic patterns would therefore represent regional differences in the concentrations of the two substances whose interaction has generated an order from seemingly unrelated chaotic processes.

An example demonstrating that this process is likely to be operational in developmental biology is recent work examining the morphogenesis of the zebra fish's stripes (Asai *et al*, 1999). They describe several mutations within a single gene, each allele of which produces a characteristically different pattern of spot size, density and connectivity on the skin of the zebra fish. These patterns can be modelled using reaction-diffusion kinetics by substituting certain parameter values. This suggests that the gene products are components of a similar operational system that exists in the generation of the skin pattern.

1.1.3 Symmetry, broken symmetry and underlying mechanisms

> "Something in the human mind is attracted to symmetry. Symmetry appeals to our visual sense of beauty. However, perfect symmetry is repetitive and predictable, and our minds also like surprises, so we often consider imperfect symmetry to be more beautiful than exact mathematical symmetry. Nature, too, seems to be attracted to symmetry, for many of the most striking patterns in the natural world are symmetric. And nature also seems to be dissatisfied with too much symmetry, for nearly all the symmetric patterns in nature are less symmetric than the causes that give rise to them."
>
> (Stewart and Golubitsky, 1992)

Symmetry as a mathematical concept allows classification and discernment of different types of regular patterns. Biological systems operate as equilibria. Breaking of symmetry to a less mathematically symmetrical form is significant and indicates the presence of an additional influence within the biological system.

The external human phenotype is bilaterally symmetrical based on a reflection transformation around the mid-sagittal plane. The human egg however is grossly spherically symmetrical with rotational as well as reflective symmetry. In a similar vein to Turing's work, the disruption of this spherical symmetry to a more restricted form has been recognised and explored at an embryological level.

The symmetry of the ball of cells in the very early developing embryo is broken several times so that at approximately day 15 in the embryo's development there are a prechordal plate and a primitive streak defining the anteroposterior and dorsoventral axes, and thus also defining left and right. Different genes and promoters are thought to be important each time that the symmetry is broken. Although not identified in mammalian embryos yet some of these have been described in other species. In *Drosophila* the follicle surrounding the egg recognises the Spätze ligand and activates a Toll receptor to induce a breaking of symmetry. In the amphibian embryo prelocalised VegT (Vegetal T-box gene) mRNA in the maternal egg has been identified as being important in symmetry breaking, as well as

another unidentified factor that activates Wnt (Wingless-type MMTV integration site family) signalling pathways (Fraser SE and Harland RM, 2000).

Observing form in biology can therefore guide more detailed investigations into basic processes. Can this same approach be used to study and inform mechanisms of disease?

1.2.1 Patterns of disease

Disease patterns are constrained by a number of factors, including the organism's anatomy, environment and systems organisation. The following patterns, their examples and inferred conclusions are included here for illustrative reasons only, the central thrust being that underlying mechanisms of disease can be suggested by carefully studying the pattern of disease involvement.

1.2.2 Local pattern of disease

Diseases that induce local patterns of involvement include, in the initial stages, tumours, infection and trauma. This pattern simplistically suggests that a single event local to the affected tissue has been an important factor in the aetiology. For example, the introduction of a pathogenic organism in the case of an abscess or the novel generation of a neoplastic cell lineage in the case of a tumour are the known causes for these diseases. The origin of the problem is to be found locally, either through internal or external factors.

1.2.3 Widespread pattern of disease

Conversely there are those diseases where widespread damage is seen and most structures and cells are affected in most systems. This points more to a fundamental problem in the metabolism or genetic make-up of the individual. Such patterns of pathology might include metabolic diseases such as diabetes or genetic problems that may similarly affect the functioning of a wide variety of cells, such as cystic fibrosis. Whilst the problem may well be found locally, it also exists on a more global nature with specific manifestations exhibiting themselves dependent upon conditions peculiar to their local environment. Studying these diseases is probably better performed on a more global nature.

1.2.4 Systemic pattern of disease

Another pattern of disease points to a specific problem with one particular part of the cell or structure even though the pattern of the disease might be widespread. Again these diseases are often genetic, such as Duchenne Muscular Dystrophy or Huntington's chorea. Identifying that the pattern of disease involvement is restricted to one particular system, such as the musculoskeletal or neurological, is important in understanding these diseases better.

1.2.5 Symmetrical pattern of disease

Finally, symmetrical diseases follow neither a local nor a widespread distribution. For example in rheumatoid arthritis, the joints affected are far more likely to be the second and third metacarpophalangeal (MCP) and proximal interphalangeal (PIP) joints symmetrically, than any distal interphalangeal (DIP) joint or the fifth MCP joint unilaterally (see chapter 4). It appears that the property of their symmetrical distribution is an important part of the disease process. Several diseases that have bilaterally symmetrical patterns will now be discussed.

1.3.1 Symmetrical diseases: Rheumatoid arthritis (RA)

A symmetrical pattern of involvement in rheumatoid arthritis is so important that it is a feature of the diagnostic criteria (Arnett *et al*, 1988). Rheumatoid arthritis affects about 1% of the population, mainly women, and typically presents between the third and fifth decades of life although it can affect an individual of any age. It is characterised by inflammatory exudates with immune components accumulating mainly in, but importantly not limited to, synovial joints. Pain and swelling coupled with the destruction of the joint cartilage and underlying bone prevents normal functioning. There are genetic associations, the strongest described being HLA-DR4 and immune dysregulation has been documented in countless publications involving both T-cell and B-cell dominated pathways. Current treatments aimed at correcting immune dysregulation are partially successful at slowing and controlling the disease, but an effective cure has yet to be demonstrated (Gordon and Hastings, 1997).

Rheumatoid arthritis has long been recognised to be bilaterally symmetrical in the distribution of joints affected (Flemming *et al*, 1976; Fuchs *et al*, 1988). This is discussed in more detail in chapter 4.

The pattern of RA is not locally confined. For example, patients with a chronic knee monoarthritis rarely develop RA and rarely give a histological picture consistent with RA (Devlin *et al*, 2000, Gallagher *et al*, 1985). Neither is the disease widespread as the internal organs, such as the liver, gastrointestinal tract and kidneys are invariably never involved. There may be a case to suggest that RA is confined to one particular system (immune dysregulation) and that the disease's effects are the result of the misdirection of the autoimmune process. This is clearly the current thinking and undoubtedly there is strong evidence to support such an argument. This does not explain the symmetrical distribution of the disease. Why should an autoimmune process have a predilection for particular MCP joints with a relative sparing of the DIP joints and a predisposition for radially located digit joints with a relative sparing of the ulnar joints? Are there other influential mechanisms in the pathogenesis of the disease that produce such patterns?

1.3.2 Other forms of chronic inflammatory arthritis

Seronegative arthritides, such as psoriatic arthritis, reactive arthritis, ankylosing spondylitis and colitis-associated arthritis are seronegative for rheumatoid factor and viewed clinically as being asymmetrical diseases. These diseases have different genetic associations, immunological abnormalities and clinical presentations. It is likely however that the arthritic asymmetry is a reflection of the paucity of joints that are involved. As the number of affected joints increase a symmetrical pattern becomes evident. For example Bhukari *et al* (2002) described the location of erosions from X-rays taken over the course of 5 years in all patients presenting with inflammatory arthritis, regardless of whether they were rheumatoid factor positive, from patients in the Norfolk Arthritis Register. There were no differences in the amount of symmetry exhibited by the erosive damage between the group that was rheumatoid factor positive, and those who were not. This implies that in this unselected group of patients it is not the presence of rheumatoid factor (i.e. the diagnosis of rheumatoid arthritis) that is influential in determining the symmetry of disease, but that all chronic polyarthritis is symmetrical.

This view is further supported by Helliwell *et al* (2000) who studied the distribution of erosions in patients with early and late disease in both psoriatic arthritis and RA. Using a mathematical model they demonstrated that the presence of symmetry was

related to the number of joints involved and that when this confounder was corrected psoriatic arthritis was as symmetrical as RA. Perhaps the same factors that are influential in producing the symmetrical expression in RA are at work in all forms of chronic inflammatory polyarthritis?

1.3.3 Osteoarthritis (OA)

Osteoarthritis affects generally an older population or those with a predisposition to the disease through previous trauma, infection or metabolic abnormality. This degenerative disease affects up to 60% of 60 year olds and the prevalence increases further as the age increases. There are genetic influences in the expression of OA. Although asymptomatic in a large proportion of people, sufferers are affected by pain, swelling and deformities. Non-surgical treatment is targeted towards muscle strengthening and palliation, and when indicated, joint replacement is the most effective treatment.

Osteoarthritis is both a symmetrical disease and it is limited to the articular system. Examining articular cartilage loss in the ankles and knees of post-mortem specimens accentuated a symmetry for osteoarthritis that was not as clear clinically (Koepp *et al*, 1999). Symmetry of OA in the hands is demonstrated by a recent epidemiological survey from the Framingham population (Niu *et al*, 2003), especially in women.

1.3.4 Psoriasis

This chronic inflammatory disease, predominantly of the skin, affects about 2% of the population and can occur at any age, although there are two peaks at the second and sixth decades (Langley *et al*, 2005). Patients suffer with itchy scaly skin that is sometimes sore and prone to complications such as infection. Up to 25% can have joint involvement. Although the patches of skin are typically on the extensor surfaces and scalp, they can occur anywhere on the body. Genetic associations have been made, most strongly with HLA-Cw6. Immune dysregulation has been shown to be important in the pathophysiology of psoriasis, mainly involving T-cell processes. Treatments for severe psoriasis are immunosuppressive and can include vitamin A derivatives and ultraviolet light treatments.

Image 1.1 Symmetrical pattern of skin psoriasis (Langley *et al*, 2005)

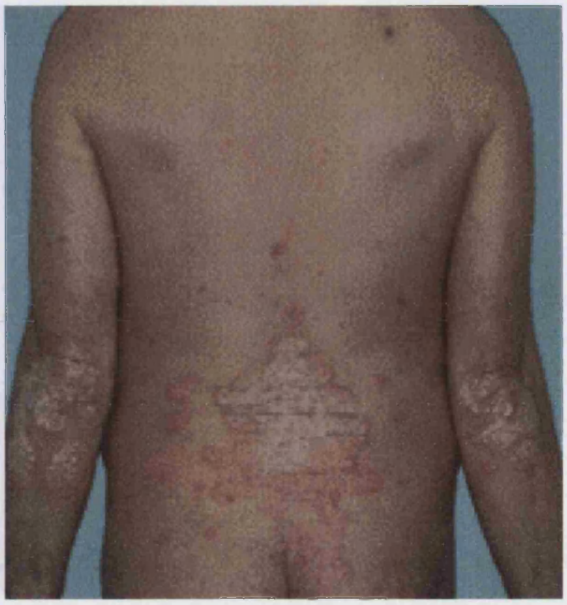

Reproduced with permission from BMJ Publishing Group Ltd

Image 1.2 Symmetrical pattern of vitiligo

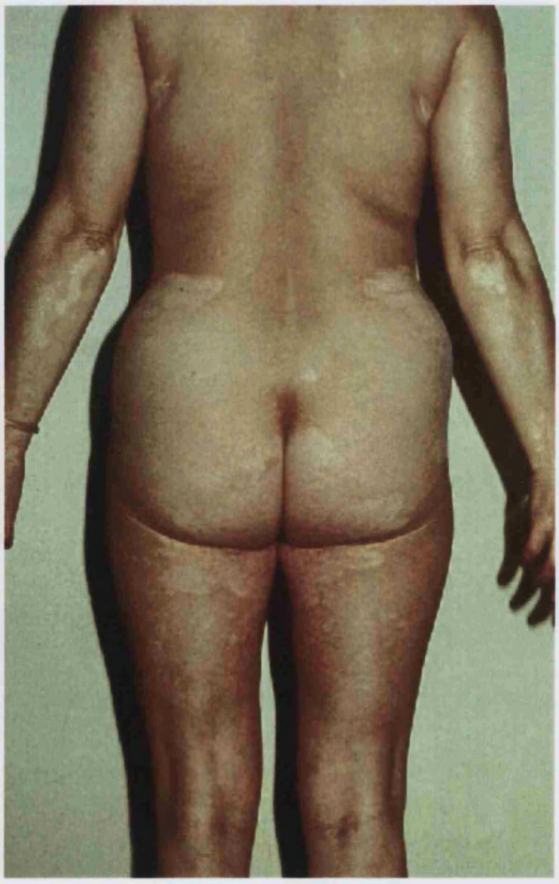

Skin psoriasis is classically described as being symmetrical (Farber *et al*, 1986) although there is a poverty of literature to document this. However when symmetry of skin psoriasis is encountered clinically, it is striking (see Image 1.1).

1.3.5 Vitiligo

Progressive symmetrical vitiligo is a condition that affects 1-2% of the population and whose peak incidence (about 50% of cases) is between 10-30 years old although it can affect individuals of any age. Individuals suffer a loss of melanocytes in a patchy albeit sometimes strikingly symmetrical pattern (Image 1.2). The resultant discolouration can lead to psychosocial disadvantages. Vitiligo is limited to the skin in its disease effects, but links with other 'autoimmune' diseases such as RA and thyroiditis have been observed. No clear cause of vitiligo has been suggested although an interplay of genetic and autoimmune hypotheses involving activated cytotoxic T-cells have been advanced, as well as neurotrophic, toxic metabolite and melanocyte growth factor hypotheses. There are no effective treatments directed against this process although there have been reports of success with ultraviolet light and immunosuppressive treatments (Njoo *et al*, 2001).

1.3.6 Sympathetic ophthalmia

This diffuse chronic uveitis occurs in both eyes several weeks, or even months and years, after penetrating eye injury. It can affect any age group susceptible to such trauma. Thought to be an autoimmune condition of the delayed hypersensitivity type it is characterised by an accumulation of epithelioid, multinucleated giant cells and lymphocytes while classically sparing the choriocapillaris. Treatment is based on immunosuppression although removal of the traumatised eye will prevent the development of the reaction.

1.4.1 Common factors between the symmetrical diseases

These diseases are directed against structures that have anatomical bilaterality, i.e. joints, skin and eyes. The presence of disease symmetry may merely reflect a widespread effect on these structures which then in turn appear to be bilaterally symmetrical. With respect to rheumatoid arthritis, this is examined in more detail in chapter 4 and refuted. The distribution of erosions occurs in a symmetrical distribution greater than by chance.

A common thread running through the aetiology of these symmetrical diseases is the presence of immunologically directed inflammatory processes. These diseases have genetic susceptibility and they affect, broadly, the mature young adult, premenopausally if female. These conditions are examples of a group that have broadly been categorised as Immune-Mediated Inflammatory Diseases (IMID). Other examples of IMID are Crohn's disease and multiple sclerosis (MS).

Whilst Crohn's disease affects an asymmetrical organ the distribution of white matter plaques of MS in the central nervous system has been examined by Werring *et al* (2000). Interestingly, they found subtle white matter changes occurring exactly contralateral to the appearance of a new demyelinating lesion and persisting for up to 6 months using sensitive serial gadolinium enhanced MRI sequences in 5 patients with multiple sclerosis. These results were similar to de Stefano *et al* (1999) who also found subtle contralateral white matter changes in the metabolism of *N*-acetyl aspartate appearing about 1 month after the appearance of three large areas of demyelination in a patient with MS. The MRI changes seen by Werring *et al* and the metabolic changes seen by de Stefano *et al*, both indicate a change in the functional state and integrity of the neurons and surrounding structures different to that expected by chance. MS has not been included in the list of bilaterally symmetrical diseases above because clinically the lesions have not been hitherto described. As neuroimaging techniques improve however, this may perhaps change.

The presence of one of the IMID predisposes the individual to developing another. For example, affected individuals with vitiligo are more likely to have rheumatoid arthritis and psoriasis, as well as the more focal auto-immune diseases affecting the thyroid and adrenal glands (Addison's disease) (Laberge *et al*, 2005; Liu *et al*, 2005). Could the same mechanism that is influential in the pattern formation in one disease predispose an individual to another IMID?

The symmetrical disease that is the exception in the above descriptions is degenerative arthritis. The epidemiology and aetiology of this disease is clearly different to that of the other symmetrical diseases. Are there different factors that could cause the symmetry seen in OA?

1.5.1 Underlying mechanisms to account for symmetrical phenotype of disease

Three hypotheses to explain bilaterally symmetrical pathology are now outlined and discussed.

1.5.2 The neurogenic hypothesis

The nervous system is anatomically bilaterally symmetrical. Neurons decussate across the midline and contain immune and inflammation modulating substances, including substance P (SP), calcitonin gene related peptide (CGRP), neuropeptide Y (NPY) and vasoactive intestinal peptide (VIP), amongst others. As will be discussed in Chapter 2 in more detail the physiology and distribution of these components in the nervous system suggest a role for the mediation of a symmetrical phenotype. An autoregulatory neurogenically mediated immuno-inflammatory loop might therefore exist between homologous structures symmetrical to the midline.

This hypothesis was first advanced by Levine *et al* (1985a) as a possible mechanism for the symmetry seen in rheumatoid arthritis. Farber *et al* (1986) then applied a similar hypothesis to skin psoriasis. Kidd *et al* (1989) expanded on this basic hypothesis by suggesting an evolutionary advantage was to be gained by having a rapid contralateral upregulation of immune and inflammatory defensive mechanisms. This hypothesis is examined in more detail in chapters 2 and 3.

A neurogenic hypothesis is attractive to evaluate in more detail. It offers the possibility of a deeper understanding of the pathophysiological processes in IMIDs as well as suggesting the potential for new therapeutic targets. These would include blocking or augmenting neuropeptides and neuronal mechanisms for the induction of an anti-inflammatory effect.

1.5.3 The biomechanical and anatomical hypothesis

This states that the pattern of symmetry in the observed diseases arises because of the individual having bilateral anatomy and being exposed to similar external and internal biomechanical forces. Biomechanical stress acting as an external force and the intrinsic anatomy acting as the internal force are inextricably combined to give symmetrical structures similar environments (Chaisson *et al*, 1999; Niu *et al*, 2003). Even though there is a 'handedness' in humans defining a laterality of function

between the sides, it is suggested that this is either minimal in the generation of excessive forces (being more restricted to fine motor movements and acts of coordination) or that there is a discernable break in the bilateral symmetry that can be detected on careful examination. One example of support for this in the literature is the study of the distribution of erosions in patients with RA (Mattingley *et al*, 1979; Halla *et al*, 1986; Möttönen *et al*, 1988; Owsianik *et al*, 1980; Boonsaner *et al*, 1992). This is a controversial finding however and as will be seen in chapter 4, the observation of dominance sided erosion preference was not made in the cohort studied.

There is evidence to suggest that biomechanical forces are important in the pathophysiology of IMID. For example, patches of psoriasis are often seen over pressure points and areas of excessive skin stretching such as the buttocks, elbows and knees. Pressure is known to change cellular adhesion molecule and proinflammatory cytokine profiles in the skin (Takeuchi *et al*, 2003). The Koebner phenomenon is a direct consequence on the actions of significant pressure on the subsequent manifestation of psoriasis. Similarly immobilisation is beneficial in the short term (Harris and Copp, 1962; Partridge and Duthie, 1963; Gault and Spyker, 1969) and hand splinting has also been reported to be of benefit (Ziljstra *et al*, 2004; Li-Tsang *et al*, 2002) to some patients with active RA.

Studies have examined the effects of immobilisation on inflammation in animal models (see section 3.4.1) through neural injury. There is confusion as to the cause of the anti-inflammatory effects of this neural injury though because, by its very nature, neural injury immobilises. Similarly, experiments that splint a limb are also confounded by the fact that the animal tends to compensate by 'over-using' its non-splinted limb. Likewise, clinical observations of neural injuries which immobilise (e.g. strokes, spinal and lower motor neuron lesions) might also obfuscate the causal effects of neuropeptides and biomechanical forces on the immuno-inflammatory process. This is an unresolved issue although as will be seen in Chapter 3, there are well designed experiments which attempt to account for this by the use of selective, non-immobilising nerve lesions or pharmacological agents. The results of these suggest that neuropeptides are important in their anti-inflammatory effects, over and above that seen by immobilisation.

The biomechanical and anatomical hypothesis fails to explain why the pattern of disease, whilst symmetrical, is different between individuals and for different diseases? Why should some individuals have predominantly a wrist distribution of erosive RA, and others have MCP and PIP disease? Why should individuals with osteoarthritis develop changes in their DIP and PIP joints, but be spared their MCP joints, when individuals with RA have their MCP and PIP joints more affected than their DIP joints? This is not difficult to explain using a neurogenic hypothesis, but is problematic for a biomechanical hypothesis.

1.5.4 A genetic hypothesis based on fractals

Non-linear dynamical systems (e.g. y=ax(1-x)) demonstrate important and unpredicted temporal and spatial biological patterns that have previously been missed following analysis with a linear modelling system (e.g. y=ax + b) that is based on proportionality and superposition properties. An example of a useful non-linear system is that of fractals, that is geometric shapes which are rough or irregular on all dimensions of scale and time. Fractals also demonstrate recurring self-similar shapes in all of these dimensions and have the universal property that includes bifurcations, that is the ability to flip between two apparently unrelated phenotypes (Goldberger *et al*, 2000).

Examples of fractals occurring in nature include the shape of coral and branches of a tree. Human networks of blood vessels and bronchi have been elucidated fractally and interestingly several groups report that the fractal dimension of relative structures is 1.7. This is the same ratio as that seen in diffusion-limited growth processes (see section 1.1.2) and very close to ϕ. This suggests that mathematically defined processes may be important in the development of form across a very wide range of biological structures (Masters, 2004).

Now, assume that joints demonstrate a fractal pattern in that there is a resonance of anatomy along a limited diminishing size scale as the proximal joints are compared with the distal joints. Certain diseases therefore have a predilection for particular rows of the homunculus. For example, osteoarthritis in the hands rarely affects the

MCP row. Only when it is associated with haemachromatosis is such an anatomical distribution favoured. Similarly, RA has a focus on the wrist, MCP and PIP rays in the upper limb, although can certainly affect any other ray.

As has already been discussed, the breaking of symmetry in the embryo is associated with different genetic expressions. In the case of fractal patterns, symmetry is upheld, but the scaling is different between repeated forms. Although fractal arrangements appear to follow physiological principles, primarily those of maintaining equilibria following Murray's principle of minimal work, this is not a perfect fit according to the known parameters in an arterial branching model (Murray, 1926a and 1926b; Zamir, 2001). Do genetic factors account for this additional role in fractal phenotypes, their expression influenced by local environmental pressures in the developing embryo? Are different genes expressed in a lower fractal scale when compared to a higher one?

Many studies have expounded genetic influences on RA, but none have accounted for its pattern of disease. Fractal analysis of affected joints may account for this pattern.

The genetic hypothesis for bilateral symmetry in disease is that the pattern is influenced genetically by the expression of different genes in the susceptible areas when compared to protected areas.

There are several problems regarding this hypothesis. To the best of my knowledge, the arrangement of joints in the homunculus has not been studied using a fractal analysis. It is predicated on the premise that a change in scale is reflected from a change in genomic expression. Evidence for this however is circumstantial based on mathematical modelling on related systems (Zamir, 2001), i.e. circulatory compared to joint anatomy. There is a paucity of evidence to suggest that genomic expression is different between rows of the homunculus.

The scale difference between joints in one limb is not characteristic of many fractal systems that have minimal and maximal patterns expressed over many logarithms, even infinitely. This does not preclude such an analysis being productive however.

Finally, non-linear dynamical modelling predicts that form can be generated from seemingly unrelated mechanisms to give unexpected outcomes. Using a defined set of genes and their associated proteins, fractal systems might predict different outcomes based on local environmental factors using physiological laws, such as those outlined by Murray in 1926. The need for a differing set of gene expression to generate a different scale may not be required.

For these reasons, a genetic hypothesis to account for disease symmetry appears unlikely.

1.6.1 Conclusion

It is possible that a varying combination of these explanatory mechanisms come to influence the phenotype of the different symmetrical diseases. For example, osteoarthritis may be primarily influenced by genetic and biomechanical factors; RA by neurogenic and anatomical factors; and psoriasis by neurogenic and biomechanical factors. Using Ockham's razor however, it would be more likely for the universal observation of symmetry to be explained by a unifying hypothesis. The neurogenic hypothesis appears to be the most convincing single hypothesis for this purpose. Furthermore, this hypothesis is important as it may offer a deeper understanding of the processes in symmetrical diseases and suggest new therapeutic targets.

Chapter 2. Neurogenic hypothesis: a crossed afferent pathway to explain the symmetrical phenotype in chronic inflammatory disease

Summary

The neurogenic hypothesis with a crossed spinal afferent pathway is presented as a possible explanation for the symmetrical pattern seen in chronic immune-mediated inflammatory disease. Evidence from animal models using either neuronal or inflammatory lesions is presented to support this hypothesis through the development of central sensitisation and a peripheral response. Anatomical, physiological and pharmacological studies of neurons and neuropeptides provide supporting evidence for the existence of such crossed afferent pathways. Finally, evidence is presented for contralateral sensitisation in man following intradermal capsaicin.

2.1.1 Spatially remote inflammatory responses

In 1978, Denko and Petricevic noted that the injection of arthritogenic crystals into the hindpaws of adult male Sprague-Dawley rats induced sympathetic or reflex footpad swelling in the opposite foot, a response that was augmented if the footpad had been 'primed' by a previous injection of crystals, such as urate or pyrophosphate. This observation was investigated in more detail by Levine *et al* (1985b).

They injected 150 μl of normal saline into a plantar surface of the midfoot of male adult Sprague-Dawley rats on three consecutive days and then measured withdrawal thresholds and paw thickness in the contralateral hindpaw each day. By the third day they had detected a reduction in the threshold to withdraw away from pressure applied linearly to the hindpaw and an increase in the paw thickness judged by constant pressure callipers applied perpendicular to the paw with the plantar surface resting between the footpads. These rats were then considered 'primed' in that they had exhibited contralateral responses and these responses recrudesced with a fourth day of saline injection. No tachyphylaxis was seen when the ipsilateral limb was stimulated 3 times over 8 hours. In fact, the contralateral responses were seen to augment and sustain to this increased input. This argues against a general arousal response that might be expected to habituate to repeated stimuli.

Levine *et al* (1985b) then investigated the mechanism of this remarkable observation by performing a variety of lesions on the rats. For one group of rats they exposed the femoral and sciatic nerves on both sides and applied capsaicin solution for 15 minutes to either the ipsilateral or contralateral side, using vehicle on the other side as a control. This treatment is relatively selective for neuropeptide containing fibres. To demonstrate the efficacy of this operation, they were then able to detect an increase in response latency to noxious heat in the paw of the treated hindlimb 3 days after treatment. Another group underwent chemical sympathectomy with guanethidine in which tissue epinephrine subsequently decreased by at least two orders of magnitude by radioimmunoassay compared to a control population. A third group underwent saphenous ligature immediately prior to the inflammatory stimulus. A fourth group had a section of sciatic nerve removed either 2 days or 6 days **before** the stimulus. Finally, a fifth group underwent a local nerve block immediately **after** the stimulus that was made irreversible by removing a section of nerve distal to the block. Control sham operations for all of these groups were also performed.

The use of capsaicin, sympathectomy and nerve lesions before the stimulus all attenuated the contralateral responses of hyperalgesia and paw swelling. Nerve lesions after the stimulus partially attenuated the contralateral responses whereas venous ligation did not attenuate the contralateral responses. The contralateral responses persisted throughout all of the sham operation groups.

Levine and colleagues (1985b) concluded by suggesting that crossed spinal reflexes could mediate neurogenic inflammatory responses and that their magnitude, duration and failure to attenuate pointed to a biological role.

There were two outstanding issues that could have thrown doubt on their observations. First, forepaws as a topographical control were not analysed. Did they too demonstrate similar responses? If they did, this might suggest a circulatory component not controlled by a saphenous ligature. Secondly, although the outcome measures were compared to baseline, the standard error of which was very small, these were not assessed by a blinded observer. However these issues founder on the reproducibility test as this experimental model has been repeated with similar results by several groups albeit using different techniques.

2.2.1 Reproduction of Levine *et al*'s (1985b) results

A comprehensive literature review was performed to assess publications that have successfully repeated Levine *et al's* results. A Medline search (Ovid) was performed in October, 2001 to find relevant papers. The terms "symmetry", "inflammation", "contralateral", and "mirror-image" were used in combinations. Abstracts were then scanned. Papers were included if a contralateral effect was observed in response to a unilateral inflammatory stimulus. Original papers were obtained and appraised. References were scanned to identify further papers until no more relevant papers were identified. Papers were excluded if the inflammatory insult caused systemic features. For example, high-doses (e.g. 250μg) of CFA (Complete Freund's Adjuvant) are known to induce a systemic arthritis in rats, whereas 50-150μg induces only a monoarthritis (Donaldson *et al*, 1993). Papers that showed the contralateral effects occurring in the CNS at levels higher than the spinal cord segment of the lesion were also excluded. Duplicate results published in different forms were excluded. Each paper was appraised on the following criteria: *a priori* hypothesis; appropriate unilateral lesion; controls that were not exposed to the unilateral lesion; alternative explanation offered by investigators.

2.2.2 Results of the literature search

The Medline search yielded 710 titles. From these abstracts, 31 papers were identified as satisfying the inclusion criteria and the original papers were obtained. References of these papers were scanned and a further 9 articles were identified. Of these 40 papers, the appraisal process excluded 23. These are listed with the reason for their exclusion in Table 2.2. A number of papers identified an anti-inflammatory contralateral response following a unilateral anti-inflammatory stimulus. These were excluded from this analysis because all of these animals had pre-existing polyarthritis.

Therefore 17 papers were identified and found to fulfil the criteria applied in the appraisal process and support Levine *et al*'s original work. In all of the papers, the *a priori* hypothesis had been that an appropriate unilateral inflammatory lesion might cause contralateral effects and controls that had not been exposed to this lesion were used. These papers are presented in Table 2.1.

Table 2.1 The contralateral effects of localised unilateral inflammation

Monoarthritis stimulus	*Contralateral arthritic effect with peripheral mechanism*	*Reference*
CFA (1μg) in knee	Decrease in anabolism of cartilage for 6-72 hours	Decaris 1999
Freund's adjuvant in knee (0.05ml of 1mg/ml)	Increase in SP, CGRP and NPY in knee for 2-24 h Increase in NK-A in knee at 2 h and at 24 h	Bileviciute 1993
Carrageenan 2% (0.05ml) In knee	Increase in CGRP and NPY for 2-24 h Increase in SP at 2 h and at 24 h; and NK-A at 24 h	Bileviciute 1993
Human recombinant IL-1 (0.05ml of 1mg/ml) in knee	Increase in CGRP and NPY for 2-24 h Increase in NK-A at 2-6 h and SP at 2 h	Bileviciute 1993
SP (0.05ml of 10^{-5}M) in knee	Increase in SP for 2-24 h; CGRP for 6-24 h; NPY for 2-6 h No increase in NK-A	Bileviciute 1993
SP in knee (0.2,1,2,10,20 μg in 50μl)	Decrease in anabolism of cartilage for 6-72 hours	Decaris 1999
500μl of mBSA in knee pre-immunised with 1ml CFA	Histopathological and biochemical evidence of joint destruction up to 80 d	Meyer 2000
500μg (50μl) mBSA in pre-sensitised knee	Increased proteoglycan loss and mechanical hyperalgesia up to 9 days	V Banchet 2000
100μl of 1% latex spheres in knee	Bradykinin-induced plasma extravasation enhanced between 10-21 days. Macrophage infiltration noted between 3-10 days	Kidd 1995
Hindpaw stimulus	***Contralateral hindpaw effect with peripheral mechanism***	
CFA (100μl)	TNF-alpha levels elevated up to 120 hours	Woolf 1997
Carrageenan (0.1ml of 2%)	CGRP levels increase in hindpaw perfusate at 3-4 hours Thermal and mechanical withdrawal latencies reduced at 3-4 h	Yu 1996
Urate, pyrophosphate and oxalate crystals (3mg/150μl)	Swelling observed, maximal at 5 hours	Denko 1978
CGRP 100μl (300pmol)	Oedema induced at 5-24h	Bileviciute 1998

All of these studies were performed in rats, unless otherwise indicated

KEY: CFA – complete Freund's adjuvant; SP – substance P; NPY – neuropeptide Y; CGRP – calcitonin gene related peptide; NK-A – neurokinin A; IL-1 – interleukin 1; MBSA – methylated bovine serum albumin; MTb – *mycobacterium tuberculosis*; TNF – tumour necrosis factor; NGF – nerve growth factor; RNA – ribonucleic acid.

Table continued overleaf

Table 2.1 The contralateral effects of localised unilateral inflammation (continued)

Hindpaw stimulus	*Contralateral hindpaw with central (neural) mechanism*	*Reference*
Carrageenan 100µl of 2%	Mechanical hyperalgesia between 3-5 days	Kissin 1998
Formaldehyde 50µl (0.1%,5%,10%)	Licking responses occur at 10-60 minutes	Aloisi 1993
Bee venom 100µl (0.2mg)	Heat (not mechanical) withdrawal latency reduced for 2-48 h	Chen 1999
NGF injections (3 days of 4µg/day) in hindpaw or ear or forepaw.	Increased expression of preprotachykinin and preproCGRP mRNA in nerve (sciatic; trigeminal; or brachial plexus)	Amann 1996
IL-1beta (10ng)	B1 receptor-mediated mechanical hyperalgesia for 1-6 h	Ganju 2001
Thermal stimuli (55C for 15s)	Thermal foot withdrawal latencies reduced at 24 hours	Coderre 1985
Thermal stimuli (55C for 15-20s)	Thermal foot withdrawal latencies reduced at 24 hours	Coderre 1987
Thermal stimuli to decerebrate rat (75C for 60s)	Reduction in the flexor reflex threshold to mechanical and thermal stimuli at 1h	Woolf 1983

Table 2.2 Papers excluded after appraisal

Hypothesis not a priori (inadequately controlled / not unilateral lesion)
Feige *et al*, 1989; Chandrasekhar *et al*, 1990; Mentzel *et al*, 1998
No controls
Boyle *et al*, 1999; Badavi *et al*, 2000; Ianaro *et al*, 2000
Polyarthritis / Pre-induced arthritis
Esselinckx *et al*, 1978; Bird HA *et al*, 1979; Bhattacharya *et al*, 1987; Kayser and Guilbaud, 1987; Kayser *et al*, 1988; Pinter and Szolcsanyi, 1988; Millan and Colpaert, 1990; Millan and Colpaert, 1991; Donaldson *et al*, 1993; Betoin *et al*, 1994; Andersson *et al*, 1998; Ceccherelli *et al*, 1998; Koch *et al*, 1998; Miagkov *et al*, 1998; Lechman *et al*, 1999; Bileviciute-Ljungar and Lundeberg, 2000; Bileviciute-Ljungar and Spetea, 2001

Contralateral responses were seen in many different laboratories and they were consistently identified independent of the type of stimulus (CFA, thermal injury, substance P for example) and the various strains of rats used (Wistar, Lewis and Sprague-Dawley) of both males and females. No alternative explanations were offered by the investigators to explain their findings. This suggests that these distant responses are not artefactual.

2.2.3 Neural mechanisms are implicated in contralateral responses

Aside from Levine *et al*'s (1985b) work, several other groups provide evidence to support the mediating of contralateral responses through neural mechanisms rather than reflecting a systemic or circulatory effect.

Coderre and Melzack (1985) abolished the contralateral hyperalgesia response to a noxious thermal stimulus by sectioning the sciatic nerve prior to the injury. Like Levine *et al* (1985b), they were unable to attenuate the contralateral response if they performed the nerve lesion after the thermal injury.

Decaris *et al*'s work (1999) perhaps provides the most convincing evidence for the distant neurogenic transmission of inflammation. They took male Wistar rats and induced a local degree of inflammation by injecting 1 μg of complete Freund's adjuvant. There was no associated rise in temperature or serum IL-6 to indicate a significant systemic response but proteoglycan activity was seen to be significantly decreased in both knees when compared to baseline and IL-1β mRNA was detected in both knees. IL-1β mRNA had previously been shown to be absent in the normal synovium. These contralateral responses were abolished when spinal cord injury was induced 2 days prior by an extradural balloon method. This operation did not alter proteoglycan synthesis nor IL-1β mRNA expression in either patella.

Bileviciute-Ljungar published two papers (2000 and 2001) demonstrating the anti-nociceptive capacity of contralateral stimuli on a defined inflammatory response. Carrageenan (1% of 50 μl) was injected into the right hindpaw of male adult albino Sprague-Dawley rats. The contralateral paw then received 100 μl of 5mg/ml of bupivacaine. Controls were injected with saline. Hindpaw withdrawal latencies were

seen to increase when compared to controls. No such increase was observed when the bupivacaine was injected systemically, suggesting a neuronal rather than a systemic anti-nociceptive effect (Bileviciute and Lunderberg, 2000). A similar experimental protocol yielded similar results with the experimental κ-opioid agonist, U-50,488H, whereby contralateral but not systemic administration was seen to have an anti-nociceptive effect (Bileviciute and Spetea, 2001).

Kidd *et al* (1995) and Donaldson *et al* (1995) both used capsaicin, a similar method to Levine *et al* (1985b), in disrupting neuropeptide containing nerves and interrupting contralateral responses. Kidd *et al* (1995) induced a monoarthritis using latex spheres injected into the right knee of male Wistar rats. Contralateral knee cellular infiltrates, mainly monocytes, were significantly elevated when compared to control animals and joints elsewhere in the affected rat. The neonatal administration of capsaicin however reduced this contralateral cell count whilst having no effect on the ipsilateral arthritic joint.

Donaldson *et al* (1995) induced a monoarthritis with Freund's Complete Adjuvant in the left ankle of adult male Han Wistar rats that had previously been shown to spread to the contralateral joint. However the application of capsaicin to the sciatic nerve in a method similar to that of Levine *et al* (1985b) two weeks prior to the arthritis induction prevented the full expression of this contralateral arthritis.

2.2.4 Central versus peripheral contralateral responses

A distinction must be made between the central changes that occur on the contralateral spinal cord and can lead to hyperalgesic and allodynic sensory changes on the contralateral limb and those changes that are peripheral. Peripheral responses are polysynaptic and could only occur in the contralateral limb secondary to an antidromic impulse releasing neuropeptides in the periphery. This distinction is important when considering experimental models to test.

Including Levine *et al* (1985b), 10 studies were seen to manifest peripheral contralateral responses and 9 studies detected changes consistent with central spinal cord sensitisation. Some studies detected both peripheral and central spinal changes.

For example, Yu *et al* (1996) detected the release of CGRP in the joint perfusate contralateral to a carrageenan-induced monoarthritis as well as the lowering of withdrawal latency to mechanical and thermal stimuli.

2.3.1 Properties of the observed contralateral responses

Taken together, these studies strongly support the hypothesis that neuronal mechanisms influence distant inflammation. It is tempting to speculate on properties that relate to these contralateral responses.

2.3.2 Magnitude of inflammatory stimulus

These contralateral responses appear to require the inflammatory stimulus to be of a certain magnitude before appearing. There are several examples in the literature of this 'threshold' effect. Bileviciute *et al* (1998) did not demonstrate contralateral hindpaw oedema with low doses of subcutaneous CGRP (75 and 150pmol), but did with a higher concentration (300pmol). Adjuvant arthritis in the rat induced with intradermal injections of small doses of CFA around the tibiotarsal joint causes a contralateral arthritis if the dose is increased from 75 to 150μg (Donaldson *et al*, 1993). Nociceptive behaviours towards the contralateral paw were not seen after 0.1% formaldehyde injections, but were observed after injections of 5% solution, and were even more frequent after injection with a 10% solution (Aloisi *et al*, 1993). Other papers did not examine the effects of varying the dose of the initial stimulus upon the contralateral responses.

2.3.3 Topographical precision

Where studied, the contralateral responses appear to be topographically precise. Topographically precise contralateral responses can only be mediated through the nervous system. Three separate studies were designed to identify this.

Kidd *et al* (1995) placed latex spheres within one knee joint of a rat before examining the inflammatory response in the contralateral knee, ankle and hip joints using bradykinin-induced plasma extravasation and histological examination of the joints. They found that only the contralateral knee exhibited enhanced plasma extravasation and macrophage infiltration and that these responses were not seen in the contralateral hip or the contralateral ankle.

Meyer *et al* (2000) examined the contralateral knee and both ankles for cartilage metabolism and histological damage. They too found that only the contralateral knee showed a decrease in cartilage anabolism and signs of histological damage and that these were not seen in either ankle.

Amann *et al* (1996) used repeated injections of nerve growth factor (NGF) and examined the mRNA of neuropeptides in the contralateral nerves. They found increases only in the contralateral sciatic nerve if the hindpaw was injected, only in the contralateral trigeminal nerve if the ear was injected and only in the contralateral brachial plexus if the forepaw was injected.

2.3.4 Stimulus specificity

The contralateral responses are broadly stimulus specific. If a pro-inflammatory stimulus is induced unilaterally, the contralateral response is pro-inflammatory, as evidenced by the identified papers, all of which show contralateral pro-inflammatory responses. However, if the unilateral response is neurological in nature, such as the sectioning of a peripheral nerve, then the contralateral response is also appropriately neurological: the corresponding neuromuscular junction exhibits nerve sprouting. Also, if the insult is anti-inflammatory, such as detailed in some of the papers in Table 2.2, the contralateral response is anti-inflammatory.

2.3.5 Reduced response

The contralateral responses are only a 'shadow' of the original lesion both in magnitude and temporally. In all of the identified papers, the contralateral findings were less than the ipsilateral changes. The withdrawal latencies were more greatly reduced on the side of the lesion than the contralateral side; the magnitude of the biochemical or histopathological abnormalities was greater on the side of the lesion; and the macroscopic changes such as oedema were also greater on the side of the lesion.

2.3.6 Sensitisation and the lack of tachyphylaxis

As described above (section 2.1.1), Levine *et al* (1985b) performed experiments to test the property of tachyphylaxis in this system and they did not find any evidence of its existence. They found instead that the contralateral side had been sensitised and

this priming could be augmented by increasing the frequency of the stimulus. No other group has tested these properties, although, as will be discussed later, this fits well into the sensitisation of the contralateral spinal horn and the release of neuropeptides contralaterally.

2.4.1 Does the right side know what the left is doing?

In 1999, Koltzenburg, Wall and McMahon reviewed a wide range of examples of unilateral neural interventions that produced bilateral effects. While acknowledging that many of these examples could be readily understood within existing frameworks of knowledge they too proposed the existence of a new signalling system across the midline of the body. They were focussed on unilateral neural lesions rather than inflammatory insults. However remarkably similar observations were made between the literature that they summarised (Table 2.3) and those that have been identified in Table 2.1 above.

The results of the experiments are not the provenance of but a few laboratories and the diversity of the results range from gene expression through to anatomical remodelling and physiology. These contralateral responses were also noted to be stimulus-specific, delayed temporally and smaller in magnitude.

Focussing on Rotshenker and Tal's (1985) experiments they note the occurrence of the degeneration of the ipsilateral neuromuscular junction distal to the nerve lesion and the new sprouting that is seen in the contralateral intact neuromuscular junction. Appropriate controls of sprouting neuromuscular junctions were obtained from normal muscles. Interestingly the sprouting contralateral to the sectioned nerve was first seen 5 days after a proximal lesion in the sciatic nerve, but it took 12 days to occur when similar numbers of axons were cut more distally.

They suggest several mechanisms for such contralateral responses, rejecting systemic and circulatory causes due to a variety of experimental parameters that were controlled. They favour the passing of a slow messenger through the dorsal commissural system, probably a neurotrophin, although acknowledge that electrical and direct trans-median signalling could occur.

Table 2.3 Does the right side know what the left side is doing? (Koltzenburg *et al*, 1999)

Lesioned nerve	Species	Effect in contralateral homonymous neurones
Motoneurones		
Facial, hypoglossal nerve	Rat	Chromatolysis, changes in RNA levels
Facial, hypoglossal nerve	Rat	Increase in acid phosphatase succinoxidase
Hypoglossal nerve	Rat	Proliferation of microglia, invasion of the nucleus by leukocytes
Sciatic nerve	Rat, mouse	Increase in mRNA for tubulin, CGRP, CCK, GAP-43
Sciatic nerve	Rat	Increase in CGRP, pro-opiomelanocortin derived peptides, B-endorphin and α-melanotropin levels
Muscle nerves	Frog, rat, mouse	Sprouting of endplates
Muscle nerves	Frog	Increased release of ACh
Sciatic nerve	Cat	Increase of extra-junctional ACh receptors
Autonomic neurones		
Superior cervical ganglion	Rat	Decrease in ACh levels
Superior cervical ganglion	Rat	Transmedian sprouting, upregulation of the neurotrophin receptor p75
Pelvic ganglion	Rat	Transmedian sprouting of fibres; increase of cell size
Lumbar sympathetic ganglion	Rat	Sprouting into DRG or spinal roots
Sensory neurones		
Inferior alveolar & infraorbital nerves	Ferret, rat	Transmedian sprouting
Sciatic nerve	Rat	Increase of mRNA for B-tubulin and decrease in mRNA for the low-molecular-weight neurofilament
Sciatic, saphenous nerve	Rat	Change of expression of genes for SP, CGRP, neuropeptide Y and galanin
Sciatic nerve	Rat	Upregulation of bradykinin receptors
Sciatic nerve	Rat	Downregulation of the mRNA for the tetrodotoxin-resistant sodium channel
Sciatic nerve	Rat	Macrophage invasion of the DRG
Sciatic nerve	Rat	Increased expression of the neurotrophin receptor, p75, on satellite cells of the DRG
Sciatic nerve	Rat	Intraplantar injection of NGF increases CGRP, SP, preprotachykinin and prepro-CGRP content
Saphenous nerve	Rat	Reduced cutaneous plasma extravasation

The following sections go on to describe the anatomical, physiological and biochemical mechanisms that outline a crossed afferent spinal pathway and that could account for the contralateral observations and associated properties.

2.5.1 The anatomy of crossed spinal afferent fibres

Cajal and von Lenhossek separately hypothesised at the end of the 19th Century that a significant part of the dorsal commissure is comprised of fibres from one substantia gelatinosa travelling to the contralateral dorsal horn through posterior decussation. The first experimental demonstration of crossed afferents came in the 1930s (Ranson *et al*, 1932) and was quickly followed by other groups.

Szentagothai described in great detail the anatomy of the dorsal horn. He depicted rich connections between the two opposite gelatinous substances (Rexed's laminae I, II and III) through the dorsal most bundle of the posterior gray commissure (Szentagothai, 1964). He studied young cats and dogs and, as well as using Golgi analysis and experimentally induced degeneration, he pioneered the method of 'persisting elements' thus permitting whole neuronal architecture to be preserved by securing the local blood supply. He found that most crossed fibres are secondary and higher order neurons, although direct primary sensory collaterals are occasionally seen in degeneration studies.

His findings explain those of Culberson *et al* who revisited this subject in 1979. They studied opossums, possums and bushbabies as well as cats and stained alternate sections with the Fink-Heimer method (silver impregnation) and cresyl violet acetate. Crossed afferent projections were a constant feature of all the animals at the sacral and higher cervical levels of the spinal cord. However there were much fewer crossed projections between C5 – T12. Most fibres diverged to reach laminae III and IV in the contralateral dorsal horn. The caveat to this study was that the methodology employed differed from that of Szentagothai (1964) and not all afferents were identified due to differing degeneration times, and interneurons were not specifically studied.

In the same year, Light and Perl (1979) also published their observations on the primary afferent projections of several mammals, including cats, rats and macaque

monkeys. They used a tool that was novel at the time, horseradish peroxidase to anterogradely stain neuronal projections. They noted that small fibres streamed through the posterior commissure on a regular basis running along the base of the dorsal horn (lamina V in the cat) or the marginal zone (lamina I). In the monkey, the highest density of contralateral fibres occurred in the thoracic, sacral and caudal sections. Many fibres were also seen to terminate just dorsal to the central canal in the midline. Again, the interneurons were not stained using this method.

In summary, several groups have looked and found somatosensory afferent projections crossing the dorsal commissure in a number of mammalian species. This provides anatomical evidence that crossed spinal afferent pathways exist to transmit signals across the midline. Figure 2.1 summarises this data in a cartoon.

Figure 2.1 Scheme demonstrating identified routes through the dorsal commissure of sensory fibres entering the dorsal horn (Culberson *et al*, 1979; Light and Perl, 1979; Szentagothai, 1961)

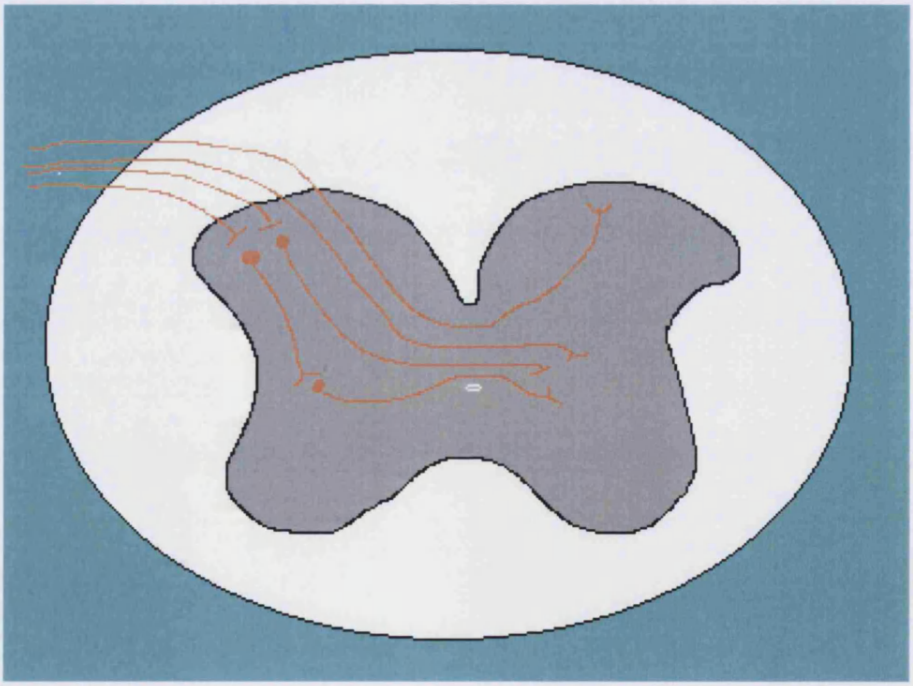

2.5.2 Function of the crossed afferent pathway

Spinal reflexes that cross the midline have long been reported. The oldest and most commonly recognised are those of the crossed extensor and adductor reflexes, recognised at the end of 19th Century. Recent studies have demonstrated that this pathway involves both short and medium latencies and are therefore both monosynaptic and polysynaptic in nature (Corna *et al*, 1996; Alexander and Harrison, 2002).

However these reflexes necessitate synaptic interface with the ventral horn to stimulate the contralateral motor command. This is incongruent with the anatomical studies that rarely find such connections through the posterior decussation, although Light and Perl (1979) did describe ventral decussations synapsing in the ventral horn. It seems unlikely therefore that the observed fibres are mediating motor spinal reflexes.

Culberson *et al* (1979) suggested that the afferents innervated dermal tissue that was near the ventral and dorsal midlines. The mammals that they studied had tails and this correlated well with the predominant decussating neurons being located sacrally and caudally. However, Szentagothai (1964) described interconnections between the two sides of the spinal cord at all levels in cats and dogs. Light and Perl's study (1979) of macaque monkeys demonstrated decussations occurred prominently in the thoracic spinal cord. It would seem unlikely therefore that all decussations would be innervating midline structures. Indeed this is born out by neurophysiological studies.

2.6.1 The neurophysiology of crossed afferent pathways in the dorsal horn

The observation that some neurons in the dorsal horn have bilateral receptive fields is of significance in the neurophysiology of contralateral pathways. This is not a new observation. Taub (1964) described the inhibitory effects of C-fibre stimulation either by electrical or noxious stimulation on the contralateral dorsal horn as had Wagman and Price (1969). Fitzgerald (1982b) demonstrated that this inhibitory effect could be modulated by capsaicin treatment. The following sections break down the findings into spinal and supra-spinal effects.

2.6.2 Crossed afferent neurophysiology at the spinal level

Fitzgerald (1982a) best illustrates this in her studies on decerebrate and spinalised rats, used to investigate this phenomenon in more detail at the segmental spinal level. She studied the deeper laminae IV, V and VI of the spinal cord and stimulated the contralateral limb with a functional stimulus such as a small paint brush, fine toothed forceps or noxious heat (45-50°C), as well as C-fibre or A-fibre electrical stimulation of the contralateral sciatic nerve. 53 separate neurons were identified, 90% of the cells having ipsilateral fields on the toes or foot and the other 10% of cells having large ipsilateral fields involving most of the leg. Most cells responded to all of the stimuli (Wide Dynamic Range (WDR) cells) but others were more Nociceptive Specific (NS). 5 Long Term Memory cells were identified and none of these had contralateral inhibitory fields, although one had a contralateral excitatory field.

When the contralateral leg and tail were noxiously (heat or pinch) stimulated 29 / 53 cells were found to have inhibitory contralateral fields, whereas there were some cells (3) with excitatory contralateral fields. The contralateral inhibitory field was in the 'mirror-image' distribution of the ipsilateral excitatory field for the majority of the cells, although 5 cells had contralateral inhibitory fields throughout the whole contralateral leg and tail. The contralateral inhibition was invariably related to noxious stimuli and could be quite profound. The inhibited cells received A- and A/C stimulation electrically, but no cell was inhibited by receiving only C-fibre input. Electrical stimulation of the sciatic nerve produced excitation in 22 / 53 contralateral cells followed by a period of inhibition. These were not necessarily the same cells affected by the contralateral functional stimuli.

This demonstrates the physiological existence at the spinal segmental level of cross-midline afferent pathways, the majority of which appear to be inhibitory and mediated by A-fibres.

Fitzgerald went on (1982b) to describe the effects of capsaicin, applied directly to the exposed sciatic nerve for 15 minutes 7-21 days prior to the experiment, on the contralateral fields. Reproducing the above results in control (sham-operated) and normal rats, she found that the contralateral fields had turned from being predominantly inhibitory in the control rates to being predominantly excitatory in the

capsaicin treated group. This contralateral field was never larger than the ipsilateral field with again the majority occurring on the foot and toes. The contralateral excitation was never as strong as ipsilateral excitation.

Interestingly, the dorsal horns on **both** sides of the spinal cord changed their contralateral fields from inhibitory to more excitatory following unilateral capsaicin treatment. Several explanations may account for this including the removal of the inhibitory C-fibre effect modulating the A-fibre input from an inhibitory to a stimulatory signal; the changing role of interneurons following capsaicin treatment; and the role of neuropeptides as neuromodulating agents. These are yet to be explored.

Expanding on these observations, Neugebauer and Schaible (1990) examined a spinalised cat model before and after the introduction of a kaolin and carrageenan knee monoarthritis. They noted that 18 / 32 neurons located in laminae VI, VII and VIII of the lumbar spinal cord had bilateral receptive fields. Following the arthritis, more neurons exhibited contralateral fields and the contralateral fields that had previously been detected in some neurons became expanded and their thresholds lowered. They acknowledged that the global effect of such changes may be masked by supraspinal influences, but the 'bottom-up' effect of an inflammatory stimulus on the physiological properties of both sides of the spinal cord is undeniable. As can be seen in Table 2.1 and has previously been discussed, it is likely that these changes are transmitted to the behaviour of the animal.

2.6.3 Crossed afferent neurophysiology in intact animals

The influence of supraspinal pathways can be studied by examining intact animals. Grubb *et al* (1993) examined the dorsal horns of male Wistar rats following the induction of a chronic arthritis by Freund's complete adjuvant. Rats were examined between 2 and 20 days post induction. Similar to Fitzgerald (1982a and b) they found 42/82 spinal neurons exhibited contralateral limb fields, the majority of these cells were WDR (36/42) and that the fields were mainly inhibitory (28/36). Also similar to Fitzgerald's study using capsaicin (1982b), the numbers of cells expressing excitatory contralateral fields increased significantly at day 20, but not prior. This increase was mainly due to an increase in activity of the ventral horn cells. Little change was seen

in the number of neurons expressing inhibitory contralateral fields at any time point. They concluded by suggesting that these changes were indicative of central spinal processing.

It is noteworthy that the changes in these rats were minimal compared to Fitzgerald's studies (1982a and b) and that the role of a significant inhibitory role for supraspinal influences may be large (Eccles and Sherrington, 1931).

This pathway has recently been further explored by Sotgui *et al* (2004). They recognise that WDR neurones are not functionally altered by normal pre-synaptic input from the contralateral side in intact animals based on experimental evidence such as Grubb *et al*'s (1993). However augmenting the contralateral pre-synaptic signal, by either infusing an excitatory neurotransmitter (NMDA) or inhibiting the inhibitory neurotransmitter glycine with strychnine, recruited 50% more of the post-synaptic dorsal horn WDR neurons and their global activity was more spontaneous and sustained following a noxious stimuli applied contralaterally than when compared to that recorded before the pre-synaptic augmentation. It therefore appears that supraspinal influences may be overcome.

Perhaps relevant to this is that substance P appears to have modulating properties on the post-synaptic membrane potential resembling long term potentiation in neurokinin-1 receptor positive neurons, a population that is less than 5% of the total neuronal population in the dorsal horn (Carrasquillo and Gereau, 2004). These fibres are required for central sensitisation following capsaicin injection and perceptual wind-up following repeated non-traumatic stimulus.

2.6.4 The metabolism of the spinal cord to a unilateral inflammatory stimulus.

Metabolic studies suggest that neuronal activity is bilateral in the spinal cord following a unilateral stimulus. This provides further evidence that the crossed spinal afferent pathway is physiological in intact animals.

The uptake of 2-deoxyglucose (2-DG) has been used as a marker of neuronal activation to study cellular activity in the rat spinal cord. Increases in metabolism have been measured in the contralateral regions of the spinal cord following unilateral

hindpaw inflammation caused by formalin, thermal injury or complete Freund's adjuvant.

Porro *et al* (1991) and Aloisi *et al* (1993) studied the cervical spinal cord uptake of [^{14}C] 2-deoxyglucose in adult male Sprague-Dawley rats at 2 and 60 minutes following the injection of 5% formalin compared with control groups of saline injected or uninjected rats. They found bilateral increases in the dorsal horns, predominantly on the ipsilateral side at 2 minutes in a broadly symmetrical fashion whereas activation was only in the medial part of the contralateral dorsal horn at 60 minutes.

Coghill *et al* (1991) used a similar technique to study the effects of non-noxious and noxious heat stimuli applied to one hindpaw of adult male Sprague-Dawley rats. They found contralateral spinal changes in the level of 2-DG uptake, mainly in the deeper layers (laminae V-X) and the medial ventral horn.

Similarly, Schadrack *et al* (1999) studied the effects of complete Freund's adjuvant injection into the ankle of Sprague-Dawley rats on spinal cord metabolism between 2 and 14 days. They too found bilateral increases in 2-DG uptake, initially within all laminae, but then focussing more on laminae V-VII. There was more uptake in the cord ipsilateral to the arthritis.

The conclusion is that the metabolic and neurophysiological potential for the contralateral spinal cord to be influenced by, and affect the process of, a unilateral lesion is supported by the presented evidence.

2.7.1 Pharmacology of crossed afferent spinal pathways

Certain populations of afferent unmyelinated sensory fibres are remarkable in containing neuropeptides within their nerve terminals. The commonest of these peptides are the co-localised substance P (SP) and calcitonin gene-related peptide (CGRP). It is these neuropeptide containing fibres that are affected by capsaicin (Caterina *et al*, 1997) and they are heavily implicated in all of the pain pathways. SP and CGRP both have effects on local inflammatory processes and immunomodulation. It is therefore of interest to note that the contralateral effects can

be abrogated by the use of capsaicin (see section 2.2.3), further implicating the role of these neuropeptides in putative contralateral pathways. Of particular relevance would be the expression of neuropeptides and their receptors centrally.

Increases in substance P, CGRP and their receptors appear to be consistent findings whether the stimulus is mBSA, latex spheres or CFA. These increases have been seen in the spinal cord (Kantner *et al*, 1985; Galeazza *et al*, 1992; Mapp *et al*, 1993; Stucky *et al*, 1993) as well as the contralateral dorsal root ganglion (Kidd *et al*, 1995; Mapp *et al*, 1995; von Banchet *et al*, 2000). Only de Ceballos *et al* (1990) found substance P levels to be decreased at 24 hours in the contralateral spinal cord following a thermal injury.

For example, Mapp *et al* (1993) took male Wistar rats and induced an arthritis using methylated bovine serum albumin following sensitisation with Freund's complete adjuvant 21 days prior. They used controls of unsensitised and sensitised animals with normal saline. Increases in the number of cells expressing CGRP and SP were observed at day 3 in the contralateral dorsal horn when compared with the control groups. These differences disappeared at day 28 post inoculation. Interestingly, on the ipsilateral side to the inflammation, only CGRP immunoreactivity was seen to increase at day 3 and both CGRP and SP were seen to decrease at day 28.

The ability to block neuropeptides pharmacologically reduces the expression of contralateral responses. Yu *et al* (1996) demonstrated that a unilateral injection of carrageenan into the plantar region of the hindpaw was sufficient to produce bilateral changes in the withdrawal latencies to thermal and pressure stimulation and increase the concentrations of CGRP in the spinal cord and the contralateral joint. However, following the administration of intrathecal $CGRP^{8-37}$, a selective antagonist of CGRP, the central sensitisation was significantly abrogated. The effects of $CGRP^{8-37}$ were only partially reversed by the application of naloxone.

Similarly Decaris *et al* (1999) were able to block the contralateral effects (see section 2.2.3) with the prior administration of a neurokinin-1 antagonist into the spinal canal.

2.8.1 Molecular and genetic mechanisms of crossed afferent pathways

The proteins of immediate-early genes and transcription factors in dorsal horn cells are rapidly expressed in response to many peripheral stimuli. Such products include fos, jun and krox-24. The expression of these genes and their products has been seen contralaterally in the spinal cord.

After CFA was placed into either the hindpaw (Menetrey *et al*, 1989) or the ankle (Leah *et al*, 1996), c-fos was expressed in lamina VIII contralaterally. After thermal stimulation immediate-early genes and their products were also seen in the deep laminae contralaterally (Williams *et al*, 1990; Herdegen *et al*, 1991a). After electrical stimulation of unmyelinated sensory afferents (Herdegen *et al*, 1990 and 1991b) early gene products were expressed in laminae IV and VI. After carrageenan was used to cause hindpaw oedema, fos-like immunoreactivity was seen in laminae V and VI (Noguchi *et al*, 1991). All of these studies would support the hypothesis that there is significant activation of contralateral neurons.

2.9.1 Evolutionary role for contralateral responses through crossed afferent pathways

For any biological pathway to be teleologically conserved there should be clear physiological advantages. One hypothesised role for a crossed afferent pathway is that it can rapidly upregulate protective pro-inflammatory responses in the contralateral limb in preparation for an insult that has already occurred to the organism on the ipsilateral side (Kidd *et al*, 1995). Biologically this could be protective and appropriate. The inflammatory response could be focally upregulated and should a similar noxious insult appear on the contralateral side, perhaps it could be dealt with more effectively. The advantage that this precise response has over a systemic response to inflammation is that it is economic with the energy expended and limits widespread self-damage caused by inappropriate inflammation. Similarly, pain withdrawal reflexes are centrally primed so that the contralateral limb can be withdrawn more quickly. There is more chance of damage limitation from a dangerous environment if such responses existed and it could be argued that survival is enhanced through the use of such pathways.

That these pathways may now be disadvantageous, propagating chronic inflammatory diseases, is a reflection of a change in environmental conditions. The symmetrical diseases do not on the whole affect the ability to procreate and hence the genetic basis for these responses could be conserved.

2.10.1 Contralateral responses in man

Although many groups have been able to establish the existence of contralateral responses in the laboratory in a variety of different species, evidence has yet to be provided for such pathways to exist in man.

Haigh (personal communication) investigated this possibility and was able to determine that a central sensitisation could be induced contralaterally in a topographically precise manner following the intradermal injection of capsaicin.

2.10.2 Protocol for demonstrating contralateral central sensitisation to capsaicin

Volunteers were seated in a quiet temperature-controlled room (23-24°C) for 30 minutes. The exact contralateral site was identified. 100µl of 1% capsaicin (Sigma, 80% Tween solution) was then injected intradermally into one forearm. The capsaicin had been made up on site and stored at 4°C throughout the study. Allodynia and hyperalgesia were then mapped every 10 minutes over the following hour (Image 2.1). This was done both ipsi- and contralaterally using Semmes-Weinstein monofilaments and standard quantitative techniques (Simone *et al*, 1989; Pedersen and Kehlet, 1998). Due to possible suggestion bias the volunteers were not told of the study objective and both arms were mapped. Volunteers were told to avoid smoking, caffeine, strenuous exercise and alcohol on the day of the study.

2.10.3 Sensory detection of hyperalgesia and allodynia.

Pinprick hyperalgesia was detected using a stiff Semmes Weinstein monofilament (6.45; 1500mN) (Finnerup *et al*, 2003). This was first tested on an area of skin (anterior chest wall) that was not anatomically related to the capsaicin injection or the contralateral side. Most volunteers reported that this felt like a pinprick but was not very painful. Volunteers were asked to rate whether the 6.45 monofilament felt different on the forearm compared to the sensation felt over the anterior chest wall.

Responses were positive for hyperalgesia if the volunteer reported that the sensation was different to the surrounding skin and was more painful than previously experienced.

Allodynia was detected using a 4.74 (51.9mN) monofilament, and again the anterior chest wall was used prior to the experiment as a reference. This force is not normally perceived as painful (Brennum *et al*, 1989), but is well above the sensory threshold. Reponses were positive for allodynia if the volunteer reported that the sensation was different to the surrounding skin and painful.

Points referring to positive responses to allodynia and hyperalgesia were then transferred using transparent acetate onto blank paper. Free drawn areas were described by connecting these points and the surface area was measured using image analysis (MAVIS, Plassman and Jones, 1998).

Image 2.1 Capsaicin injection is given into the left arm (white arrow). Hyperalgesia (lines) and allodynia (crosses) are mapped every ten minutes in different colours to both arms over 1 hour

Figure 2.2 The percentage of responders to intradermal capsaicin over time (n=32)

Purple and magenta bars are **ipsilateral** hyperalgesia and allodynia respectively. Yellow and turquoise are **contralateral** hyperalgesia and allodynia respectively. The horizontal red line represents the responses of those subjects not exposed to capsaicin.

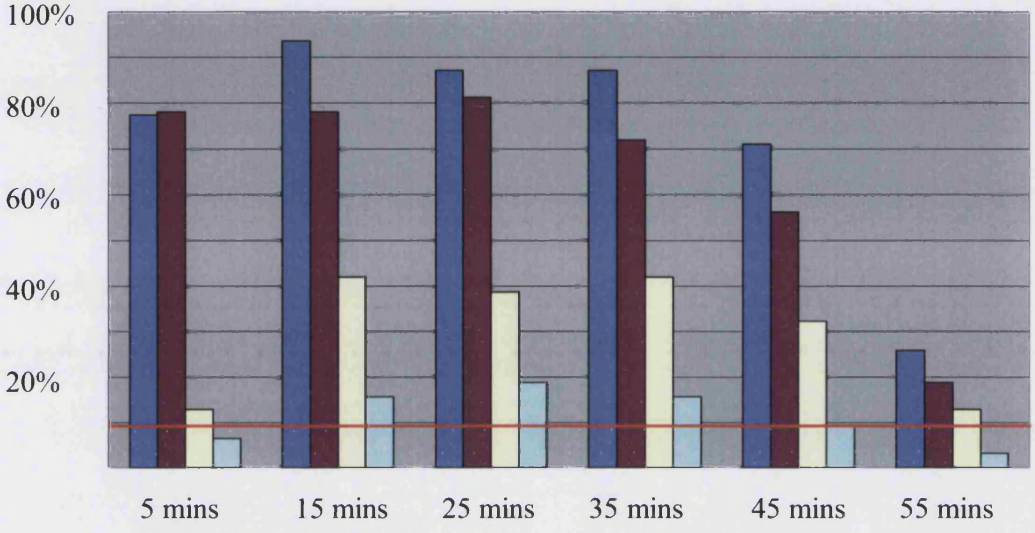

2.10.4 Volunteers for the protocol and controls

Volunteers were recruited at the Royal National Hospital for Rheumatic Diseases and the University of Bath. Two groups were recruited, healthy volunteers and patients with RA.

Because skin differs in the density of nociceptors and thresholds to sensory stimuli vary within the same individual depending upon the location, comparing forearm responses to anterior chest wall responses might be misleading and generate false positive responses. To help control such bias, and also control for suggestion bias, the control group of healthy volunteers was recruited. They had not been exposed to the intradermal capsaicin. Areas of hyperalgesia and allodynia were mapped as outlined above on the forearm.

Recruitment was over 9 months at the RNHRD Trust. Bath Local Research and Ethics Committee approved the protocol (BA110). Baseline characteristics including

disease duration, medication and disease activity were collected. All volunteers gave their informed consent.

2.10.5 Outcomes and statistical analysis

A non-parametric signed rank test was used to compare the frequency of contralateral hyperalgesia and allodynia in the group exposed to capsaicin to the frequency of such response in the healthy control group not exposed to capsaicin.

The secondary outcome was to compare the contralateral responses between the rheumatoid and healthy groups.

2.10.6 Contralateral sensitisation following intradermal capsaicin

In the control (non-capsaicin) group, 23 volunteers (mean age 27 years, 43% male) were recruited. 3 of these volunteers also had a diagnosis of rheumatoid arthritis (all female). 2/23 (8.7%) volunteers demonstrated areas of hyperalgesia and allodynia that both felt different and was more painful than the surrounding tissue. Both volunteers were healthy. One of these volunteers had a very large area of hyperalgesia with ill-defined boundaries. The other had a small area.

In the group who were administered capsaicin 9/14 (64.3%) healthy controls demonstrated contralateral hyperalgesia or allodynia within an hour. 12/18 (66.7%) patients with RA demonstrated contralateral sensory changes. Both groups demonstrated statistically significant differences in the frequency of contralateral responses when compared to the control group at ($p<0.05$) (Figure 2.2). In the healthy group, this achieved significance for hyperalgesia at 5, 15 and 25 minutes and for allodynia at 15, 25, 35 and 45 minutes. In the rheumatoid arthritis group, this achieved significance for hyperalgesia at 15, 25, 35 and 45 minutes but did not achieve significance for allodynia at any time point.

The area of the contralateral responses varied in magnitude between 5-50% of the ipsilateral response to capsaicin (Figure 2.2) in both groups.

The mean mechanical hyperalgesia area in the contralateral arm in both groups was 18 cm^2 (SEM +/-5.3). The mean mechanical allodynia area was 14 cm^2 (SEM +/-

4.7). Both of these were significant ($p<0.05$) when compared to the control group's mechanical hyperalgesia and allodynia, 4 cm^2 (SEM +/- 3) and 3 cm^2 (SEM +/- 2.7) respectively.

There were no significant differences between the proportions of healthy volunteers and patients with rheumatoid arthritis who described contralateral sensations. There was no difference in the temporal pattern of the responses between these two groups. There was no correlation between the baseline characteristics of the volunteer groups and the presence a contralateral response.

In summary, contralateral sensitisation to a stimulus of intradermal capsaicin is robust and topographically precise in this group of volunteers. This is the first demonstration of a neurogenic contralateral responses occurring in man and provides evidence of a central sensitisation pathway's existence.

2.11.1 Conclusion

The neurogenic hypothesis has been advanced. Both central and peripheral mechanisms can be induced contralaterally following unilateral inflammatory stimulus. Multiple examples appear in the literature using a variety of inflammatory stimuli in different experimental models. There are clear anatomical pathways that have been described in the literature to account for these contralateral responses. Neurophysiological and morphological molecular studies also support the implication of the contralateral dorsal horn in the response to an acute inflammatory stimulus. Finally, central sensitisation has been shown to occur in man following intradermal capsaicin injection.

Chapter 3. Neurogenic influences on inflammation and symmetrical diseases

Summary

This chapter summarises the effects that nerves, and specifically neuropeptides, have on inflammation with particular reference to the possible peripheral modulation of inflammatory and immune processes. The distribution of nerves is briefly summarised in normal joints and those of patients with rheumatoid arthritis, as well as the skin of patients with psoriasis. The role of neuropeptides is then discussed and it can be seen that they can significantly influence local inflammatory and more systemic immune processes. Evidence is given for the effects of neural lesions on the course of inflammatory and immune processes in animal models of arthritis. Finally, clinical observations of the effects of neural lesions, both upper and lower, on the phenotypic manifestation of symmetrical diseases are summarised. All of this evidence supports the hypothesis that an autoregulatory neurogenic loop can peripherally influence the course of diseases such as RA and can therefore account for the symmetry seen in these diseases.

3.1.1 Introduction

The possible role of a neurogenic autoregulatory loop to explain the symmetry observed in bilaterally symmetrical diseases has been outlined. If this hypothesis is correct, then nerves and in particular neuropeptides should be appositely positioned to influence this process. Furthermore, disease development should be slowed, arrested or ameliorated by interrupting the nerve supply to the affected areas. The following sections pay particular attention to rheumatoid arthritis, although other diseases such as skin psoriasis are considered. The innervation of the joint is outlined, the influence of neuropeptides on immune and inflammatory mechanisms is considered, and observations of the interruption of the neural supply are summarised.

3.2.1 The anatomical distribution of nerves in joints

Although previously thought to be poorly innervated, the joint in fact has a rich and varied nerve supply, both in terms of large fibres mediating mainly proprioception

and small unmyelinated fibres mediating mainly nociception. The neurally dense areas are located in the joint capsule, at the insertion of ligaments and tendons, and in the synovium (Kellgren and Samuel, 1950; Dye *et al*, 1998).

Mapp (1995) described the histological innervation of the normal synovium. Most joints derive their neural supply from at least one spinal level. About 50% of articular nerves are small in diameter and sympathetic or nociceptive in nature. Sympathetic fibres generally follow the larger blood vessels within the joint and their role appears suited to controlling the local blood supply. Unmyelinated C fibres not only surround the blood vessels but end freely in the synovium unrelated to any blood supply. These fibres are nociceptive and are generally quiescent to normal physiological stimuli and range of movements. They are sensitised in the presence of inflammatory mediators or painful stimuli and, upon being sensitised, can induce a discharge following a normal stimuli.

3.2.2 The distribution of nerves in rheumatoid arthritis

Mapp (1995) went on to describe the innervation of the synovium in rheumatoid arthritis and noted that this is markedly different to that of the normal synovium. Using immunohistochemical studies, deep vessels appear to maintain their innervation, which is confirmed to be sympathetic in origin on specific staining. However, smaller vessels more superficial to the joint cavity are apparently denuded and the number of free fibres is greatly reduced in the synovium, especially in the intimal layer. No staining was seen in intensely inflamed and 'lymphoid' areas of the diseased synovium.

The destruction, or overgrowth, of nerve fibres in RA and OA is supported by observations from other groups (Gronblad *et al*, 1988; da Silva and Carmo-Fonseca, 1990) and implicates the nervous system in the pathophysiology of such diseases.

3.2.3 The distribution of nerves in skin of patients with psoriasis

Pergolizzi *et al* (1998) examined the epidermal nerves from 10 patients with skin psoriasis. They took biopsies from three areas; long-standing lesions; mature, but not long-standing lesions; and apparently uninvolved skin. They found that both of the psoriatic lesions had significantly decreased expression of neural fibres and there was

almost a complete lack of epidermal nerve fibres in long-standing psoriatic lesions. Johansson *et al* (1991) also found a profound reduction in the expression of protein gene product (PGP 9.5), a pan-neuronal marker, in the lesions of mature psoriatic plaques when compared to non-lesional skin.

However, these results are in counterpoint to Chan *et al* (1997) and Al'Abadie *et al* (1995) both of whom noted that the expression of substance P (SP) and calcitonin gene-related peptide (CGRP) are increased in the lesions with psoriasis. Little detail was available however on the temporal history of these biopsies and the conflicting results may therefore not be incongruent.

The early involvement of neuropeptides in the developing psoriatic plaque is provided by Naukkarinen *et al* (1993) who studied plaques induced by the Koebner phenomenon, non-lesional skin and skin from healthy volunteers. They found a steady increase in levels of SP and vasoactive intestinal peptide (VIP) in the developing lesions. There was a clear increased density of these neuropeptides in the mature psoriatic lesion.

From histological studies, nerves are clearly involved in the pathophysiology of both RA and skin psoriasis. The role of various neuropeptides in the immune and inflammatory processes will now be discussed.

3.3.1 Neuropeptides

Histochemical and immunological studies have revealed the presence of a variety of peptides in neurons. A summary of these peptides to date is provided in Table 3.1. The role for these peptides outside the traditional neurotransmitter and neuromodulation roles for neuronally stored substances is wide and varied. Many of these neuropeptides are located in neurons found in synovium. These include substance P, calcitonin gene-related peptide, neuropeptide Y, vasoactive intestinal peptide, somatostatin and dynorphin. It should be noted that the production of these peptides is not limited to the nervous system, but monocytes, dendritic cells, eosinophils and mast cells are all capable of their production.

Table 3.1 Some Mammalian Neuropeptides and Neuropeptide Families (adapted from Hokfelt *et al*, 2004)

Hypothalamic hormones

Oxytocin; Vasopressin

Hypothalamic releasing and inhibiting hormones

Corticotropin releasing hormone (CRH); Growth hormone releasing hormone (GHRH); Luteinizing hormone releasing hormone (LHRH); Somatostatin growth hormone release inhibiting hormone; Thyrotropin releasing hormone (TRH)

Tachykinins

Neurokinin α; Neurokinin β; Neuropeptide K; Substance P

Opioid peptides

β-endorphin; Dynorphin; Met- and leu-enkephalin

NPY and related peptides

Neuropeptide tyrosine (NPY); Pancreatic polypeptide; Peptide tyrosine-tyrosine (PYY)

VIP-glucagon family

Glucagon-like peptide-1 (GLP-1); Peptide histidine isoleucine (PHI); Pituitary adenylate cyclase activating peptide (PACAP); Vasoactive intestinal polypeptide (VIP)

Other peptides

Brain natriuretic peptide; Calcitonin gene-related peptide (CGRP) (α- and β-form); Cholecystokinin (CCK); Galanin; Islet amyloid polypeptide (IAPP) or amylin; Melanin concentrating hormone (MCH); Melanocortins (ACTH, α-MSH and others); Neuropeptide FF (F8Fa); Neurotensin; Parathyroid hormone related protein

'Novel' neuropeptides

Agouti gene-related protein (AGRP); Cocaine and amphetamine regulated transcript (CART)/peptide; Endomorphin-1 and -2; 5-HT-moduline; Hypocretins/orexins; Nociceptin/orphanin FQ; Nocistatin; Prolactin releasing peptide; Secretoneurin; Urocortin

As will be seen the physiological effects *in vitro* and *in vivo* of these neuropeptides support the view that they can influence the immune-mediated inflammatory processes present in bilaterally symmetrical diseases. Pharmacological evidence is given by their actions, either through agonists or antagonists, in the development and maintenance of experimentally-induced animal models of arthritis. The generalised central effect of neuropeptides appears to be more of a modulating, rather than transmitting, nature. The peripheral effects of the relevant neuropeptides are more relevant to the contralateral responses of crossed afferent pathways. Some of these neuropeptides will now be briefly summarised. This review is not intended to be exhaustive, merely reflect the influence that these neuropeptides might have upon the periphery.

3.3.2 Substance P (SP)

Substance P (Powderable) was first discovered by von Euler and Gaddum in 1931. Although they isolated a heterogeneous collection of substances, they immediately demonstrated powerful vasodilatory actions and effects on gastric motility that have been confirmed in studies using the synthetic peptide performed after SP was finally isolated in the 1970s. Vascular effects include the margination of neutrophils and, in synergy with chemotactic peptides and complement, the migration and cytotoxic activation of these neutrophils.

Local inflammatory properties occurring at physiological concentrations of SP include the degranulation of mast cells (many unmyelinated nerve endings are seen to interact closely with mast cells); secretion of prostaglandins and thromboxane from macrophages; and the modulation of immunoglobulin production from lymphoid tissue (Holzer, 1988; Garrett *et al*, 1992; Mapp, 1995; Lotz, 1997).

Lymphocytes have specific receptors for SP and, when stimulated, proliferate more in its presence. It is considered to be immunostimulatory. Lymphocytes also have receptors for CGRP, somatostatin and various amines which are considered to have more suppressive activities (see below, Lambrecht, 2001). Anatomical studies demonstrate the interaction between the SP neuropeptide containing neurons and the high endothelial venules in lymph nodes. This is the putative interface between the draining antigen presenting cells and circulating lymphocytes' access to the inner

cytoarchitecture of the lymph gland. Interestingly, the local application of capsaicin into these draining lymph nodes attenuates adjuvant-induced arthritis (Lorton *et al*, 2000).

An interesting effect of various neuropeptides has been described by Levite (1998) Whilst naïve T-helper cells (TH0) are driven by antigenic stimulation to induce rather fixed patterns of cytokine secretion characterised by the 'pro-inflammatory' TH1 (e.g. IL-2, IFNγ) and the 'anti-inflammatory' TH2 (e.g. IL-4, IL10) cytokine profiles, neuropeptides cause these TH0 cells to produce a rather different and distinctive pattern described as 'forbidden'. This forbidden pattern combines both the characteristic TH1 responses with the additional secretion of IL4 and IL10, and the characteristic TH2 responses with the additional secretion of IL2 and IFNγ. These effects seem to be not only a property of SP, but also CGRP, somatostatin and VIP.

In patients with inflammatory arthritis there are several reports of elevated concentrations of SP in the synovial fluid (reviewed by Garrett *et al*, 1992). These levels are far in excess of those found in paired plasma levels suggesting a joint origin. Similarly there is an increased expression in the joints of patients with RA when compared to healthy controls of the enzyme neutral endopeptidase which is an important catabolic enzyme of SP. Finally it has also been shown that there is a large increase in the number of SP receptors in the rheumatoid synovium when compared to a healthy population (Garrett *et al*, 1992).

Levine *et al* (1984) demonstrated that SP infusion into the knees of rats increased the severity of adjuvant induced arthritis and that the administration of a putative receptor antagonist reduced this arthritis to the level of moderate soft tissue swelling and osteoporosis, findings corroborated by Lam and Ferrell (1989) with a carrageenan model of tissue inflammation.

In conclusion, the pro-inflammatory peripheral effects of substance P and its role in rheumatoid arthritis are well described.

3.3.3 Calcitonin gene-related peptide (CGRP)

CGRP is colocalised with SP in vesicles contained in the synaptic terminals of unmyelinated and thinly myelinated neurons. The actions of CGRP are synergistic with those of SP (Lotz, 2000). It is recognised that CGRP is more potent as a vasodilator than SP (Brain *et al*, 1985) but has a similar action on microvascular permeability and neutrophil accumulation. CGRP however has immunomodulatory activities that are more suppressive including the suppression of the proliferation of murine T cells and dendritic cell activation (Lambrecht, 2001).

3.3.4 Somatostatin (SS)

Somatostatin's activities as an inhibitory neuropeptide were described in 1968 (Hokfelt *et al*, 2004). However it wasn't until 1973, when SS was isolated and structurally characterised that it was realised to be identical to the gut hormone described in 1969. SS is considered to be more of an anti-inflammatory neuropeptide. It too is released from capsaicin-sensitive nerve endings and it has a tendency for suppressive effects on the immune system, specifically on the proliferation of T-cells and in causing a reduction of IFN-γ production from both murine and human T lymphocytes (Hokfelt *et al*, 2004).

Somatostatin has been studied in the setting of arthritis induced by complete Freund's adjuvant. An agonist has been found to ameliorate the course of the arthritis whereas an antagonist exacerbates the histological and clinical picture (Helyes *et al*, 2004).

3.3.5 Vasoactive intestinal peptide (VIP)

VIP was isolated in the 1970s from the duodenum and its chemical structure elucidated a short time later (Delgado *et al*, 2004). VIP has a mixed effect on inflammation and the immune system. Several studies demonstrated an immunosuppressive effect of VIP on T-lymphocytes by reducing their proliferation and cytokine expression of IL-2. However more recent studies have suggested augmented immune and inflammatory actions of VIP with the activation of dendritic cells and the generation of IL-12.

Promising experimental data has come from the administration of intraperitoneal injections of VIP after the development of an arthritis induced by sensitisation to collagen type II in complete Freund's adjuvant in DBA/1 mice. Mice treated with VIP showed delayed onset, lower incidence and decreased severity of their collagen-induced arthritis when compared to the control groups, and these responses were dose-related (Delgado *et al*, 2001).

3.3.6 Neuropeptide Y

Neuropeptide Y is part of the 'pancreatic polypeptide family' and is peripherally widely located in the sympathetic nervous system. Although more studied in relation to anxiety, obesity and cardiovascular disease, there is evidence to suggest a role for it in the interface between the immune and sympathetic nervous systems. It is recognised to be a messenger and a modulator of the immune system by its functions on the differentiation of T helper cells, monokine release, NK cell activation and immune cell redistribution (Bedoui *et al*, 2003).

3.3.7 Nerve Growth Factor (NGF)

Although not strictly a neuropeptide, neuropeptide-containing nerves are dependent upon the neurotrophin Nerve Growth Factor (NGF). Its effects have been studied in skin psoriasis models as well as arthritis. Epidermal keratinocytes are known to synthesise and release nerve growth factor (NGF) and express its low affinity (p75) and high affinity (trkA) receptors (Pincelli, 2000). NGF is known to stimulate keratinocyte proliferation and induce apoptosis in its absence. NGF is also expressed in higher levels in psoriatic skin when compared to non-lesional skin from the same patients and skin from healthy controls (Pincelli, 2000). Moreover, NGF blockade through a specific trkA receptor antagonist ameliorated psoriatic plaques transplanted onto the severe combined immunodeficient mouse in a double-blinded placebo-controlled study (Raychaudhuri *et al*, 2004).

It should be noted that synovial cells also release NGF and that this is augmented by inflammatory cytokines. Elevated levels of NGF have been found in the synovial fluid of patients with inflammatory joint disease when compared with normal healthy volunteers and plasma NGF is increased in patients with juvenile chronic arthritis.

NGF levels are higher in active rheumatoid disease when compared to quiescent. (Falcini *et al*, 1996; Halliday *et al*, 1998).

Agonists and antagonists have not directly been studied in experimental arthritis. However, one study did suggest that an indirect method to reduce the amount of NGF in a carrageenan model of active joint inflammation using cholecystokinin antagonism resulted in an increase in joint swelling, suggesting that NGF has an ameliorating influence in this model (Manni *et al*, 2002).

3.4.1 Denervation and arthritis in animal models

Hood *et al* (2001) induced a monoarthritis in male Dunkin-Hartley guinea pigs using a suspension of heat-killed *M. tuberculosis* in paraffin oil (CFA). She had pre-treated a group of 10 guinea pigs with systemic capsaicin. This group had significantly attenuated disease after day 1 of arthritis induction. Initial macrophage infiltration was followed by a lymphocyte population at day 3, which was again significantly attenuated in the capsaicin-treated group.

Courtright and Kuzell (1965) showed that sectioning one sciatic nerve 7 days before the induction of adjuvant arthritis delayed the onset and reduced the severity of disease in that limb.

As noted in chapter 1 (section 1.5.3) a criticism of this manipulation for studying the neurogenic effect on the development of arthritis is the accompanying paralysis induced by the neural lesion. Kane *et al* (2005) have recently circumvented this criticism by severing only the sensory afferent nerves, leaving the motor neurons intact. That they found similar results to the other groups strongly supports a neurogenic role in the development of acute arthritis.

Levine *et al* (1986) used a variety of neural lesions and concluded that not one single lesion could consistently account for the improvement or accentuation of adjuvant-induced arthritis. He used groups of rats that were genetically bred to have a high sympathetic tone or had been exposed to neonatal capsaicin or had a unilateral dorsal rhizotomy performed or underwent peripheral sympathectomy. Deafferented rats had a worsening of their arthritis whilst with those treated with neonatal capsaicin had a

less severe arthritis. Rats with a high sympathetic tone also had a more severe arthritis and the sympathectomised rats had less severe disease.

These animal models provide several different illustrations of the effects of neural depletion on the course of arthritis. Most, but not all, have beneficial effects. Another way to examine this issue is to assess the effects of neural injuries on IMID by clinical observations.

3.5.1 Denervation and the attenuation of inflammation in clinical disease

The appropriate innervation of normal tissue is essential for the development of inflammation. In a striking clinical case report, Schade Willis *et al* (2001) reported the sparing of a limb affected by a brachial plexus injury secondary to birth trauma from necrotic skin rash due to *N. meningitidis* infection in a young boy. Tarkowski *et al* (1996) demonstrated a lateralisation of the tuberculin response favouring the non-paralysed side in patients with poliomyelitis affecting one of their upper limbs.

It is therefore of no surprise to see sparing of disease progression in the diseases that have so far been described. A selection of these is summarised in Table 3.2.

These examples are self explanatory, but the effect of denervation to a lesion of psoriasis is shown in Image 3.1. The superior part of a chronic plaque of psoriasis has demonstrably improved following denervation whereas the innervated lower half is still chronically inflamed.

3.6.1 Conclusion

From the review of the evidence in these first three introductory chapters, it seems plausible, if not likely, that a neurogenic loop affecting the peripheral contralateral side in a topographically precise manner exists and should therefore be demonstrable in man.

Table 3.2 Reports in the literature of the development of arthritic diseases in partially paralysed patients (Dixon, 1989)

Disease	Nerve lesion	Outcome suppressed	Reference
OA	Hemiplegia	Heberden's nodes	Forestier (1935)
OA	Hemiplegia	Heberden's nodes	Coste (1935)
OA	Hemiplegia	Heberden's nodes	Winter (1952)
OA	Poliomyelitis	OA knee or hip	Glyn (1966)
OA	Nerve injury	OA and Heberden's nodes	Stecher (1947)
OA	Hemiparalysis	OA	Segal (1998)
RA	All nerve lesions	Erosions	Yaighmai (1977)
RA	Hemiplegia	Arthritis	Bland (1968)
RA	Hemiplegia	Digital vasculitis, arthritis and RA nodules	Nava (1953)
RA	Hemiplegia	Arthritis	Jacqueline (1953)
RA	Hand dominance	Radiological changes of arthritis	Soila (1963)
RA	Disuse caused by elbow trauma	Arthritis	Kamerman (1966)
RA	Poliomyelitis	Arthritis	Glick (1967)
Psoriatic arthritis (PsA)	Nerve injury in one finger	Arthritis mutilans in one finger	Kane (2005)
PsA	Hemiplegia	Arthritis	Veale (1993)
PsA	Denervation	DIP arthritis and nail pitting	Mulherin (1995)
Psoriasis	Lower motor	Plaque amelioration	Raines (2002)

Image 3.1 Partially denervated psoriatic plaque (Raines and Cox, 2002)

This gentleman had undergone an oesophagectomy (scar arrowed) and the intercostal nerves were severed. These supplied the skin that included the superior aspect of the chronic psoriatic plaque and it can be seen that this has greatly improved.

Chapter 4. Symmetry of early erosions in patients with rheumatoid arthritis

Summary

Erosive disease in patients with rheumatoid arthritis (RA) is classically described as symmetrical in nature. In this chapter, this symmetry is described in the erosions of patients with RA with 6 months of symptoms. The progression of this symmetry is described 17 months later and compared to the baseline reading. It can be seen that not only is early RA symmetrical, but that this symmetry increases as time passes. Either a neurogenic or anatomical hypothesis may explain the symmetry of these erosions. There was no dominant side predilection at any time point however and this does not support a biomechanical hypothesis. A neurogenic hypothesis would best fit these observations.

4.1.1 Symmetry of disease in rheumatoid arthritis

Rheumatoid arthritis affects the joints in many different dimensions and these can be measured. Measurements can be made clinically or through a variety of imaging techniques. For example, clinical assessments can be made of pain, tenderness, stiffness, swelling, range of movement, and function. Imaging assessments include radiography, ultrasonography, scintigraphy, thermography, magnetic resonance imaging (MRI) and computed topography (CT). Many studies have been conducted into examining the effects of RA on patients' joints using these assessments. However, few studies have looked specifically at the distribution of the disease. Studies that have been performed have mainly used radiographic techniques. These will now be briefly summarised and discussed.

4.1.2 Previous radiographic studies of the symmetrical distribution of erosions in RA

Halla *et al*'s study (1986) exemplifies a number of problems that occurred in previous studies when examining the symmetrical distribution of erosions in patients with RA. Other studies with similar methodological weaknesses include those of Martel *et al* (1965), Mattingley *et al* (1979), and Owsianik *et al* (1980). Halla *et al* (1986) examined radiographs for marginal erosions in 200 consecutive patients attending an

outpatient clinic using 3 independent examiners. They found only 21% of the erosions in the metacarpophalangeal (MCP) and metatarsophalangeal (MTP) joints were classified as asymmetrical, with nearly 80% having symmetry. However, this study used radiographs which are a relatively insensitive means of detecting erosions. Several joints were grouped together rather than being analysed individually thus exaggerating the symmetry finding. They also failed to take into account the temporally dynamic nature of RA by only analysing their cohort at one point in time thus potentially underestimating any symmetry.

Zangger *et al* (2005) identified asymmetry to occur between 9.7-14.4% of joints in patients with RA, slowly increasing dependent upon disease duration. They found that the wrist, when divided into quadrants, and the MCPs exhibited more asymmetry than the PIPs. Furthermore, by studying 77 erosions, they found that the overall probability of small joints in the foot and hand becoming symmetrical over two years was 28.5% and this symmetry was predicted by rheumatoid factor. This study is limited not only in its imaging methodology but also by its analysis. By not determining the background rate of erosion development in these patients it is difficult to predict the significance of the number of symmetrical erosions. For example, 28.5% of erosions may be very significant if the rate of joints being affected is small (say 5% per year), but not very significant if the rates of new erosions are higher (say 20% per year).

Möttönen *et al* (1988) commented upon the symmetry of erosive disease by using a relatively more sensitive combination of scintigraphic and radiological assessment and following up a group of 13 patients for the following 2 years. They noted 4 erosions at baseline and the development of 47 new erosions in 387 joints (13.2%). Although noting a relative asymmetry in the distribution of these erosions, the small numbers of patients and erosions meant that there was a lack of power to detect significant differences.

Boonsaner *et al* (1992) specifically tested the hypothesis that there is a discrepancy between the dominant and non-dominant sides. They studied the radiographs of 93 patients with RA. They found significant differences between the two sides (dominant and non-dominant) in both joint space narrowing and erosions. However in their

analysis they did not make joint-to joint comparisons, preferring to use a total load of erosions when comparing both sides. This may introduce bias into their results should one side develop an erosion prior to the contralateral. This could have been obviated if they had undertaken a longitudinal study.

Brook and Corbett (1977) examined the hands and feet of 94 patients with early RA radiographically and followed them up for 5 years. They found symmetrical changes occurring in the joints. However they did not specifically design their study for this analysis and their inclusion criteria could be questioned as nearly 30% of their cohort did not develop any erosions.

A more sensitive technique to standard radiography is that of microfocal radiography.

4.2.1 Microfocal Radiography

The advantage of microfocal radiography is that it increases the radiographic magnification without losing any spatial resolution thereby allowing better identification of the imaged structures. Magnifying standard radiographs loses resolution dependent primarily on the focal length of the X-ray spot source, typically more than 0.3mm. With very small X-ray sources however (<20μm) this loss of resolution is overcome (Figure 4.1). The development of fast rare-earth screen-film systems in the late 1980s permitted the development of these microfocal imaging systems. High magnification (up to 10 times) and the retained resolution of microfocal radiography permit measurements of structures as small as 40υm (Buckland-Wright *et al*, 1986; Buckland-Wright and Bradshaw, 1989). Macroradiographs are produced from microfocal radiography (Figure 4.2).

Figure 4.1 Microfocal X-ray unit demonstrating very small focal point

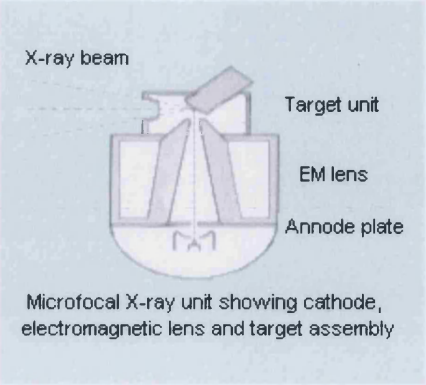

Microfocal X-ray unit showing cathode, electromagnetic lens and target assembly

Figure 4.2 Microfocal radiography

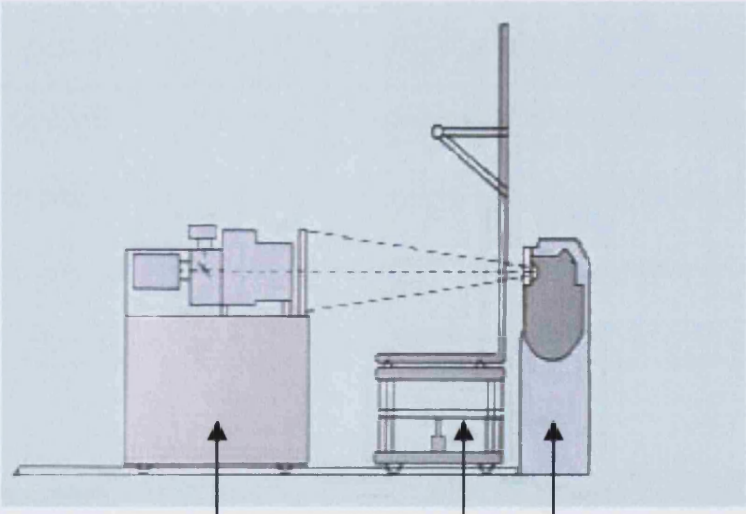

The microfocal radiographic unit arrangement demonstrates the juxtaposition of the patient gantry with the microfocal unit. Magnification of the image occurs by removing the film processor from the gantry.

4.2.2 The use of microfocal radiography to assess erosions in RA

Erosions on macroradiographs of the wrist and hand in patients with RA can be seen within 3 months of symptom onset (Buckland-Wright, 1984) and these measurements have previously been shown to be both accurate and reproducible (Buckland-Wright and Walker, 1987).

Buckland-Wright (1984) used this technique to assess the presence of erosions in the hand and wrist joints of 26 patients with early and moderately advanced disease. He found that this technique was more sensitive than standard radiography and he was able to discern erosions that were unidentifiable on standard films. He described the earliest erosions occurring in the medial (radial) side of the carpus; the 2nd and 3rd MCPs; and the 3rd and 4th PIPs. He noted that the erosions appeared to be symmetrical although this study was not primarily powered nor structured to assess this in more detail.

4.2.3 The use of microfocal radiography to assess the symmetry of erosions in RA

Clarke *et al* (1994) assessed the distribution of symmetry in the joints of patients with early RA using microfocal radiography longitudinally at four separate time points over 18 months. They took 51 patients with a mean disease duration of 36 months (range 3-276 months) and analysed the erosion area at 142 sites and the joint space width in 25 sites in the wrist and hand of each side. They analysed the erosion scores in three ways. Firstly, they summed the areas for each hand to give a total erosion area load per hand. Secondly, they summed the areas for each of the 142 sites to give an erosion area per site. Thirdly, they compared the size of the erosion with the contralateral side in individual patients using the signed rank test. They compared differences for the first outcome (total erosion area per hand) at all 4 time points, and the other two outcomes at baseline and 18 months.

They found no difference between the dominant and non-dominant hands in total erosion load per hand at three of the four time points. At the 12 month assessment visit they noted that the dominant hand had a smaller total erosion load when compared to the non-dominant hand.

They found two of the 142 sites demonstrated significant differences at baseline between the two extremities and six of the sites demonstrated differences at 18 months. There was an equal split in which side the erosion area was larger. Neither of the sites demonstrating asymmetry at baseline did so at 18 months.

They also found that 6 patients had significant differences in the number of sites exhibiting larger erosions at baseline, and 5 patients exhibited significant differences at 18 months. Again, there was an equal split between dominant and non-dominant (5 and 6 respectively) and none of the patients demonstrating asymmetry at baseline did so at 18 months.

They concluded by stating that over the 18 month study there was almost no evidence of the group progressing asymmetrically.

This study addressed many of the criticisms outlined towards studies in section 4.1.2, namely the use of a sensitive method longitudinally, but it did study a heterogeneous group of patients with different disease durations and treatments.

Interestingly, they chose to analyse the erosions by using a measure of area rather than frequency. Previous publications had shown that erosion area is more useful measure of disease progression than frequency due to its increased ability to detect disease progression in disease longer than 48 months duration. The number of erosions as an outcome measure for the assessment of symmetry is probably more appropriate. This is because biomechanical forces are important in the size of an erosion although not in their initiation (Jayson *et al*, 1970). Clarke *et al*'s (1994) methodology will therefore confound a study designed to test the hypothesis of neurogenic symmetry or biomechanical.

It was felt that this study could therefore be repeated in a different cohort and using different outcome and analytical methods.

4.3.1 A macroradiographic study of the distribution and progression of erosions in the hand and wrist joints of patients with early rheumatoid arthritis

From the evidence above, it was decided to study the presence of erosions in the joints of a group of patients with very early rheumatoid arthritis longitudinally. Such a cohort existed in Professor Buckland-Wright's X-ray library at the Department of Clinical Anatomy, School of Biomedical Sciences at the Guy's Hospital campus in King's College, London. This cohort provided the bulk of the patients for a randomised controlled trial into the effects of myocrisin (Buckland-Wright *et al*, 1993).

4.3.2 Cohort of RA patients

The X-rays of hands and wrists from 42 patients with RA were identified. Their average age was 55.3 (range 29-79, SD 13.5) and they had had symptoms for a mean of 6.4 months (range 2-15, SD 3.6). 25/42 (59.5%) were women; 20/42 (47.6%) had a positive rheumatoid factor; and 15/42 (35.7%) smoked. The mean number of joints involved at recruitment on a 28-joint count was 6.4 (range 1-18, SD 3.6), ESR 31.9 (range 1-110, SD 28.0), and morning stiffness 528 minutes (range 0-1440, SD 652.2). Patients rated themselves as 23.1 on a 100-point visual analogue scale (range 0-95, SD 23.5) and their average uncorrected Health Assessment Questionnaire (HAQ) score was 16.0 (range 4-32, SD 10.9). None of the patients had commenced a Disease Modifying Anti-Rheumatic Drug (DMARD). 34/42 (81.0%) were taking non-steroidal anti-inflammatory drugs. 7 patients were taking other medications. These included atenolol (2 patients); thyroxine (2); dyazide (2); amitriptylline (2); nifedipine (2); ranitidine; ferrous sulphate; dothiepin; uniphyllin; timolol eye drops; ventolin and becotide inhalers.

In summary, this appeared to be a slightly older group of patients than classically described with mild–to–moderate disease. This cohort had early disease with more than 90% having symptoms of less than 12 months duration.

Only patients with definite Rheumatoid Arthritis (ARA Criteria) were included into the trial. Patients had been excluded if they had been treated with DMARDs; they had severe systemic, renal, or hepatic disease; significant laboratory findings; a history of blood disease, exfoliative dermatitis or SLE; an allergy to gold; a history of urticaria,

eczema or colitis. Patients had also been excluded if they were currently taking phenylbutazone or oxyphenbutazone; or were pregnant or nursing.

The trial necessitated obtaining macroradiographs at 6-monthly intervals for 18 months. Of the 42 patients studied, 10 did not have X-rays at 18 months, and therefore their X-rays at 12 months were used instead. One other patient had films at 24 months rather than 18. The average difference between the baseline and follow-up X-rays (time 1: T1) was for all 42 patients was 16.7 months.

4.3.3 Protocol of the study

The presence of an erosion, no erosion, or other X-ray pattern was classified from 142 sites on each hand and wrist at two time points: baseline (T0) and follow-up macroradiographs (T1). Each film was read twice and only if an erosion was seen at both viewings was it determined to be present (see sections 4.3.4 and 4.3.5). The thumb was excluded from the macroradiographs.

For an erosion to be included for the purposes of the study, all three of the following features must exist. There must be a clear disruption of the cortical line and there must be loss of trabeculation in the underlying bone, and both of these changes must be seen on both reviews of the microradiograph.

A database in Microsoft Excel was compiled for analysis. Expected numbers of symmetrical erosions were determined depending on the prevalence of erosions and compared with observed values with the Z-test, a generalised version of the Chi-squared test. Progression of the erosions was then assessed.

In brief, normal bone, erosions and abnormalities that were not erosions were coded 0, 2 and 3 respectively. Because each macroradiograph was assessed twice the possible scores were 0, 2, 3, 4, 5 and 6. Only a score of 4 represents an erosion to be included in the count. Using combinations of Excel functions, data could be extracted to provide details on the symmetry of erosions and their progression.

Baseline values (T0) reflected an average of 6 months from the start of the patient's symptoms and the follow-up film to assess progression (T1) was taken 17 months

later. Two different levels of analysis were performed on the database: 'point-to-point' (142 points per side) and 'joint-to-joint' (22 joints per side). The wrist was divided on anatomical grounds into 10 separate regions (see Figure 4.3), and there were 4 MCPs, 4 PIPs and 4 DIPs on each side making a total of 22 joints.

Figure 4.3 Division of the wrist joint into 10 regions

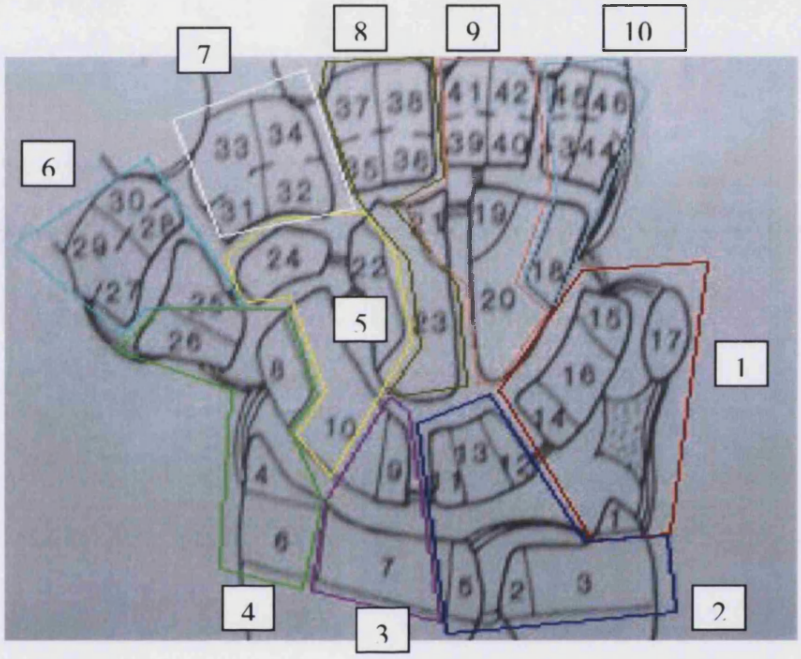

The regions were formed on anatomical grounds for the analysis of the wrist:

1	Styloid-pisiform-triquetrum	1, 14, 15, 16, 17
2	Radio-ulnar-lunate	2, 3, 5, 11, 12, 13
3	Radio-scaphoid flexor	7, 9
4	Radio-scaphoid-trapezium	4, 6, 8, 26
5	Scaphoid-capitate-trapezoid	10, 22, 24
6	Carpo-metacarpal (CMC) 1	25, 27, 28, 29, 30
7	CMC 2	31, 32, 33, 34
8	CMC 3	23, 35, 36, 37, 38
9	CMC 4	19, 20, 21, 39, 40, 41, 42
10	CMC 5	18, 43, 44, 45, 46

4.4.1 Measuring the reproducibility of microfocal radiography

Reproducibility of the scoring is paramount to the use of microfocal radiographic techniques being useful in the study of erosions in RA. Both interobserver and intraobserver scores were therefore obtained in a blinded fashion. Blinding was achieved by covering any identifying features on the macroradiographs. For the purposes of intraobserver readings, these were obtained more than 3 months apart. Both observers were blinded to the original results.

The unweighted kappa score is an appropriate test to use to assess the consistency between two observers of radiographic readings organised into categorical data (i.e. coded values of 0, 1, 2 etc...) (Landis and Koch, 1977; Ruckman *et al*, 1995; Zangger *et al*, 2004).

4.4.2 Intraobserver kappa value

For intraobserver values, 1111 separate points were analysed on 10 different macroradiographs. The overall erosion prevalence for this cohort was 7.8%, representative of that in the overall sample (6.8 – 13% dependent upon whether the sample was from T0 or T1). The interobserver kappa value was 0.71 (0.62-0.80 95% confidence intervals) (GraphPad). This is a substantial agreement according to Landis and Koch's (1977) scale.

Table 4.1 2x2 table for intraobserver reliability score (n=1111)

		Reading 2		
		No erosion	*Erosion*	***Total***
Reading 1	*No erosion*	1019	13	1032
	Erosion	26	53	79
	Total	1045	66	**1111**

Table 4.2 Kappa values and their strengths of agreement (Landis and Koch, 1977)

Kappa value	Strength of agreement.
<0	Poor
0 - 0.2	Slight
0.21 - 0.4	Fair
0.41 - 0.6	Moderate
0.61 - 0.8	Substantial
0.81 - 1	Almost perfect

From this kappa value, the minimum detectable difference can be calculated (Lassere *et al*, 1999). This was found to be 30 erosions to an alpha of 0.05. This means that any difference between groups that was more than 30 erosions was unlikely to be due to the observer error.

4.4.3 Interobserver kappa value

The interobserver scoring was performed by Ms. Elizabeth Messent, a doctoral student working with Professor Buckland-Wright and experienced in evaluating macroradiographs. A random selection of 20 different points was used on 5 separate macroradiographs producing a series of 100 points for analysis. The criteria for erosion identification were identical and training had occurred prior to the scoring cohort. The erosion prevalence for this cohort was 5%, slightly lower than in the intraobserver sample. The kappa value for her interobserver score was found to be 0.59 (0.28-0.91 95% confidence intervals). This agreement is moderate on the Landis and Koch scale (1977).

4.5.1 Results: Distribution of the erosions

There were equal numbers of erosions on both left and right sides at both time points. Table 4.3 details the frequency of the points where the erosions were most prevalent. Table 4.4 details the joints where these were seen the most. This is represented pictorially at and between the different time points in Figures 4.4-6.

Table 4.3 Distribution of the 12 most frequently eroded points

Rank	ND side At T0 (n)	Dom at T0 (n)	New ND side at T1 (n)	New Dom at T1 (n)	TOTAL (n)
1	8 (24)	8 (26)	44 (28)	8 (36)	8 (112)
2	44 (20)	4 (19)	1 (26)	11 (21)	44 (85)
3	6 (20)	44 (17)	8 (24)	44 (20)	4 (75)
4	18 (18)	6 (15)	18 (23)	1 (20)	6 (74)
5	4 (18)	1 (14)	19 (20)	7 (19)	1 (72)
6	7 (18)	18 (13)	6 (20)	6 (19)	18 (71)
7	26 (16)	51 (11)*	4 (20)	26 (18)	7 (64)
8	1 (14)	39 (11)	11 (19)	19 (18)	26 (60)
9	17 (13)	19 (11)	39 (18)	4 (18)	19 (60)
10	52 (11)*	11 (10)	26 (18)	18 (17)	11 (59)
11	19 (11)	26 (9)	7 (18)	27 (16)	39 (52)
12	39 (10)	7 (9)	21 (17)	14 and 21 (14)	21 (48)

The figures represent the region (142 in total) with the frequency of the erosions in brackets. All of these points are in the wrist apart from points 51 and 52, marked *. These are respectively on the medial and lateral 2nd metacarpal head, closest to the joint space. Please see Figure 4.3 to identify the wrist regions.

Table 4.4 Distribution of the most frequently eroded joints (not including wrist)

Rank	ND side at T0 (n)	Dom at T0 (n)	New ND side at T1 (n)	New Dom At T1 (n)	TOTAL (n)
1	DIP 3 (6)	MCP 2 (11)	PIP 4 (9)	DIP 4 (7)	MCP 2 (24)
2	MCP 3 (5)	PIP 2 (4)	MCP 2 (7)	PIP 5 (6)	PIP 2 (18)
3	MCP 4 (5)	MCP 3 (3)	MCP 4 (6)	DIP 5 (5)	PIP 4 (18)
4	MCP 5 (5)	DIP 2 (3)	PIP 2 (6)	MCP 3 (4)	MCP 3 (17)
5	PIP 2 (5)	MCP 4 (2)	DIP 4 (6)	DIP 2 (4)	PIP 5 (17)
6	PIP 3 (5)	DIP 3 (2)	DIP 5 (6)	PIP 4 (4)	DIP 2 (16)
7	PIP 5 (5)	PIP 3 (2)	MCP 3 (5)	PIP 2 (3)	DIP 4 (16)
8	MCP 2 (4)	PIP 4 (2)	PIP 3 (5)	MCP 2 (2)	MCP 4 (15)
9	DIP 2 (4)	MCP 5 (1)	PIP 5 (5)	MCP 4 (2)	PIP 3 (14)
10	PIP 4 (3)	PIP 5 (1)	DIP 2 (5)	MCP 5 (2)	DIP 5 (12)
11	DIP 4 (3)	DIP 4 (0)	MCP 5 (3)	PIP 3 (2)	MCP 5 (11)
12	DIP 5 (1)	DIP 5 (0)	DIP 3 (0)	DIP 3 (2)	DIP 3 (10)

It can be seen that the majority of erosions occur in the wrist, then in the MCPs, PIPs and DIPs respectively. In the digits, the concentration of erosions is focussed on the second MCP and then radially fans out both across the row of MCPs and the distally along the columns.

The points that have the most numbers of erosions are the scaphoid, trapezium, hook of hamate and lunate; the distal end of the radius; the ulnar styloid; and the bases of the 4^{th} and 5^{th} metacarpals. All of these concur with previous publications on the distribution of erosions early in course of RA both using microfocal radiography (Buckland-Wright and Walker, 1987; Clarke *et al*, 1994) which are mentioned above and standard radiographic techniques (Leak *et al*, 2003). Leak *et al* (2003) found that the radioulnar, radiolunate, scaphoid, styloid process and the heads of the 2^{nd} and 3^{rd} MCPs were all affected early and relatively more in frequency than other joints. Interestingly, they found that the fourth finger was relatively spared irrespective of dominance - not a finding repeated here.

Figure 4.4 Colour-coded distribution of the points affected by erosions in the digits and wrists at baseline (T0)

NON-DOMINANT

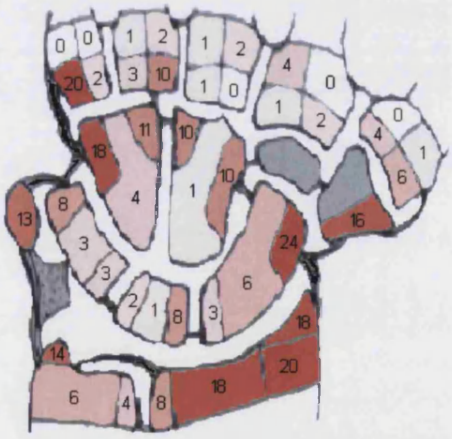

DOMINANT

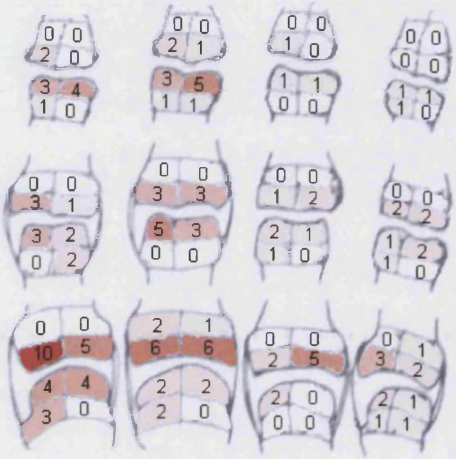

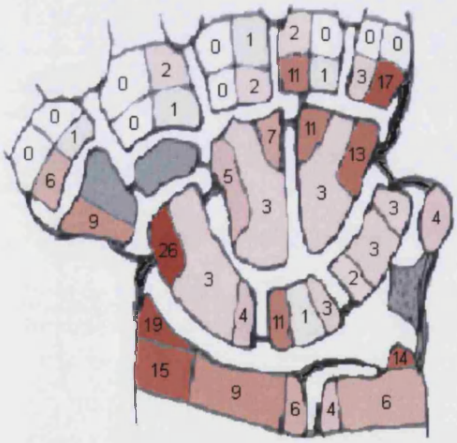

Figure 4.5 Colour-coded distribution of the points affected by new erosions in the digits and wrists at between the time points (T1 - T0)

NON-DOMINANT DOMINANT

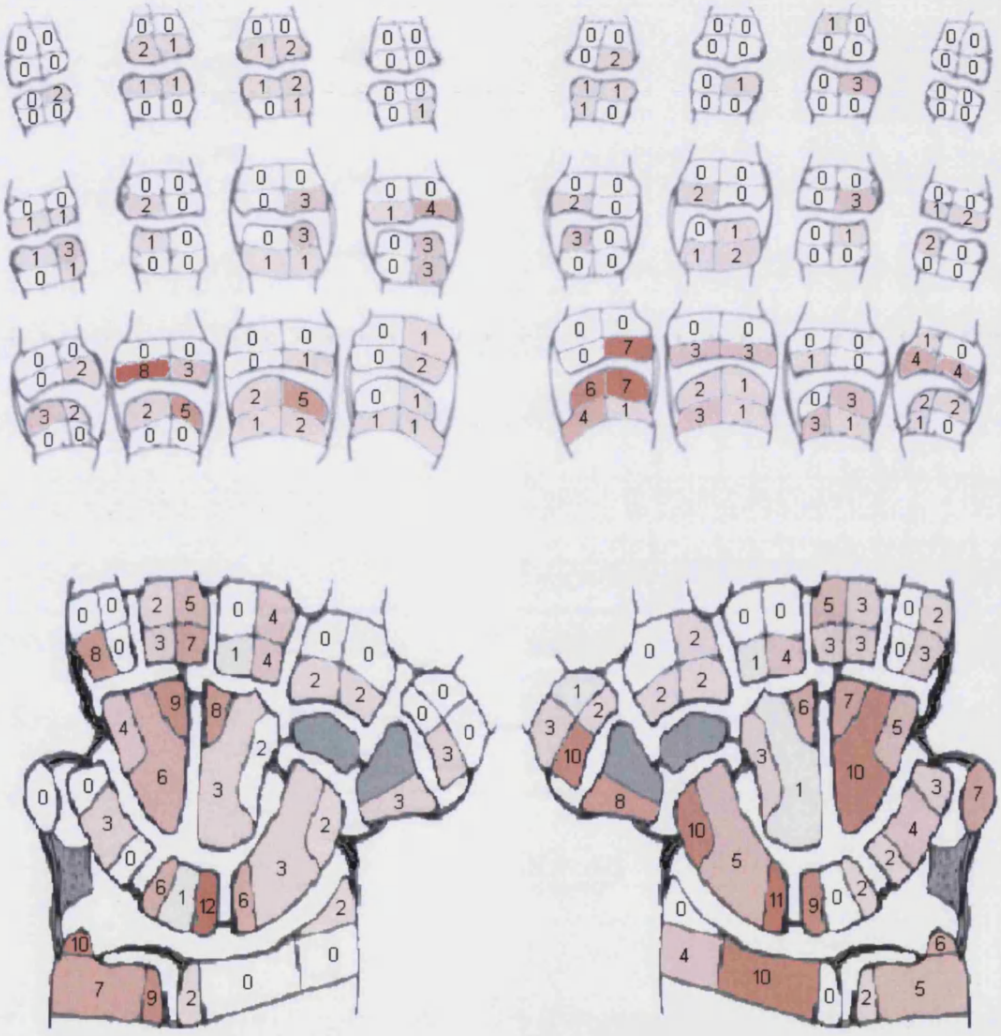

Figure 4.6 Colour-coded distribution of the points affected by erosions in the digits and wrists 17 months later (T1)

NON-DOMINANT DOMINANT

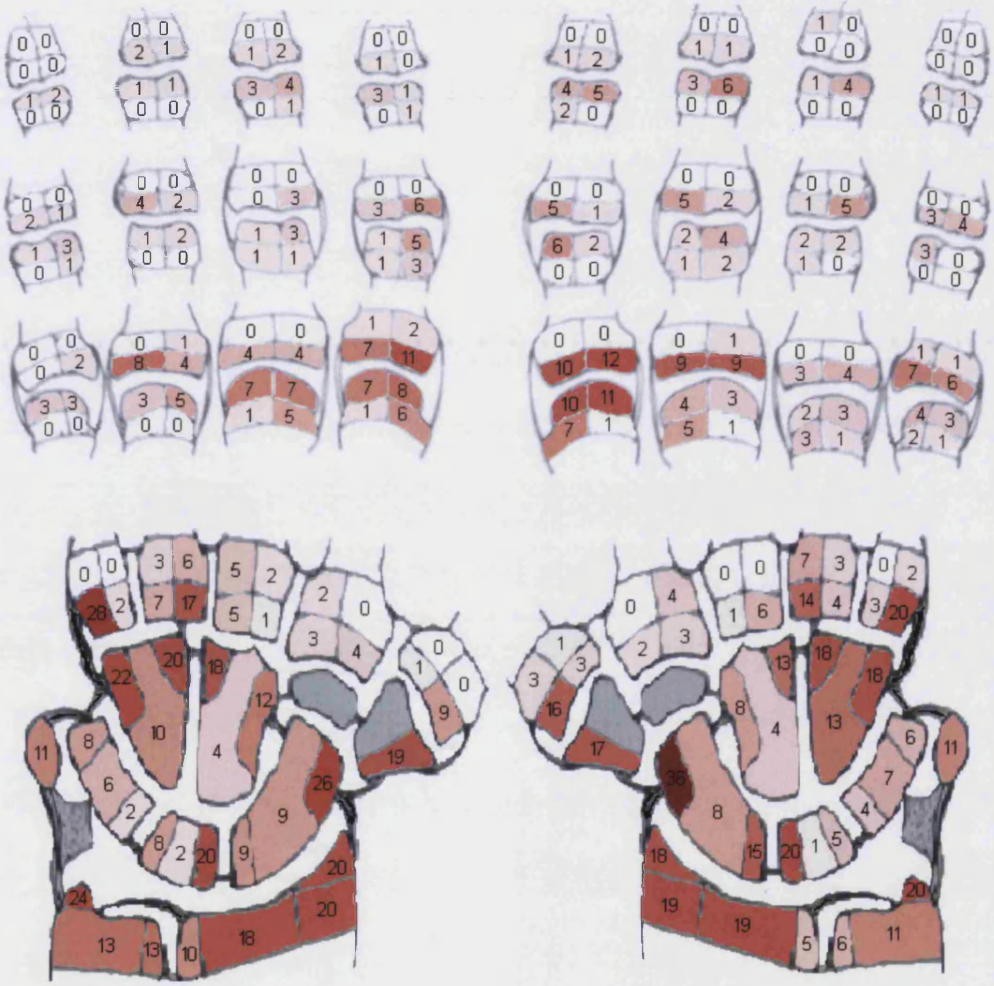

4.5.2 Distribution of erosions at T0

There were no differences between the numbers of erosions on the dominant (369 (6.61%)) and non-dominant (384 (6.79%)) sides. This was less than the smallest detectable change (30 erosions).

With respect to the digits, the frequency of erosions per row in decreasing order was MCPs followed by PIPs and then DIPs. The frequency of erosions per digit in decreasing order was 2nd, 3rd, 4th and then 5th. The highest frequency of erosions occurred in the 2nd MCP and the distribution fanned out in a radial form in decreasing order so that the joint with the fewest number of erosions was the 5th DIP.

The erosions have a predilection for the joint surfaces rather than the capsular insertion. This was highly significant when tested with a Chi-squared test ($p<0.001$). The erosions predominate on the radial side of the 2nd and 3rd MCP where they occur around the capsular insertion. This however was not significant when tested. There was a suggestion that the erosions in the DIPs occurred on the distal portion of the joint surface; the erosions of the PIPs were equally distributed; and the erosions in the MCPs occurred on the proximal side of the joint surface.

With respect to the wrist, there was a greater prevalence of erosions in these bones than in the digits. The erosions occurred in regions with large supporting ligaments attached. They occurred in high numbers on both the radial side of the carpus (trapezium; scaphoid and radial head) and the ulnar side (base of 4th and 5th metacarpals; hook of hamate; and ulnar styloid). These findings were very similar to those of Buckland-Wright's (1984) who noted that the erosions in RA occurred around the ligamentous insertions.

4.5.3 Distribution of new erosions in the intervening 17 months (T1-T0)

There were again equal numbers of new erosions occurring on the dominant (355 (6.29%)) and the non-dominant sides (335 (5.93%)). This was again less than the smallest detectable change.

In the digits, the distribution was identical to that seen at baseline, namely centred around the 2nd MCP and fanning out. There was a slight preponderance of erosions

towards the dominant side at this point, although this was non-significant on a Chi-squared test.

In the wrist the distribution was again reflected from the baseline image with both the radial and ulnar sides equally affected and the erosions predominated in those areas with ligamentous insertions. There was a preponderance of erosions towards the non-dominant side, again non-significant. Overall there was no difference in the number of new erosions in the hands and wrists between the sides.

4.5.4 Distribution of erosions at T1

The total number of erosions on the dominant side was 607 (10.7%). The total number of erosions on the non-dominant side was 592 (10.5%). This was again less than the smallest detectable difference. It should be noted that the total seen at T1 did not represent the sum of erosions seen at T0 and new erosions. This was because there was some healing of erosions seen in this cohort (Buckland-Wright *et al*, 1993) and there was a degree error in the observation process.

The picture seen at T0 was accentuated with replicable findings. At T1 however the Chi-squared test reached significance for both the radial distribution of erosions in the capsular regions of the 2nd and 3rd MCPs ($p<0.05$) as well as the proximal prevalence of erosions in the DIPs ($p<0.05$).

4.5.5 Summary of the erosion distribution

The distribution of erosions found in this study was in agreement with other descriptions of the erosion development in patients with early rheumatoid arthritis, namely that both radial and ulnar sides of the wrist were involved and that the MCPs and the radial columns were more affected than the DIPs and ulnar columns in the digits.

Certain points within these areas, mainly in the wrists, were much more likely to develop an erosion than any other. Understanding why certain areas were predisposed to developing erosions may help in understanding the pathophysiology of rheumatoid arthritis (see section 4.8.1).

At neither time point was there a difference in the total number of erosions between the non-dominant and dominant sides. This was also true in the distribution of new erosions between the two time points.

4.6.1 Results of the symmetry analysis

Two different levels of analysis were performed on the database: 'point-to-point' (142 points per side) and 'joint-to-joint' (22 joints per side). Baseline values (T0) reflected an average of 6 months from the start of the patient's symptoms and the follow-up film to assess progression (T1) was taken 17 months later.

4.6.2 Point-to-point analysis

There were a maximum of 5964 available points on Non-Dominant (ND) side and 5964 available points on Dominant (D) side. The number of excluded points for each side at each time point were 305 (ND, T0), 380 (D, T0), 288 (ND, T1), and 282 (D, T1). Points were excluded if they could not be assessed because of either overlapping bone or had not been imaged.

Table 4.5 The total number of points available for analysis

	MAX	ND T0	D T0	ND T1	D T1
	5964	5659	5584	5674	5682
DIPs	1344	1312	1289	1316	1306
PIPs	1344	1288	1281	1301	1303
MCPs	1344	1298	1287	1312	1317
Wrist	1932	1761	1727	1745	1756

Table 4.6 Total number of points available for the symmetry analysis

	MAX	T0	T1
	5964	5450	5510
DIPs	1344	1272	1282
PIPs	1344	1255	1272
MCPs	1344	1264	1297
Wrist	1932	1659	1659

4.6.3 Point-to-point symmetry at baseline (T0)

If one point has an erosion at T0, what were the odds of an erosion occurring in exactly the same point on the other side compared to any other contralateral point?

At baseline there were	384 / 5659 erosions on the ND side	(6.79%)
And	369 / 5584 erosions on the D side	(6.61%)
Of which	150 were bilateral	

Odds ratio = **6.1** ** (95%CI: 5.1 – 7.1)

Therefore the number of symmetrical erosions was 6 times greater than by chance.

Table 4.7 Regional subgroup analysis for point-to-point analysis at T0

	ND side (%)	D side (%)	Bilateral (%)	Odds Ratio(CI)
Wrist	290/1761(16.5)	233/1727 (13.5)	122 (10.7)	**3.3** (2.2-4.5)**
MCP	63/1288 (4.9)	67/1287 (5.2)	21 (4.6)	**6.5** (3.7-9.4)**
PIP	20/1298 (1.5)	40/1281 (3.1)	3 (1.7)	**5.0** (-0.8-10.8)
DIP	11/1312 (0.8)	29/1289 (2.3)	4 (2.0)	**16.7** (0.0-33.3)

** $p<0.01$

The symmetry of the erosions was therefore not a mathematical quirk and was present at baseline. It appeared to be more accentuated distally, although the PIP and DIP odds ratios did not reach significance. Therefore, as the prevalence of erosions diminished, the chance of symmetry increased.

4.6.4 Potential confounding variables in the point-to-point analysis

The above calculations were based on the assumptions that the erosions were distributed equally between the 142 points on each side and that each individual was equally likely to develop an erosion. As described above, the erosions have a predilection for particular points, especially around the wrist. This predilection distorts the assumption that erosions were randomly scattered. Furthermore, different individuals have different numbers of erosions. Correction factors for both of these assumptions are now detailed. After using these correction factors, it can still be seen that the observed symmetry was significantly higher than expected.

Firstly, the symmetry for each of the 142 points was calculated separately, based on the number of erosions that were present at that point. The expected numbers of symmetrical erosions were then summed for each point. When this was done, the corrected number of expected bilaterally symmetrical erosions rose from 25 to 70.1, and the new odds ratio reduced to 2.1 (1.7-2.5 95% CI). This was still highly significant on the Z test ($p<0.01$).

Secondly, the expected number of symmetrical points per individual patient was calculated in a similar fashion and summed. When this was done, the expected number of total erosions rose from 70.1 to 109.8. This individual influence on the expected erosions was less important than the anatomical preference of the erosions (1.6 versus 2.8 times the expected rate respectively).

This revised expected number of 109.8 erosions was still significantly short of the 150 observed with an odds ratio of 1.4 (1.1 – 1.6 95% CI). Although it can be seen that most of the observed symmetry was accounted for by the anatomical predisposition and the differential expression of erosions between individuals, there was still a significant influence on the expression of symmetry that was unaccounted

for. This is discussed further in section 4.7.1 when a symmetry score is calculated for each individual patient and compared to the total number of erosions (Figure 4.7).

These findings were reproduced at the T1 time interval and the details have not been listed here.

4.6.5 Point-to-point symmetry over the intervening 17 months (T1-T0)

If one point has an erosion unilaterally at T0 what were the odds of an erosion occurring in exactly the same point on the other side 17 months later compared to any other contralateral point?

145 erosions that were previously unilateral at T0 became bilateral at T1. Of these 145, 57 erosions developed on the ND side following a unilateral erosion on the D side at T0; whereas 88 erosions developed on the D side following a unilateral erosion on the ND side at T0. Furthermore, 85 *de novo* erosions occurred bilaterally. Overall at T1, there were 335 erosions new to the ND side and 355 erosions new to the D side

New symmetrical erosions occurred at	142 / 335 on ND side	(42.4%)
And	173 / 355 on D side	(48.7%)

The number of available points for an erosion occurring on ND side to be opposite an erosion on the D side was 219 / 5292 = 4.14%

OR = **10.2** ** (8.6 – 11.9)

Therefore a non-eroded point on the ND side was 10 times more likely to develop an erosion at T1 if it was opposite an erosion at T0 than if it was not opposite an erosion.

The number of available points for an erosion occurring on the D side to be opposite an erosion on the ND side was 234 / 5313 = 4.40%

OR = **11.1** ** (9.41 – 12.72)

Therefore a non-eroded point on the D side was 11 times more likely to develop an erosion at T1 if it was opposite an erosion at T0 than if it was not opposite an erosion.

Table 4.8 Regional subgroup analysis expressed as odds ratios for the point-to-point analysis for the intervening 17 months between T0 and T1

	ND side (OR, CI)		D side (OR, CI)	
Wrist	**6.8**	(5.6-8.1)**	**5.6**	(4.7-6.6)**
MCP	**8.5**	(4.4-12.7)**	**5.4**	(6.1-14.3)**
PIP	**10.9**	(4.0-17.7)**	**23.1**	(7.7-50.9)**
DIP	**15.0**	(2.8-27.2)*	**70.0**	(17.2-122.8)**

*p<0.05

**p<0.01

There was more symmetry expressed distally than proximally. As the frequency of the erosions decreased they were more likely to display symmetry.

4.6.6 Joint-to-joint analysis

There were 924 joints available for analysis on both sides. No joints were excluded from this analysis, although several joints did not have all of their points included.

4.6.7 Joint-to-joint symmetry at baseline

If one joint has an erosion what was the likelihood of another erosion occurring in exactly the same joint on the other side at baseline (T0)?

924 joints

At baseline (T0) there were	219 / 924 erosions on the ND side	(23.7%)
And	219 / 924 erosions on the D side	(23.7%)
Of which	124 bilateral	

Odds ratio = **2.4** ** (95% CI: 2.0-2.8)

Therefore the number of symmetrically eroded joints was 2.4 times greater than by chance.

Table 4.9 Regional subgroup analysis for joint-to-joint analysis at T0

	ND side (%)	D side (%)	Bilateral	OR (95% CI)
Wrist	147/420 (35)	167/420 (39.8)	103	**1.8** (1.5-2.1)**
MCP	33/168 (19.6)	31/168 (18.5)	14	**2.3** (1.1-3.5)*
PIP	21/168 (12.5)	12/168 (7.1)	3	**2.0** (-0.3-9.4)
DIP	18/168 (10.7)	9/168 (5.4)	4	**4.2** (0.0-8.3)

* $p < 0.05$

** $p < 0.01$

There was more symmetry expressed distally than proximally. As the frequency of the erosions in the joints decreased they were more likely to display symmetry.

4.6.8 Progression of erosions in joints over 17 months

If a joint has an erosion unilaterally at T0 what were the odds of an erosion occurring in exactly the same joint on the other side 17 months later compared to any other contralateral joint?

64 erosions that were unilateral at T0 became bilateral at T1. Of these 64, 29 erosions developed on the ND side when there was a unilateral erosion on the D side at T0; whereas 35 erosions developed on the D side when there was a unilateral erosion on the ND side at T0. Furthermore, 48 *de novo* erosions occurred bilaterally.

Overall at T1, there were

136 new erosions on the ND side

145 new erosions on the D side

New symmetrical erosions occurred at 77 / 136 erosions on the ND side (56.6%)

And 83 / 145 erosions on the D side (57.2%)

The number of available points for an erosion occurring on the ND side to be opposite an erosion on the D side was 95/705 = 13.48%

OR = **4.22** ** (3.30-5.10)

Therefore a non-eroded joint on the ND side was 4 times more likely to develop an erosion at T1 if it was opposite an erosion at T0 than if it was not opposite an erosion.

The number of available points where an erosion occurring on the ND side was opposite an erosion on the D side was 95/705 = 13.48%

OR = **4.25** ** (3.15-5.34)

Therefore a non-eroded point on the D side was 4 times more likely to develop an erosion at T1 if it was opposite an erosion at T0 than if it was not opposite an erosion.

** $p<0.01$

Table 4.10 Regional subgroup analysis expressed as odds ratios for the joint-to-joint analysis for expression of symmetry in the intervening 17 months between T0 and T1

	ND side (OR, CI)	D side (OR, CI)
Wrist	**5.6** (4.2-6.9)**	**3.5** (2.5-4.4)**
MCP	**5.1** (2.5-7.6)**	**3.8** (1.8-5.8)**
PIP	**3.9** (1.0-6.7)*	**7.8** (2.5-13.2)**
DIP	**3.3** (0.0-6.6)	**12.8** (1.5-24.1)*

*$p<0.05$

**$p<0.01$

The T0 baseline data can be considered to represent the erosive process over the previous 6 months. The T1 data has been corrected by subtracting the T0 data so that it can be considered to represent the erosive process over the following 17 months. The T1 data has also been analysed to represent the total erosive process over the previous 23 months.

From the T0 data, it can be seen that symmetry exists early in the course of the disease. This symmetry appears to be accentuated distally even though the frequency of the erosions in these regions decreased. However the odds ratios were not significant at this time point. The symmetry was more accentuated at a point-to-point level when compared to the joint-to-joint analysis.

Over the next 17 months, the symmetry was seen to accentuate, again more at the point-to-point level. Perhaps this accentuation does not represent a different rate of symmetry development secondary to an increase in the number of erosions, but was merely reflective of the longer time interval (17 months) of this analysis compared to that of T0 (6 months). Again, the erosive frequency diminished distally and the symmetry was more pronounced distally. This time, this reaches clear significance.

4.7.1 Univariate analysis on a symmetry score

A 'symmetry score' was given for each patient. This was calculated by expressing the ratio of the number of observed symmetrical joints to the number of expected. Symmetry scores ranged from 0 – 57.6 (median 7.5, SD 10.3).

Patient factors (age, sex, handedness, medications, NSAID use, smoking status, alcohol intake) as well as disease status (symptom duration, rheumatoid factor, hours of stiffness, number of joints affected, ESR and Health Assessment Questionnaire (HAQ)) had been recorded at baseline for the purposes of the study. These were coded and then modelled against the dependent variable (symmetry score) using a univariate analysis (SPSS 12.0). Secondary analyses tested for correlations between these variables and the student's t-test was used where appropriate to compare means. The level of significance for this secondary analysis was set as $p<0.01$ because multiple tests were performed.

The symmetry score was seen to correlate negatively with the total number of erosions in an exponential pattern. Figure 4.7 illustrates this using the log of the symmetry score. This result is counterintuitive. It might be expected that the degree of symmetry should rise as the number of erosions increases as there are fewer available sites for non-symmetrical erosions. However it can be seen that an individual who develops a single erosion was more likely to develop a second erosion

in the exact contralateral point than any other area, even the predisposed areas. This suggests that a symmetrical erosion was more likely to develop very early on in the disease process than later.

Figure 4.7 The number of erosions plotted against the log of the symmetry score

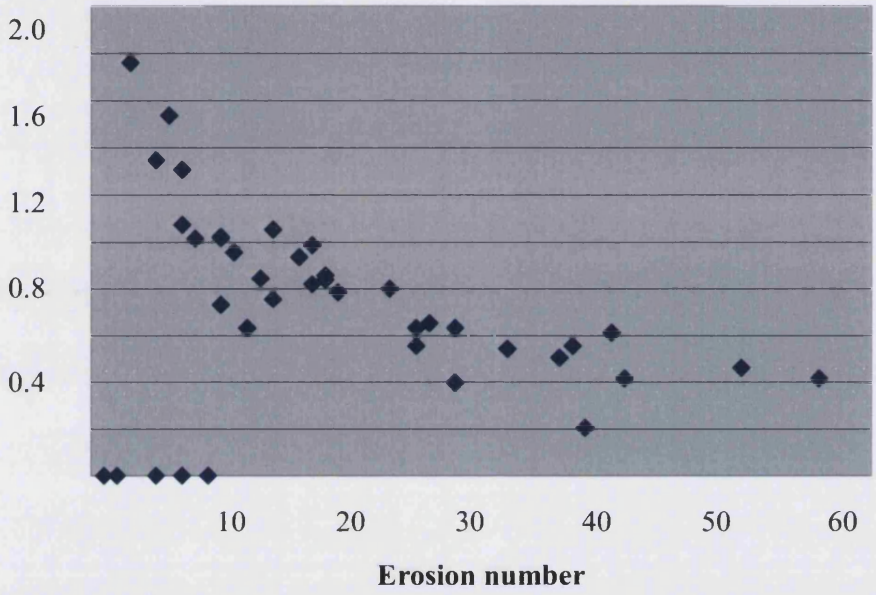

This demonstrates that the fewer the number of erosions that a patient has the more likely it was that these were to be symmetrical. (p=0.018)

To investigate this finding further the distribution of the erosions in those patients with 10 or fewer total erosions (n=17) was analysed. 8 patients in this group had no symmetrical erosions (total of 33 erosions) leaving 9 patients with a total of 13 symmetrical erosions from a total of 66 erosions. The following areas were affected with the associated frequencies in brackets: 6 (3); 44 (3); 8(2); 4, 11, 18, 22 and 26. All of these areas were in the wrist and at high risk of developing an erosion (Table 4.3). Looking at the anatomical distribution of these areas, they appear to be predominantly on the radial side of the wrist (4, 6, 8, 11 and 26) with 44 occurring on the ulnar side and 22 in the middle. It appears that another process occurred when the patient has few erosions to induce a symmetrical pattern.

The symmetry score did not correlate with any of the other patient nor disease factors. The numbers of joints affected predicted the HAQ score in a positive relationship ($p<0.001$), but no other relationships were significant. The lack of positive findings in relation to previously well described factors (e.g. rheumatoid factor and number of erosions) could have been due to the relatively small numbers (n=42) of patients that were analysed in this way.

4.8.1 Discussion of the study methods

This was a single observer retrospective study of 42 patients with the onset of rheumatoid arthritis within the past 6 months at two cross sectional times 17 months apart using the sensitive technique of microfocal radiography to identify erosions. The technique was validated using a blinded observer with moderate to good interobserver values.

The threshold for erosion detection was set high. Positive identification of an erosion in two viewings was required. For example, 'en face' erosions were obviously detectable but difficult to fulfil the above criteria due to any obvious lack of cortical disruption. This reduced sensitivity may have missed erosions and makes it more likely that any expressed symmetry was a reflection of those areas which were most likely to yield a positive erosion reading.

This study could now be repeated prospectively using a larger cohort and perhaps a different technique such as MRI to reduce any systematic mistakes from the detection strategy. Pierre-Jerome *et al* (1997) studied the wrists of 31 females with rheumatoid arthritis using MRI fast field echo sequences. They found that the symmetry of the carpal bone lesions also dissipated over time with patients who had symmetrical lesions having had RA for significantly less time than those patients with asymmetrical lesions (12 versus 6 years). The erosions predominated over the radial force-bearing column of the wrist and they also noted that more lesions occurred on the right. This group of patients however had had the disease for a significant time and very few patients had early disease. Furthermore the symmetrical analysis was cross sectional and did not take into account the evolution of erosions over time.

4.8.2 Discussion of the symmetry analysis

In section 4.6.3 it was seen that the symmetry at baseline was pronounced with an odds ratio of more than 6 ($p<0.01$).

It was then seen (section 4.6.4) that this was mainly accounted for by the predilection for erosions to occur in particular places. This distribution restriction could be seen to account for the higher than expected numbers of symmetrical erosions but only explained about half of the increased odds ratio.

The individual's number of erosions was another confounder, but this again only explained about half of the remaining increased symmetry. There was still a significant level of symmetry ($p<0.01$) seen in the distribution of the erosions that was unaccounted.

Finally (section 4.7.1), this remaining symmetry was seen to be accounted for by an interesting finding. The fewer the number of erosions that an individual had, the more likely those erosions were to be symmetrical. This influence was small because the total number of erosions that patients with a few erosions contribute towards the total number of erosions in the population was small. This effect was significant however and needs to be explained.

The implication is that in the early stages of the disease, the erosions' distribution is more likely to be symmetrical than later on in the disease. This however is counterintuitive to the finding that the erosions become more symmetrical as time progresses. This contraindication can be understood by identifying two processes as being important at different stages of the development of erosions. One process produces symmetry in the erosions (S) whereas the other produces damage in the predisposed areas (P). The 'symmetricising' process (S) is focal, transient and dominant in the early part of the disease although only affects a small number of areas. The damage caused in the predisposed areas by a more general slower process takes time to accumulate but tends to increase symmetry because of the restriction of the number of available predisposed points. It is possible that process S is an artefact of the analysing system but this is unlikely given that it is not one or two patients that

skew the results, but a general trend in the data. Identifying the different processes may enlighten the pathophysiology of rheumatoid arthritis.

The places where these erosions occurred were in exactly the same places as the commonest areas affected. By understanding why these areas were affected, and not others, an important insight into the mechanism may be realised.

4.8.3 Neurogenic hypothesis

A neurogenic hypothesis should have several predictions concerning the distribution of these erosions. Erosions should be seen to occur in areas with a high prevalence of nerves and likewise erosions should not occur in areas of low neuropeptide concentration. Neuropeptide containing nerves within joints were mainly concentrated in perivascular locations or as free nerve endings (section 3.2.1). The blood supply from the joint is derived mainly from a rich network of pericapsular arterioles feeding into finer capillary networks. The anatomical subdivision of the hand and wrist templates did not take these into account and little insight can be gained from this.

However, another area of high neuropeptide concentration occurs in the ligamentous insertions into the bone, otherwise known as the enthesis (Benjamin and McGonagle, 2001). It can be seen that the areas of highest concentrations of erosions were around the entheses of the wrists. It is attractive to consider that the neurogenic mechanism may be mediating the high expression of symmetry seen in these areas. Perhaps the neurogenic mechanism represents process S described above?

The erosions occurred on the bare areas immediately adjacent to the perimeter of the cartilage (see Image 4.1, Figures 4.4-6). In the knee, this area too has a rich blood supply with associated neuropeptide containing nerves (Mine *et al*, 2000), although this has not been studied in the finger joints.

The distribution of the erosions seen in this study supports a neurogenic hypothesis and suggests that further investigation into contralateral changes following unilateral inflammatory stimulus is warranted.

Image 4.1 The erosions occurred in the bare areas adjacent to the cartilaginous perimeter. Evidence from a DIP joint

4.8.4 Anatomical and biomechanical hypotheses

The biomechanical forces applied through the whole hand are very complicated and vary depending on the hand's position and the force applied to the extent that whole hand models have not yet been developed. However, individual joint kinetics and relative ligament influence on force dissipation and joint stabilisation is well developed and instructive for the hand surgeon's clinical management and pathological understanding.

Biomechanical forces have been best studied in osteoarthritis. The distribution of osteoarthritis with its bias for the PIPs, DIPs and carpotrapezium joint (1st carpometacarpal) with a sparing of the MCPs is very different to that of rheumatoid arthritis. This in itself might suggest that the role of biomechanical forces in the development of the pattern of erosions in rheumatoid arthritis is small.

There is evidence from both the literature and this study to suggest that load bearing is important. In the rheumatoid patient this load bearing wrist shifts more to the ulnar side whereas normal load bearing occurs through the radial columns in the wrist (Manal *et al*, 2002). There is support for this switch from radial to ulnar sides from this study by looking at the relative number of new erosions between T0 and T1 when compared to baseline. It can be seen that the new erosions occurred preferentially on

the ulnar side whereas the development of new erosions on the radial side is greatly decreased when compared to baseline distributions. The fan distribution of the erosions could fit with force vectors applied to the hand being channelled through the radial side. The development of proportionally more erosions in the ulnar MCPs over the following 17 months when compared to the first 6 months might also reflect this change in biomechanical loading emphasis. Perhaps the biomechanical hypothesis may contribute to process P described above?

The full expression of the pattern described (distal PIP and proximal MCP involvement) is not explained however, and the experience from OA would suggest that the hand is particular well designed to avoid undue load being expressed at the MCP.

The anatomical part of this hypothesis suggests that there are intrinsic anatomical abnormalities that predispose areas to an erosions. This might include a 'bear' area denuded from cartilage that exposes underlying bone to an erosion. Or it might include an area of very thin cortex, such as those that might occur next to entheses. There are, however, many entheses in the carpus, only some of which have been highlighted in the above schema.

4.9.1 Conclusion

It can be seen that the distribution of erosions in patients with early RA is symmetrical. It can also be seen that the odds ratio for this symmetry increases over time. Most of this symmetry is accounted for by two mathematical confounders: the number of erosions affecting a predisposed site, and the number of erosions an individual develops. However the remaining amount of symmetry appears to be related to a process that occurs when a patient has very few erosions. It is unclear whether this process is an accentuated predisposition of particular sites to anatomical and biomechanical factors, or a separate process that could be neurogenic in nature.

Chapter 5. Establishing the experimental model to investigate skin blood flow responses to an active immunisation

Summary

An experiment to investigate putative contralateral responses should have an appropriate stimulus; a sufficiently sensitive detection strategy and be adequately controlled. This chapter outlines the approach used to satisfy these conditions. Pilot studies are then summarised to demonstrate the reliability of the techniques selected and the development of the experimental protocol.

5.1.1 Stimulus properties

The stimulus should be local and not induce significant systemic changes that might confound any results. Adequate controls are therefore paramount. The stimulus should generate a significant response to maximise any contralateral changes. From the review of the literature, the stimulus should be either sustained over time or of sufficient magnitude in order to overcome the threshold effect and generate a contralateral response (Shenker *et al*, 2003; see Chapter 2). The stimulus should also be acceptable to sufficient numbers of subjects to allow the adequate powering of the experiment.

5.1.2 The stimulus: An active immunisation

An active immunisation was selected to be the stimulus of choice for the following reasons.

Symmetrical diseases tend to be of the Immune-Mediated Inflammatory Disease (IMID) classification. An active immunisation has persistent local inflammatory reactions (see below) as well as obvious immune stimulating actions. The combination of these is attractive when looking for a stimulus as the temporal persistence may overcome any threshold effect. Active immunisations are both common and well-tolerated in all populations and this is liable to improve recruitment.

Active immunisations that were considered for the purposes of the investigation were mumps-measles-rubella (MMR), influenza (inactivated virus), typhoid (Vi capsular polysaccharide) and hepatitis B (hepatitis B surface antigen). These immunisations were selected on the basis of their common use.

For a list of other possible local stimuli that have been used in publications involving human volunteers and reasons why these were not considered, please see Table 5.1.

Table 5.1 Excluded insults for generating a contralateral response

Stimulus	*Reason for exclusion*	*Reference*
Chemical		
Cantharadin	Inflammatory-only response	Day *et al*, 2001
Topical capsaicin	Mild and transient stimulus	Mohammadian *et al*, 1998
Histamine dihydrochloride	Mild and transient stimulus	Skaare *et al*, 1997
Platelet activating factor	Mild and transient stimulus	Turner *et al*, 2000
Methalcholine	Mild and transient stimulus	Borum *et al*, 1998
Purified Protein Derivative	Poor anticipated recruitment	Pitzalis *et al*, 1996
Physical		
Thermal burns	Specialised equipment required Poor anticipated recruitment	Pedersen *et al*, 2000
Suction-induced blisters	Difficult to standardise Poor anticipated recruitment	Pitzalis *et al*, 1996

5.1.3 Literature review of local and systemic responses following an MMR, influenza, typhoid or hepatitis B immunisation

For the purposes of the experimental model, it is desirable for the active immunisation to have a persisting local inflammatory response with a minimal systemic response. Prominent systemic (circulatory) effects would confound any topographically-precise contralateral response (neurological). A brief literature review was therefore conducted.

To summarise the results, self-reported local reactions are prevalent in a significant proportion of patients (20-30%) who had been given one of these active immunisations. In a minority of subjects (1-10%) there is some systemic activation, although this is seen to subside using laboratory measures within 24 hours in the majority of cases.

Controlling for this confounding systemic response is important and can be achieved by taking a control region that is not topographically related to the immunisation and to perform the experiment at least 24 hours following the immunisation.

Influenza

Wongsurakiat *et al* (2004) studied local and systemic effects of a split-virion attenuated influenza immunisation in 62 patients with chronic obstructive airways diseases compared with a placebo injection (63 patients). Local reactions occurred more in the influenza group (27% versus 6%) but there were no differences in systemic reactions (76% versus 81%) suggesting no significant systemic effects were occurring. A similar study was performed in Liverpool in healthy subjects aged between 65-74 years old by Allsup *et al* (2001). They also found an increased reporting of local symptoms when compared with placebo injection (11% vs. 5%) with no evidence of a systemic effect (35% vs. 42%). Less than 1% of 2150 Italian subjects immunised with either an inactivated influenza virus or subunit vaccine self-reported a temperature more than 37.5 °C in the following 3 days (Squarcione *et al*, 2003).

Typhoid

Using lab measures, typhoid (Vi capsular polysaccharide) immunisation induced a rise at 8 hours in the serum levels of tumour necrosis factor-α, interleukin-6 and interleukin-1 receptor antagonist. There was also a reduction in the endothelial responses to bradykinin with no effect on the response to glyceryl trinitrate and norepinephrine. Endothelial reactivity to sublingual nitroglycerin or 5-minutes of occlusion as measured by plethysmography and conduit vessel response using high-resolution ultrasound was altered 8 hours post-immunisation. This dysfunction had normalised by 32 hours post-immunisation (Hingorani *et al*, 2000; Kharbanda *et al*, 2002; Clapp *et al*, 2004). Sabitha *et al* (2004) obtained questionnaires from 153 healthy subjects aged between 12–25 years old who had been given typhoid Vi capsular polysaccharide immunisation. 29 (19%) reported local skin reactions of pain, redness or swelling and 5 (3%) reported symptoms of fever, headache or chills. Panchanathan (2001) obtained questionnaires from 125 Malaysian Air Force recruits who had also been immunised with a typhoid Vi polysaccharide. 28% reported local symptoms such as pain, erythema and induration and 1% self-reported systemic symptoms

Hepatitis B

Clarke *et al* (1989) studied 92 medical students following repeated intradermal Heptavax B (plasma-isolated hepatitis B surface antigen). They documented that more than 85% of subjects reported symptoms of pain, erythema or induration at 6 months following 3 immunisations. No systemic symptoms were reported. They also took skin biopsies from the injection site two months after immunisation. These skin biopsies (n=7) demonstrated a superficial and deep perivascular lympho-plasma-histiocytic inflitrations with a preponderance of T-cells over B-cells.

MMR

Gotherfors *et al* (2001) reported an incidence of between 20-30% of local skin reactions following a second MMR injection given to a population of healthy 12 year olds.

5.2.1 Detection strategy properties

The contralateral responses that have been reported in the literature are small and transient (see chapter 2). The detection system should therefore be of sufficient sensitivity to identify very small changes. The timing of the experiment is also paramount in order to maximise the contralateral response. The detection strategy should be feasible in the available setting and acceptable to sufficient numbers of subjects to allow the adequate powering of the experiment.

5.2.2 The detection strategy: a non-invasive scanning laser Doppler Imager to study microvascular skin blood flow

The velocities of moving particles can be determined from the resultant frequency shift of reflected light following its contact with a moving object according to the Doppler principle. Blood flow can therefore be semi-quantified by extrapolating from the frequency shift detected when low-power, fixed-wavelength laser light is reflected from moving red blood cells. Laser Doppler measurements are specific to the blood flow in the skin and not influenced by underlying muscle blood flow because the laser light does not penetrate more than a few millimetres (Wardell, 1993; Grossman *et al*, 1995).

Fixed laser Doppler flowmeters (LDF) have been in use for several years using these principles. However, the localised nature of the perfusion signal coupled with the gross anatomical variability of the microvasculature prohibits its use in meaningful comparisons of absolute blood perfusion measurements across different individuals. This caveat also applies when comparing readings from different sites within the same individual. LDF therefore is strictly site-specific and should be limited to monitoring dynamic responses to physiological stimuli at a single site (Grossman *et al*, 1995).

The recent development of scanning laser Doppler imaging (LDI) devices obviates some of these problems. LDI reduces the variability of single-point measurements caused by the skin's natural heterogeneity in blood vessel density. It gives an average skin blood flux for an area that can be compared more accurately over time, or across different regions, than LDF (Stucker *et al*, 1995; Morris and Shore, 1996).

Measurements obtained by laser Doppler are intrinsically of a relative nature because the factor of proportionality will be different for different tissues so an absolute, quantitative index of perfusion (e.g. number of blood cells moving through 1 g of tissue per second) can not be derived using LDF or LDI. 'Absolute' values can be derived however if the experimental conditions are carefully controlled and LDI has been successfully used experimentally to assess vascular skin responses over two experimental times and between two separate sites (Clough *et al*, 2001; Ramsay *et al*, 2003).

5.2.3 The use of capsaicin-induced vascular responses as a surrogate for neuropeptide availability

The sensitivity of any detection method can be hugely improved by using a surrogate marker. Capsaicin (8-methyl-N-vanillyl-6-noneamide) has been used as a tool for assessing neuropeptide availability, an important system in the regulation of skin blood flow. Many of the published contralateral responses in animals are directly related to or downstream from neuropeptide discharge (see Chapter 3). This would therefore be a highly relevant system to investigate as neuropeptides have properties that are functionally and anatomically appropriate to mediate contralateral responses. Furthermore, topical capsaicin is safe and in regular clinical and experimental use.

Capsaicin has separate outcomes on both the nervous and the vascular systems. In the nervous system an area of primary sensitisation is generated from the actions on the peripheral nerves. Central sensitisation occurs in the spinal cord to generate a larger area of secondary hyperalgesia surrounding the area of primary hyperalgesia (LaMotte *et al*, 1992).

Capsaicin opens the non-selective cation channel TRPV1 receptor (transient receptor potential channel vanilloid receptor 1), located on fine sensory afferent nerve fibres, to allow an influx of calcium and effect the release of substance P (SP) and calcitonin gene-related peptide (CGRP) from dense-core vesicles through an exocytotic mechanism (Merighi *et al*, 1988; Bevan and Szolcsanyi, 1990; Oh *et al*, 1996; Caterina *et al*, 1997). These neuropeptides then act as vasodilators through both endothelial-dependent and endothelial-independent mechanisms (Brizzolara

and Burnstock 1991; Lippe and Holzer, 1992). Skin blood flow responses to the application of capsaicin have therefore been used as an indirect measure of neuropeptide release.

Several techniques have been used for evaluating the skin blood flow responses to topical capsaicin. These usually include mapping out the area of flare (planimetry); colorimetry; and fixed laser Doppler flowmetry (LDF) (Helme and McKernan 1985; Jolliffe *et al*, 1995; Morris *et al*, 1995; Fang *et al*, 1997; Harding *et al*, 2001). A lack of sensitivity is seen when comparing planimetry to LDI or colorimetry (Stucker *et al,* 1995 & 1996). As mentioned above, comparably sensitive techniques such, as colorimetry and LDF, are not as reproducible as LDI (Stucker *et al*, 1995).

5.3.1 Controlling for confounding variables

Skin blood flow and vascular reactivity is dependent upon several variables. These include the region of the body that is to be studied, age, vasoactive medications, room temperature, skin temperature, posture and the time within the menstrual cycle (Charkoudian 2003). An experimental protocol should take into account these factors.

Pilot studies were undertaken to assess the variability of skin blood flow in the same region on two separate occasions. For females, the second scan was timed to be approximately at the same point within the menstrual cycle as the first. Each subject was acclimatised in a temperature-controlled room (25-27°C) for 30 minutes. This was deliberately warm to encourage a slight vasodilatation. Subjects were advised to avoid caffeine, nicotine and alcohol on the day of the study and excluded if any vasoactive medication had changed between visits. A colour thermographic camera (ThermoVision, Flir Systems, Sweden) monitored the skin temperature, and a digital thermometer (Digitron Instrumentation Ltd, Model 2751-K) monitored the room temperature. Adjustments to the temperature control were made throughout the protocol to ensure that the room temperature remained within 1°C of the starting temperature.

5.3.2 The protocol

Four regions of interest (ROI) were identified, two on each arm. These were carefully marked and recorded on the first visit so that they could be used again on the second visit. The ROI were the outer upper and ulnar lower regions on each arm. The upper ROI was approximately 15cm along a line measured from the mid-acromion point in the shoulder to the lateral epicondyle in the elbow. The lower ROI was approximately 12cm along a line measured from the lateral epicondyle in the elbow to the ulnar styloid in the wrist. Each ROI was identified to a digital camera in the LDI by using a hollow plastic circular template and a semi-permanent marker pen to circumscribe a 2.8cm^2 region. The mark used to identify the ROI was the centre of this circle.

The LDI (LDI-2, Moor Instruments Ltd, Devon, UK) was used approximately perpendicular to the skin surface at a distance of 75cm using a flux gain value of 2; scan speed of 4 pixels/ms; and a bandwidth of 250Hz – 15kHz. Scanning time was approximately 3 minutes. All four ROI were scanned simultaneously. The calibrating procedure for the LDI was conducted at monthly intervals using the manufacturer's standard and in-built software.

The LDI was used to obtain two baseline images before the topical capsaicin cream (0.075%, Axsain) was applied using the hollow template to define the contact surface area as outlined above. The cream was left on the skin for 30 minutes. The cream was completely removed with a soft tissue and care was taken to avoid a mechanically-induced flare reaction. Seven further LDI scans were then obtained over the next 21 minutes.

5.4.1 Data analysis

In addition to using the peak skin blood flow, the vasodilatory response expressed by LDI values has been corrected by different methods in the literature. Values for a pre-defined region of interest such as that used in this protocol can be expressed using the area under the curve (AUC) (Ramsay *et al*, 2003) or corrected for the baseline by either division (Newton *et al*, 2001) or subtraction (Zhelev and Bakalova, 2002). The total area of vasodilation can also be calculated (Clough *et al*, 2001).

The pilot study assessed all five of these methods. ROI were identified from the pre-drawn felt-tip pen mark on a digital camera image that had been simultaneously acquired during the flux scan. This free-drawn ROI was automatically copied onto the flux image and the average flux for that ROI calculated using the accompanying software (Moor Instruments Ltd, Version 3.11).

The five separate analyses outlined above were carried out on the same data (in addition to using the peak values) in order to establish which method would be the most reproducible for this protocol. Three analyses focussed on the increase in skin blood flow within the ROI defined by the template and the fourth analysis concerned the total area of the flare. The four methods of correcting the peak skin blood flow were:

1 Uncorrected peak flux values (in PU).
2 Subtracting the baseline blood flux from the peak flux (in PU) (Zhelev and Bakalova, 2002).
3 Expressing the peak flux as a ratio to baseline (Newton *et al*, 2001).
4 Calculating the AUC (in PU, without subtracting baseline) (Ramsay *et al*, 2003).
5 Total area (baseline areas subtracted from average of maximum 2 areas) (Clough *et al*, 2001). To identify the total area of flare a threshold value of 150 perfusion units was set and the number of pixels with values above this counted using the software.

Biological zero

The biological zero (the laser Doppler signal when arterial flow is arrested) was not measured as this was assumed to be constant at a given location in a given individual over time. Other groups have not measured the biological zero because their experience was that it makes only a small contribution to the total signal and does not change significantly under different conditions (Morris and Shore, 1996; Newton *et al*, 2001). Furthermore, subtracting the biological zero from flux readings leads to an underestimation of the net flux (Zhong *et al*, 1998).

5.4.2 Study aims

For the purposes of the initial pilot study, the primary aim of the study was to assess the reproducibility of the increase in skin blood flow following topical capsaicin over the two separate experiments using the five different methods. Reproducibility was expressed in terms of the coefficient of variation. Secondary outcome measures were to correlate the effects of skin temperature, room temperature, age, region, baseline blood flow and inter-subject variability on the response to capsaicin. This analysis was performed using univariate modelling. This fully factorial balanced, type III model had no *a priori* contrasts and a Tukey's post-hoc test was used. All analyses were performed using SPSS 12.0.

5.4.3 Reproducibility of LDI measurements

The reproducibility of the data collection was performed by using an observer who was blinded to the original data and also independent of the study. The independent observer followed the protocol for identifying the ROI from the digital camera image as outlined above and the results are displayed in Figure 5.1. 343 regions were analysed with the mean difference being 2.9 PU (SD 10.2 PU). This analysis therefore introduced only a small amount of variation into the data.

Figure 5.1 Bland-Altman plot of interobserver differences (PU) from free drawing around digital camera image of region of interest (ROI)

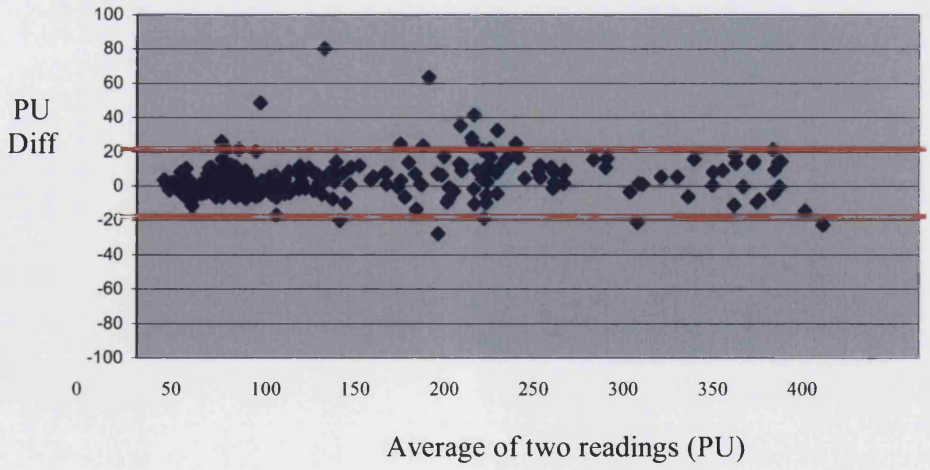

The red lines indicate 95% confidence intervals.

5.4.4 Testing the adequacy of the acclimatisation time

A period of acclimatisation is needed to give a steady state of skin blood flow. To determine whether 30 minutes was adequate, 14 subjects who had undergone pilot studies had regions identified that were not involved in the study. These were monitored over the course of the experiment and the data are summarised in Figure 5.2. Skin blood flow is seen to vary very little after 60 minutes of acclimatisation. The difference between this steady state and skin blood flow after 30 minutes was seen to be between 2-4 PU (SEM 2). 30 minutes therefore was thought to be adequate.

Figure 5.2 The role of acclimatisation in skin blood flow variability (n=14) showing mean flux at baseline and for 30 minutes following the removal of capsaicin in control regions distant to the capsaicin application

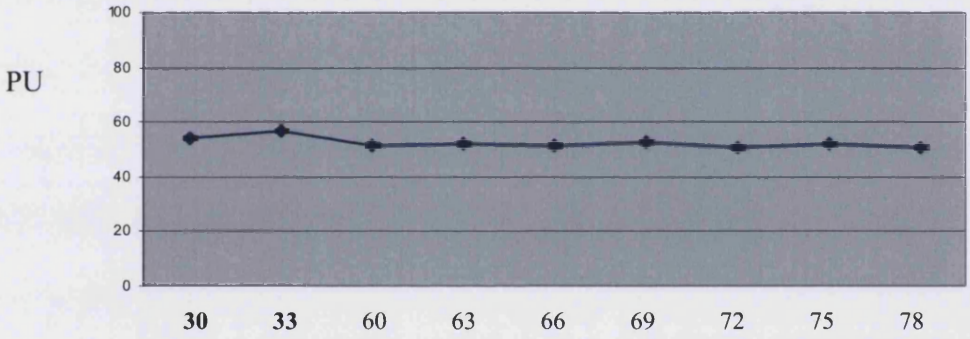

Time (minutes).
Note: non-linear scale

5.5.1 Measuring increases in skin blood flow in response to topical capsaicin in 14 healthy subjects on two separate occasions

14 subjects were recruited (7 males; mean age 41 (21-72) yrs). All were healthy and taking no medication. Two subjects smoked. Informed, written consent was obtained from every subject. The Local Research and Ethics Committee approved this study (BA172). One subject was excluded because of a skin flare reaction to mechanical abrasion prior to the experiment that had not subsided by the time of recording. Each subject had four ROI. Therefore, 52 separate areas were analysed.

Table 5.2 summarises these results and displays the mean coefficients of variation. The analytical methods with the best reproducibility over time were the AUC and subtraction of the baseline. The methods with the worst reproducibility were the the uncorrected data and the area of flare. The coefficients of variation ranged from 27.8-49.4%.

Table 5.2 Coefficients of variation of increased skin blood flow in response to topical capsaicin over time and according to the analytical method

Method	Time 1 Mean (SD)	Time 2 Mean (SD)	Coefficient of Variation
Uncorrected	197.0 (155.2)	193.2 (149.5)	49.4%
Subtraction	270.4 (121.0)	275.6 (104.2)	29.8%
Ratio	5.9 (3.0)	6.4 (3.3)	37.6%
AUC	2390.9 (1143.8)	2918.2 (1392.0)	27.8%
Total Area	400.8 (185.1)	474.7 (216.4)	43.8%

5.5.2 Baseline skin blood flow measurement over time in the control group

In the control group the skin blood flow at baseline was seen to vary by an average mean of 1.5 PU (2.9%), (SD 14.5 PU, SEM 3.9 PU), over two measurements. There were no significant differences in skin blood flow over time in any of the regions (Wilcoxon signed-rank test), nor any differences over time between the regions (ANOVA).

5.5.3 Secondary analysis in the control group

Univariate modelling showed that the increase in skin blood flow following capsaicin administration was significantly correlated with age (Figure 5.3). This increase in skin blood flow was not related to skin temperature, room temperature, region, subject, baseline skin blood flow, or time of the experiment.

In addition, there was no relationship between either the skin or room temperature and skin blood flow (Table 5.3). As expected skin temperature was significantly

correlated with room temperature (p=0.021) although r^2=0.05 meaning that this was a weak relationship at the studied temperatures. There were no significant inter-regional differences between the skin temperatures.

Figure 5.3 Secondary analysis: Increase in skin blood flow following topical capsaicin is correlated negatively with age

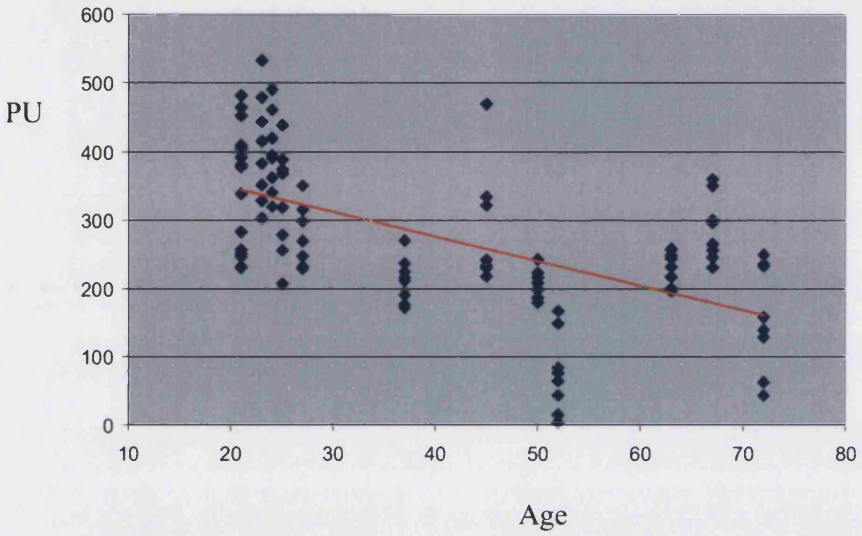

Each subject has 8 readings
Highly significant correlation with age (P<0.01)

Table 5.3 Baseline skin and room temperatures as measured by quantitative colour thermography for all ROI of each subject on the two separate occasions

	RT 1	Time 1				RT 2	Time 2			
Area		LU	RU	LL	RL		LU	RU	LL	RL
Mean	25.1	32.1	32.1	32.2	32.6	25.9	32.2	32.1	32.9	33.0
SD	0.3	1.3	1.5	1.4	1.1	0.7	1.4	1.4	1.1	1.0

RT – Room Temperature; LU – Left upper ROI; RU – Right upper ROI; LL – Left lower ROI; RL – Right lower ROI

5.5.4 Delayed responses to capsaicin as a possible confounding factor

It was estimated that 21 minutes of scanning would be adequate to capture the peak skin blood flow response to topical capsaicin based on pilot studies. However, 12 out of 104 regions had the maximal skin blood flow response at the measurement taken at 21 minutes. It was possible therefore that the skin blood flow in these 12 had not peaked and this would confound any reproducibility studies. Taking these regions out of the analysis, 42 regions were left for analysis. No significant differences were seen in the revised coefficients of variation with the range being 25.2-41.4% and the AUC and subtraction data still being the most reproducible.

5.6.1 Differences in skin blood flow in response to capsaicin following immunisation

15 immunised subjects were recruited (6 males; mean age 55 (25-81) yrs). Each subject was studied according to the protocol outline above. Informed, written consent was obtained from every subject. The Local Research and Ethics Committee approved this study (BA172). All were included in the analysis of data. The subjects had been immunised a median of 3 days prior to the study (range 2-10 days).

The primary outcome assessed was the response to capsaicin measured by subtracting the baseline from the average of the two maximal readings using absolute perfusion units (PU) (see section 3.5.1). This measurement was then subtracted from the measurement 2 months later. All 4 regions were analysed and then compared (figure 5.4). There were no differences in the increase in skin blood flow over time in response to capsaicin following an immunisation. There were no significant differences either within each region (Wilcoxon signed rank test) or between regions (ANOVA).

The value of capsaicin in detecting differences between a group of subjects who had been immunised compared to a group that had not was therefore thought to be minimal. This surrogate outcome measure was therefore dropped from the protocol.

Figure 5.4 Differences over time between the regions following immunisation.

Maximal LDI values after capsaicin corrected by subtracting the baseline (n=15)

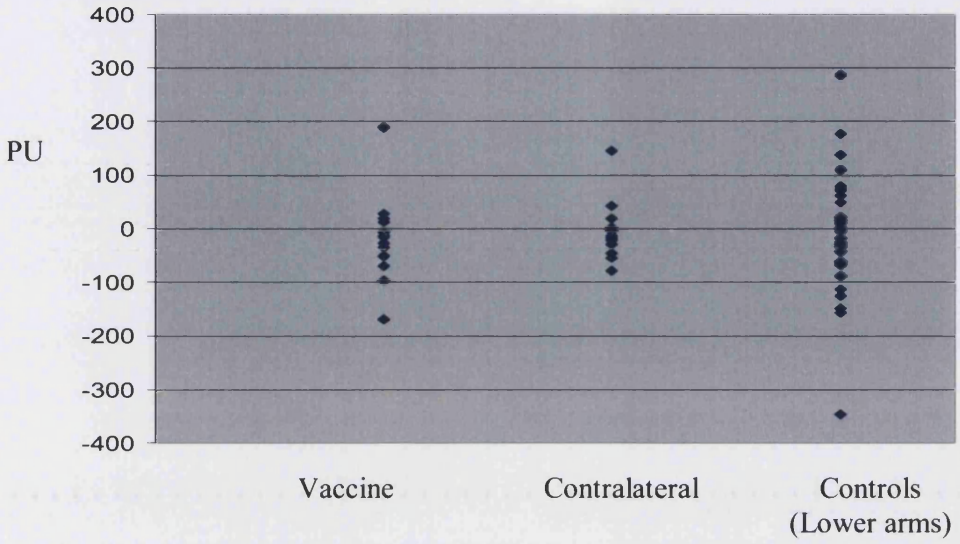

5.6.2 Differences in skin blood flow following immunisation prior to capsaicin

Figure 5.5 demonstrates the skin blood flow following an immunisation. This difference is significant when compared to the internal control two months later (Wilcoxon sign-rank test; two-sided p=0.013). This difference in skin blood flow was also significant (p=0.044) when compared to the control regions in the lower arms using a one-way ANOVA.

However, the increase in blood flow in the immunised region was not significant (p>0.05) in a one-way ANOVA comparison with the exact contralateral region. This suggests that there could have been increases in the skin blood flow occurring there that were not occurring in the control group. These differences must have been small however as there was no significant difference between the contralateral group and the control groups using this outcome.

Taken together, this pilot data does not support the null hypothesis and suggested that further studies be undertaken to investigate whether immunisation leads to an increase in blood flow in the contralateral region when compared to the control region.

Figure 5.5 Changes in skin blood flow following immunisation in the different regions

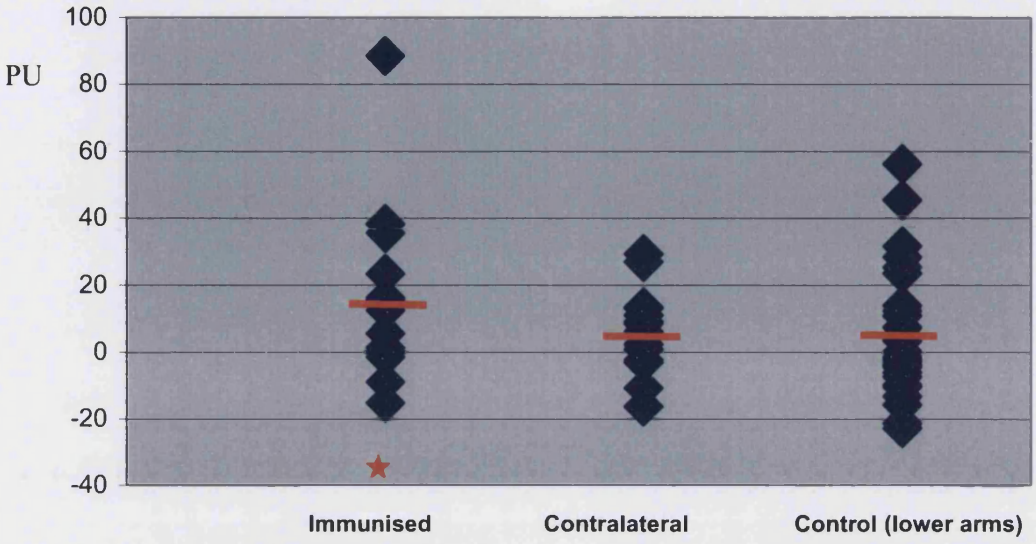

★ $p<0.05$ Immunised region compared to the other two (ANOVA) and immunised region over the two time points (Wilcoxon signed-rank test).

Changes were therefore made to this protocol in an effort to increase sensitivity. Recruitment was restricted to before 4 days following an immunisation and the distance at which the LDI scanned was reduced allowing the gain to be increased.

5.7.1 Timing of the study in relation to the immunisation

This pilot study recruited subjects who had been immunised a median of 3 days prior to the study (range 2-10 days). Figure 5.6 demonstrates that the skin blood flow response following immunisation is greatest following recruitment before day 4. It was decided that further studies should concentrate on recruiting before day 4.

Figure 5.6. Differences in skin blood flow over time since immunisation in the 4 different regions of interest

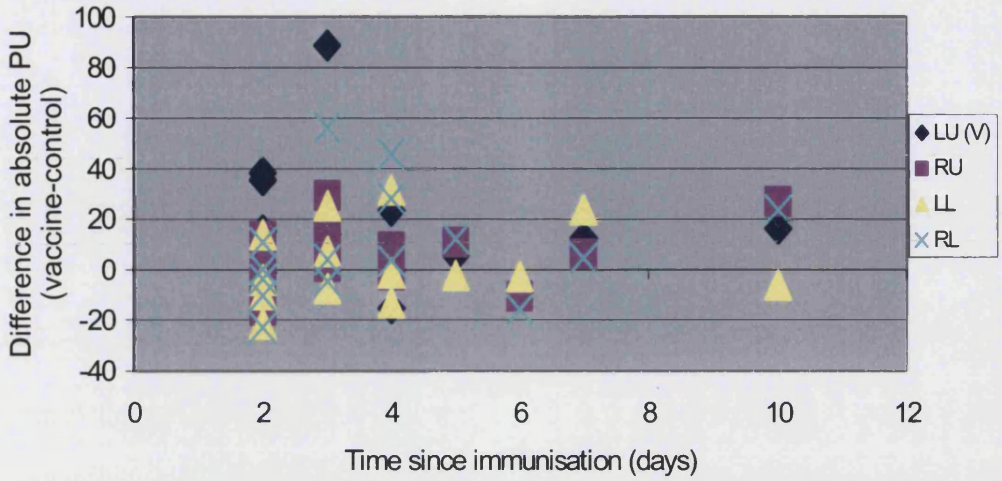

LU – Vaccinated left upper ROI; RU – Right upper ROI; LL – Left lower ROI; RL – Right lower ROI

5.7.2 Increasing the sensitivity of the LDI

An attempt was made to increase the sensitivity of the LDI to small changes in skin blood flow. This was done by reducing the distance between the LDI and subject from 80 to 20cm thereby decreasing background noise. The LDI flux gain was changed from 2 to 0 whilst all other parameters were kept constant. 8 new control subjects were scanned using these parameters to obtain new control data for the baseline skin blood flow responses.

5.8.1 Testing the variability of the new protocol on a control group (n=8)

This modified protocol was tested on a group of healthy subjects who were taking no medication at the time (n=8; 4 males; mean age 35 years (range 22-88)) over two months (see Figure 5.7). The skin blood flow over time was seen to vary by a mean of 2.1 PU (1.4%) (SD 39.2 PU, SEM 13.9 PU). There were no significant differences in skin blood flow over time controlled for region tested by Wilcoxon signed rank test; nor between the regions tested by one-way ANOVA. 95% of the data was between + / - 77 PU (50.3%) of the first scan.

5.9.1 Calculating sample size based on the pilot data

Using the pilot data from the original protocol (n=15), the baseline skin blood flow in the contralateral region (right upper) at the follow up time (i.e. when there had been no previous immunisation) was 35.5 PU (SD 14.8). Following an immunisation, this increased to 40.3 PU (SD 13.6), an increase of 4.8 PU (SD 13.5). Using these values a sample size of 57 subjects would be required with an α=0.05 (one-sided) and β=0.8 (GraphPad Stat).

Figure 5.7 Bland Altman plot of the differences over time for all four scanned regions in a control cohort

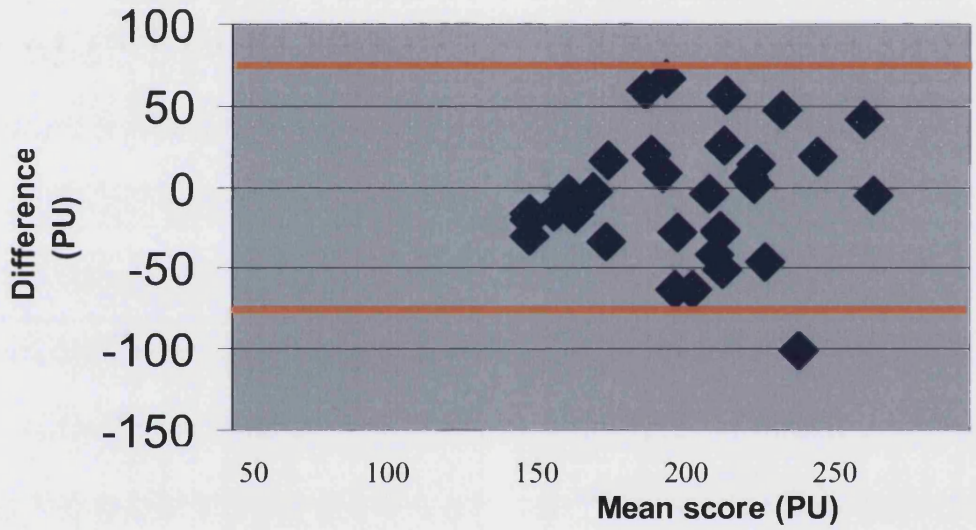

Red lines indicate 95% confidence intervals (n=8).

Chapter 6. Skin blood flow responses following active immunisation

Summary

The experimental model was tested. The null hypothesis was supported. Skin blood was seen to increase in the vaccinated region but not in either the experimental (contralateral) nor the control (lower arms) regions. Reasons for the lack of support for the hypothesis are discussed including the possibilities that the magnitude of the stimulus was insufficient to overcome the threshold required to generate a contralateral response and the timing of the experiment was not sufficient to capture a contralateral response.

6.1.1 Hypothesis

The hypothesis is that the skin blood flow in the area of the contralateral arm, precisely topographical to an active immunisation given 2-4 days prior, will be different to that of control areas in a group of healthy volunteers.

The **null** *hypothesis is that the skin blood flow in the area of the contralateral arm, precisely topographical to an active immunisation given 2-4 days prior, will be* **no** *different to that of control areas in a group of healthy volunteers.*

6.2.1 Methods

The background for this chapter has been laid out in Chapter 5.

Healthy individuals were recruited and studied on two separate occasions. Recruitment came from three sources:

1 Students at the University of Bath following mumps, measles and rubella (MMR) immunisation (32 volunteers)

2 Staff at the Royal National Hospital for Rheumatic Diseases following annual influenza immunisation (25 volunteers)

3 Patients recruited through local general practices (3 volunteers).

A £30 stipend was given to each volunteer to compensate for the time given to this study.

Anatomical landmarks were used to define four regions of interest (ROI) two in the upper and two in the lower arms. These were carefully marked and recorded on the first visit so that they could be used again on the second visit. The upper arm ROI was identified in a similar way to that in Chapter 5. It was located with reference to the anatomical line drawn from the midpoint on the lateral aspect of the acromion in the shoulder to the lateral epicondyle in the elbow. The lower arm ROI differed from that marked before as it was located with reference to the anatomical line drawn from the lateral epicondyle in elbow to the ulnar styloid in the wrist on the hairy dorsal aspect of the forearm. Each ROI was identified with a circular template (2.83 cm^2) using a semi-permanent marker pen. Each subject was then acclimatised in a warm temperature-controlled room (25-27°C) for 30 minutes.

6.2.2 Correcting for confounders

To correct for possible confounders (see Chapter 5), subjects were advised to avoid caffeine, nicotine and alcohol on the day of the study and excluded if any medication thought to affect the microcirculation had been given or changed between visits. Each subject was given a questionnaire to assess possible confounding variables to skin blood flow and microvascular assessment. The following data was collected: time since the vaccine; age; past medical history; medication; creams applied to their upper arms; smoking history; and allergies. This data is presented in Tables 6.1 and 6.2.

The second scan was timed to be 1 to 3 months later (mean 2 months), and for females this was scheduled to be approximately the same point within their menstrual cycle. A digital thermometer (Digitron Instrumentation Ltd, Model 2751-K) monitored the room temperature. The skin temperature was not monitored as it was thought irrelevant due to the shorter time course of this experiment (12 minutes) compared to the pilot studies (more than 60 minutes).

6.2.3 The Laser Doppler Imager

The LDI (LDI-2, Moor Instruments Ltd, Devon, UK) was used at a distance of 20cm perpendicular to the skin surface using a gain value of 0 for the flux; scan speed of 4 pixels/ms; and a bandwidth of 250Hz – 15kHz. Scanning time was approximately 1 minute. Each ROI was scanned individually. Two scans were taken from each ROI. Capsaicin was not used. The LDI was calibrated on each day of scanning as necessary according to calibration software.

6.2.4 Data analysis

The primary outcome was to detect whether there were any differences between the exact contralateral area and the control groups. The differences between these regions were analysed using a one-way ANOVA with a Bonferroni correction. The second primary outcome was to detect whether there was any difference in the contralateral area following immunisation compared to 2 months later.

Secondary analysis involved examining the data at the different time points using a one-way ANOVA with a Bonferroni correction and examining the effects of the recorded variables on the skin blood flow and each other using univariate modelling. SPSS 12.0 was used for all statistical analysis. Graphical data is presented using MS Excel.

6.3.1 Results: The characteristics of the studied population

60 subjects were recruited and their baseline characteristics are listed in Table 6.1. One subject did not attend for his second scan and was excluded from the analysis. His data did not significantly differ from the group data in any significant way (see Table 6.4). The results to the questionnaires are detailed in Tables 6.1 and 6.2. One student had unfortunately contracted mumps and attended his first (post-immunisation) session during his prodromal illness. His data did not vary from the mean significantly and was not excluded from the final analysis (see Table 6.4).

Table 6.1 Baseline characteristics of the experimental group

Total number	60
Age (yrs)	30.6 (range: 18-67, SD 14.6)
Gender	28 M 32 F
Immunisation	21 Influenza 2 Typhoid 37 MMR
Location of immunisation	53 L 7 R
Days since immunisation	2.5 days (range 1-4, SD 1.3)
Previous illness	15
Medication	10
Topical creams	7
Current smokers	6
Allergies	3

Table 6.2 Details of past medical history and medication

Previous illness	**Medication**	**Cream**	**Allergies**
Asthma (4)	Mini-pill (4)	Aqueous (3)	Dust mite
Hayfever (3)	Becotide (2)	Vitamin E	Opioids
Cured breast cancer	Salbutamol (2)	Moisturiser	Penicillin
Diabetes	Insulin	50/50 paraffin	Septrin
Chronic otitis media	Oral contraceptive	Papaya body butter	
Osteoporosis	Anti-histamine		
Eczema	Cod liver oil		
Urticaria			
Mumps			
Psoriasis			

6.3.2 Primary outcomes: The skin blood flow after immunisation

Table 6.3 presents the skin blood flow immediately after the immunisation; 2 months later; and the differences between the two. Figure 6.1 represents this graphically. Table 6.4 presents the data from both the volunteer who did not return for follow-up and the volunteer with mumps.

Table 6.3 The mean skin blood flow from the different regions on the arms immediately following the immunisation; 2 months later (control); and the differences between the two

	Mean	SD	SEM	Median
Immunisation				
Vaccine	258.1**	143.1	13.2	244.7**
Experimental	190.5	63.4	5.8	181.6
Lower (V)	167.4	46.5	4.3	159.3
Lower (E)	175.4	53.9	5.0	165.6
Control				
Vaccine	188.9	74.1	6.9	180.1
Experimental	186.2	66.4	6.1	177.9
Lower (V)	166.9	41.5	3.8	158.6
Lower (E)	169.5	48.6	4.5	161.2
Difference				
Vaccine	70.0**	150.8	14.0	65.4**
Experimental	4.3	58.2	5.4	3.7
Lower (V)	0.5	47.6	4.4	0.7
Lower (E)	5.8	56.9	5.2	3.7

** $p<0.01$ compared to other regions using ANOVA

Figure 6.1 Mean skin blood flow values (standard errors shown) of the four regions after immunisation (blue) and 2 months later (maroon)

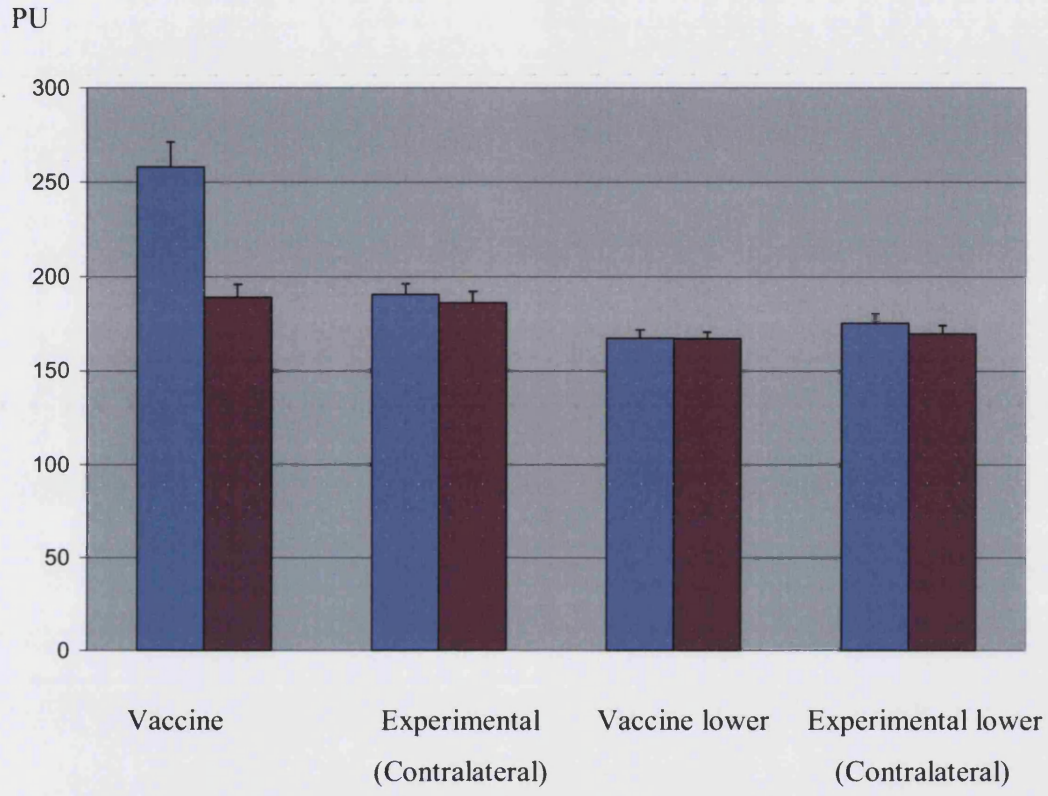

Table 6.4 Values of the subject who did not return (DNR) and the subject who had mumps (M)

Region	Mean (DNR)	Median (DNR)	Mean (M)	Median (M)
Immunisation				
Vaccine	156.7	146.5	168.4	162.2
Experimental	130.3	124.0	189.4	181.4
Lower (V)	138.0	132.0	148.4	143.3
Lower (E)	137.8	128.0	155.4	147.9
Control				
Vaccine	-	-	156.6	151.4
Experimental	-	-	187.9	173.8
Lower (V)	-	-	174.7	162.9
Lower (E)	-	-	164.9	157.2
Difference				
Vaccine	-	-	11.8	10.8
Experimental	-	-	1.5	7.6
Lower (V)	-	-	-26.3	-19.6
Lower (E)	-	-	-9.5	-9.3

From Table 6.3 and Figure 6.2, it is clear that the introduction of an immunisation causes an increase in skin blood flow in that region compared to any of the other regions ($p<0.01$). None of the other regions differed significantly between each other on a one-way ANOVA with a Bonferroni correction. It was also noted that the skin blood flow differed significantly from that recorded 2 months later only in the immunised region and not in any of the other regions using a Wilcoxon signed-rank test.

As can also be seen, after the immunisation the skin blood flow in the contralateral exact area (Experimental) is non-signficantly higher than the control areas. However this apparent increase is not due to the introduction of the vaccine because when the control skin blood flow is seen 2 months later, the same difference is evident. It appears that the anatomical area scanned in the upper arms has a higher skin blood

flow than the control areas in the lower arms. This is significant ($P<0.001$) when the upper arms are compared to the lower arms using a two-way paired t-test. Possible reasons for this are detailed in the discussion. When the skin blood flow from the two time points are subtracted then the differences between the skin blood flow in the regions disappears (Table 6.3).

There are no significant differences in the contralateral arm when compared to that in the control areas. This result supports the null hypothesis.

6.3.3 Skin blood flow after immunisation over time in the different regions

Figure 6.2 illustrates the differences in blood flow in each region against the time since the immunisation was given. Table 6.5 describes these results numerically.

As can be seen skin blood flow in the immunised region is increased for at least four days. None of the other time points in any of the other regions (experimental and control) were seen to change over the corresponding four days. This data supports the data previously presented. There was no detectable significant rise in skin blood flow following immunisation in regions distant to that of the immunisation region itself.

It is interesting to note that the range of data on the first day post-immunisation was significantly different to the ranges seen on the volunteers attending 2-4 days post-immunisation. This increased spread of data was a consistent finding across all of the regions. This variability however was not dependent upon the timing of the immunisation and is a reflection of volunteers with more variable skin blood flow being recruited 1 day following immunisation.

The skin blood flow in the experimental group one day following an immunisation was raised compared to the same region 2 months later, although this was not significant. Due to the large standard deviation of the data more than 200 more volunteers would need to be recruited to find this value significant using an alpha of 0.05 and a beta of 0.8 (see section 6.5.1).

Figure 6.2 Blood flow in the different regions over four days since immunisation

PU **Immunised region (*note different range on y-axis*)**

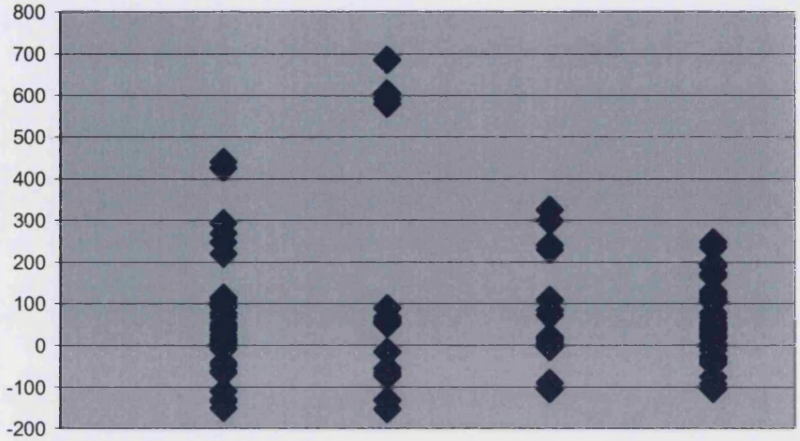

PU **Exact contralateral (experimental)**

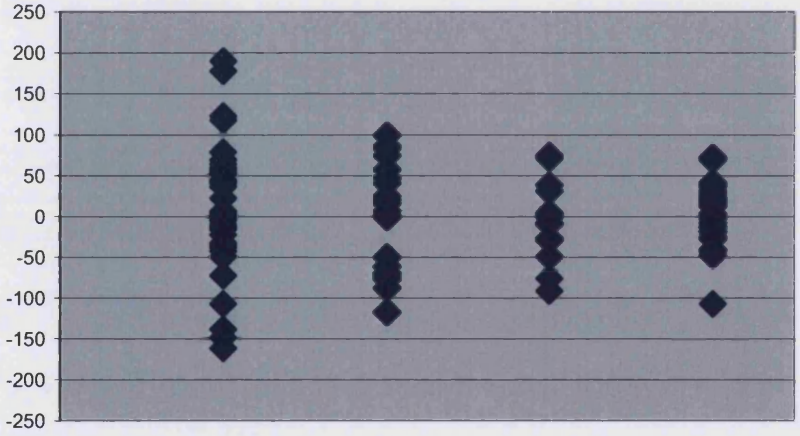

PU **Lower regions combined (control)**

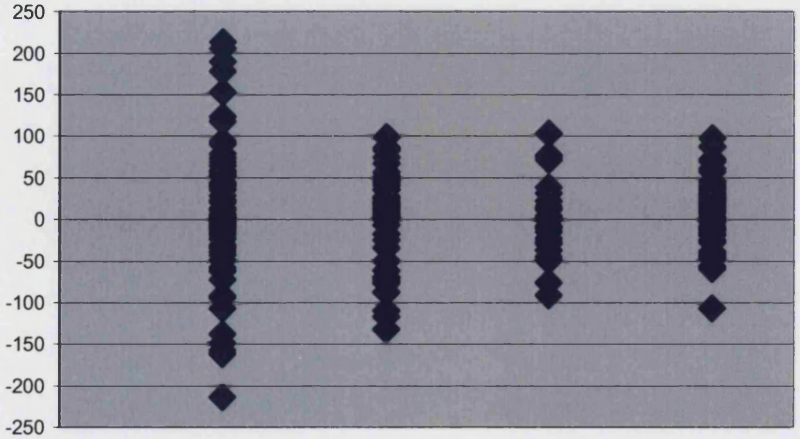

Day 1 Day 2 Day 3 Day 4

Table 6.5 The blood flow differences between immunisation and control times plotted against time since immunisation (SEM)

	Day 1	Day 2	Day 3	Day 4
Vaccine	56.5 (22.1)*	122 (52.3)*	81.7 (32.1)*	49.8 (13.8)**
Experimental	11.5 (12.0)	-2.5 (13.7)	-4.3 (11.4)	4.3 (5.6)
Lower (V)	0.1 (9.7)	0.0 (7.3)	3.7 (10.1)	0.0 (6.6)
Lower (E)	4.3 (12.7)	6.4 (10.5)	1.8 (10.2)	8.8 (5.8)

* $p<0.05$ Wilcoxon signed-rank test

** $p<0.01$ Wilcoxon signed-rank test.

6.3.4 Secondary analysis: Effects of other variables on skin blood flow

An analysis using univariate modelling (SPSS 12.0) was performed to assess whether there appeared to be any impact on skin blood flow from the variables described above. There appeared to be significant relationships between skin blood flow and the type of immunisation received; age; smoking status; and the presence of an allergy.

Type of immunisation

The 2 individuals who had the typhoid immunisation had significantly higher blood flow values in the region that was immunised, and significantly lower values in all of the other regions after the immunisation when compared to the volunteers who had received either influenza or MMR immunisations ($p<0.001$ using one-way ANOVA with a Bonferroni correction). 2 months later, these 2 individuals had significantly lower blood flows in all regions than the other groups ($p<0.001$). These findings were not explained by the presence of any other variable, but may be a reflection of very low numbers in this group.

Volunteers who received the MMR had significantly higher blood flows than those who received influenza immunisation ($p<0.01$). This was seen in the upper arms only, and occurred both after immunisation and 2 months later, suggesting that this was an intrinsic difference between the two groups rather than caused by the immunisation.

The MMR group was significantly younger than the influenza group ($p<0.01$) although there was no significant relationship between the skin blood flow in the upper arms and age ($p=0.18$). There were no other differences between the MMR and influenza groups and it is difficult to explain the observed difference using the data collected.

Age

The relationship between age, blood flow, region and immunisation was interesting (Figure 6.3). Across all of the regions, age was seen to be associated with a slight but highly significant ($p<0.001$) decrease in the skin blood flow at two months following immunisation i.e. the control time. It was seen to have a slightly negative non-significant relationship with skin blood flow after immunisation. When the differences between the two times was taken age was seen to have a significant positive relationship with differences in skin blood flow ($p<0.01$). It appears that the increase in skin blood flow following immunisation increases as age increases.

When this relationship was explored with regards to region specificity the following results were seen (Figures 6.4, 6.5, and 6.6). Skin blood flow was seen to decrease with age in all of the regions at time 2 (Figure 6.4). This was a highly significant relationship in both of the upper arms ($p<0.001$) whereas it was not significant in the lower arms.

Skin blood flow was seen to increase with age following immunisation (time 1) in all of the regions apart from the contralateral region to the immunisation site (Figure 6.5). The negative relationship with skin blood flow and age following immunisation was highly significant in this contralateral (experimental) region ($p<0.001$). The positive relationship was significant only in the lower arm on the immunised side ($p=0.028$).

Figure 6.3 Blood flow plotted against age and its relationship with immunisation

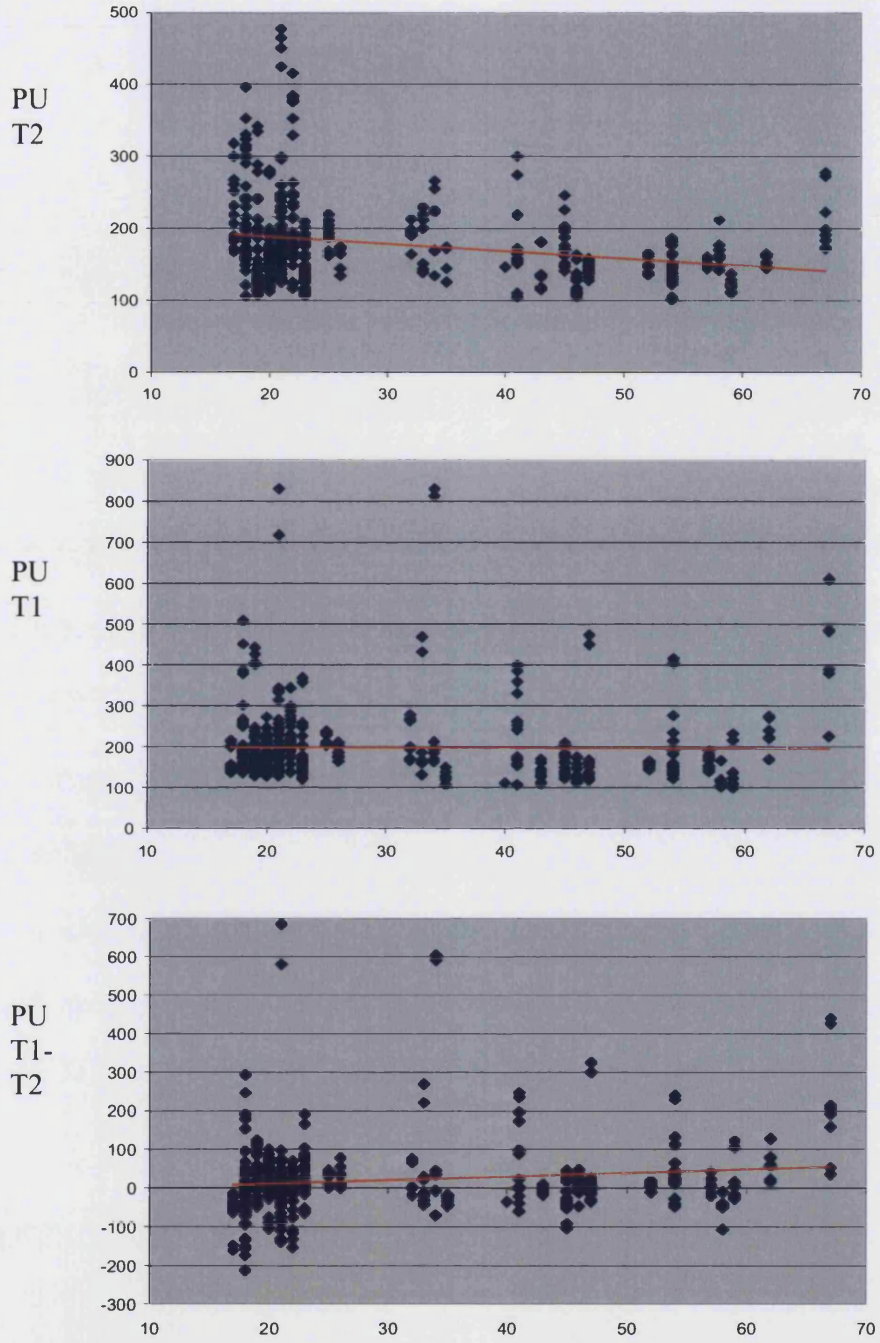

The top graph is control data (no immunisation). The middle graph is post-immunisation (experimental data). The bottom graph is the difference between the two. As can be seen there is a negative correlation of age with no immunisation that is negated after an immunisation. This means that there is a positive relationship with age if the differences are examined. (Note differing range on y-axis)

Figure 6.4 Age against skin blood flow at each region 2 months after immunisation (T2)

Vaccine
***

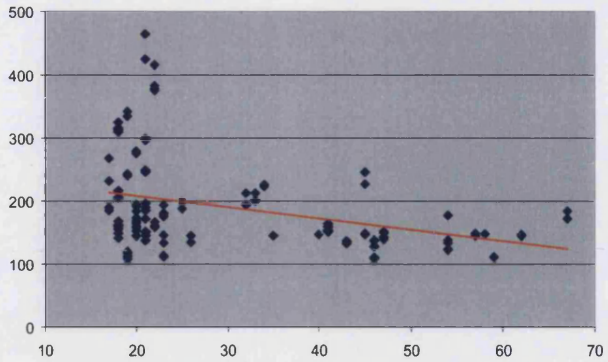

Contra
***

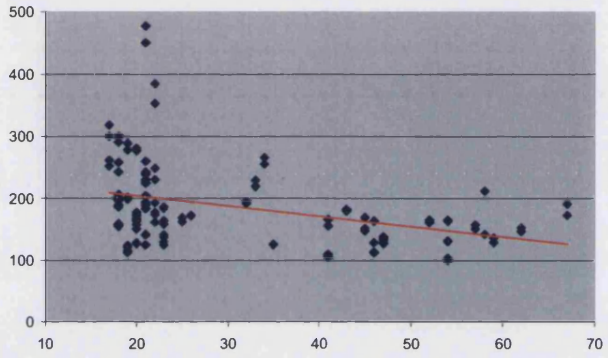

V Lower

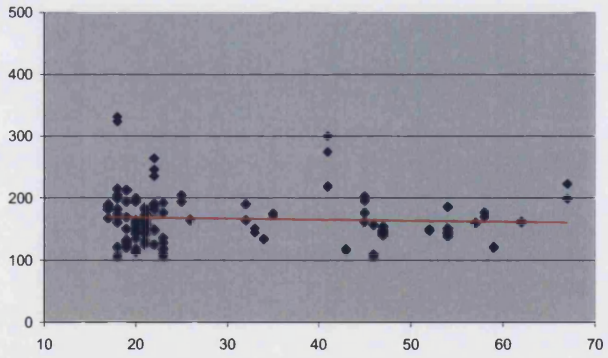

C Lower

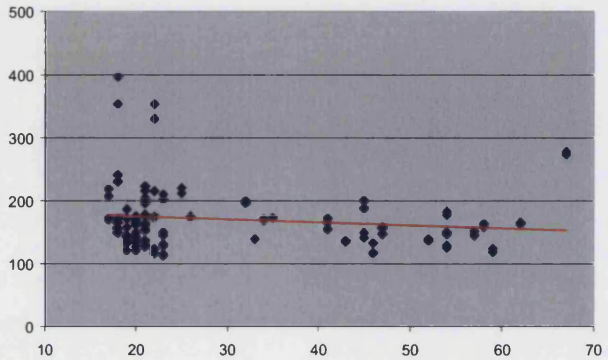

Figure 6.5 Age against skin blood flow at each region after immunisation (T1)

Vaccine

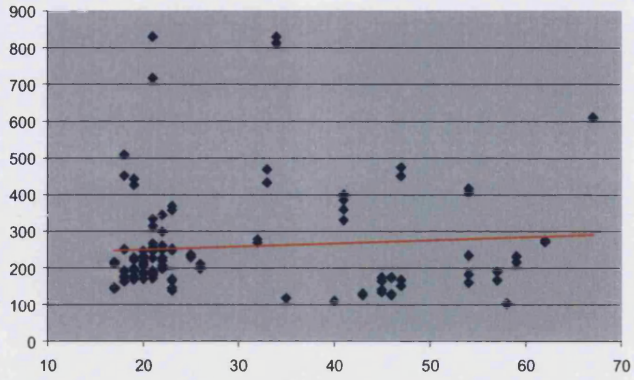

Contra
***

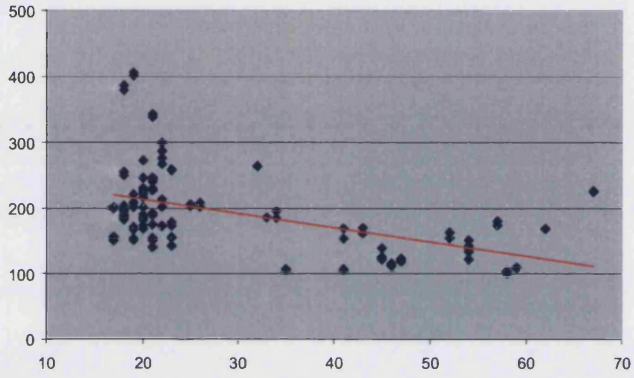

V Lower
*

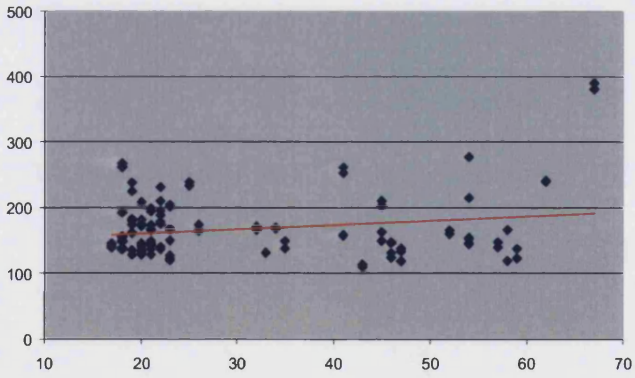

C Lower

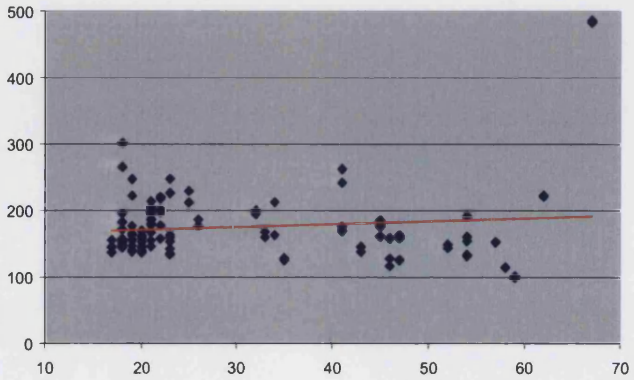

Figure 6.6 Age against skin blood flow at each region. Skin blood flow from 2 months after immunisation (T2) subtracted from immunisation (T1)

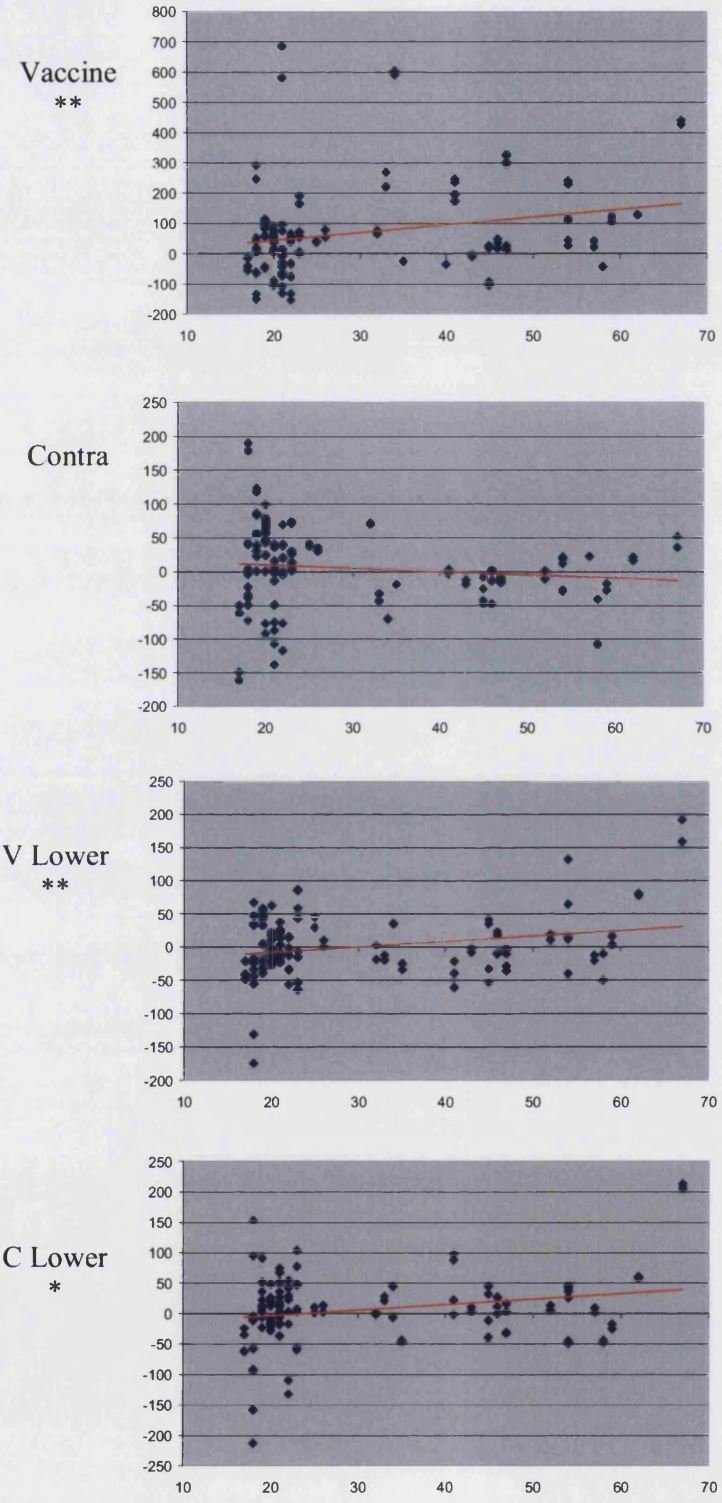

* p<0.05 ** p<0.01 ***p<0.001 (univariate modelling)

When the two time points are subtracted from each other (Figure 6.6) skin blood flow is seen to increase in all of the regions with respect to age apart from the exact region contralateral to the immunisation. This increase in skin blood flow with respect to age is significant in all of these three regions. There is no significant change in the contralateral region. These results are discussed in section 6.5.2.

When the older age group (over 50 years old, n=9) are analysed as a subgroup, skin blood flow is seen to differ significantly between the regions (Table 6.6). Both the vaccinated region and the contralateral region are seen to differ significantly from the control regions both following immunisation and when corrected for the skin blood flow 2 months following immunisation. Here it can be seen that these significant differences arise because of an increase in the skin blood flow after immunisation in the control lower arm regions. The skin blood flow does not change in the contralateral region exactly opposite to the immunisation.

Table 6.6 The mean skin blood flow from the different regions on the arms immediately following the immunisation; 2 months later (control); and the differences between the two in the over 50 age group (n=9)

	Mean	SD	SEM	Median
Immunisation				
Vaccine	275.9**	157.0	39.2	252.9
Experimental	149.8**	37.3	8.8	142.1
Lower (V)	194.3	82.2	19.4	181.4
Lower (E)	188.9	113.4	26.7	178.6
Control				
Vaccine	145.4	22.7	5.7	138.8
Experimental	150.6	27.5	6.5	152.4
Lower (V)	160.8	26.0	6.1	152.4
Lower (E)	162.0	44.9	10.6	144.7
Difference				
Vaccine	130.5**	142.4	35.6	121.928.9
Experimental	-0.8**	36.9	8.7	-2.6
Lower (V)	33.5	69.9	16.5	28.9
Lower (E)	26.9	75.6	17.8	26.1

** $p<0.01$ compared to control regions using ANOVA

Smoking

The 6 volunteers who smoked had significantly higher blood flow ($p<0.01$) after they had been immunised when compared to non-smokers. There were no significant differences in this smoking group 2 months later. On further analysis, this increased blood flow arises in all regions apart from the experimental (exact contralateral) region.

Allergies

The 3 volunteers with allergies had higher skin blood flow than those with no allergies. This was only at the control time point, 2 months after immunisation, and

was only seen in the upper arms, not the lower. This was unaccounted for by another variable.

In summary, several variables were seen to have an impact on the skin blood flow over and above the region and the immunisation.

6.4.1 Findings from the protocol

The main findings from this protocol are that an immunisation increases the skin blood flow in that region significantly for at least the following 4 days. There are no concomitant differences in the skin blood flows in any of the other regions. There are no differences in the skin blood flow in the exact contralateral region when compared to a control region taken at the same time; nor when compared to the same region 2 months later. These results support the null hypothesis.

Further findings are that age is correlated negatively with skin blood flow 2 months following immunisation and has a significant relationship with region and immunisation time as well. The type of immunisation also has a complex relationship with region and skin blood flow. Smoking and the presence of allergies also demonstrate significant differences in skin blood flow following immunisation when compared to volunteers who do not smoke and have no allergies respectively.

6.5.1 Discussion of the primary outcome findings

These findings are not consistent with the evidence that has been published and summarised in Chapter 2. Aside from the bias in the literature for the publication of positive results, there may be several other reasons for this.

As has been detailed in Chapters 2 and 5 the stimulus has to overcome the threshold properties set for the crossed afferent pathway by either being of sufficient magnitude or duration. Animal models all used very different stimuli to that used in this protocol. They were more severe and sustained (e.g. chronic monoarthritis; neural lesion; hindpaw oedema etc.) than the immunisation that the volunteers received. It would not be ethically permissible to apply a more powerful stimuli to human volunteers. It may be that the immunisation did not surmount the 'gating' of the central nervous system.

Another property of the crossed afferent pathway is that the contralateral effects that are seen are reduced in magnitude and temporally delayed, sometimes up to days following the original insult. This led Koltzenburg, Wall and MacMahon (1999) to comment that the contralateral responses might be mediated by slow signalling pathways that occur centrally. In this study the contralateral responses were not detected for 4 days following the immunisation. It may be that this time period was not long enough to capture the putative contralateral effect. The ipsilateral response to the immunisation had not subsided as there were still significant differences between the skin blood flow recorded 4 days after the immunisation compared to that of the control 2 months later. Perhaps any contralateral response could manifest itself at least 4 days after the immunisation, even after the immunisation has subsided.

It is possible that the study was not adequately powered to detect a very small and subtle contralateral effect occurring at day 1. This is the time that the skin blood flow corrected for the control 2 months later was noted to be slightly higher than the control regions (Table 6.5) to a p=0.202 with a Wilcoxon signed rank test. Using these results as the basis for powering a new study (mean 212, SD 72.7) more than 200 more volunteers would need to be recruited. This was clearly impractical in the time available.

It is possible that the contralateral responses were actually occurring but failed to be detected. A different detection technique (immunohistochemistry) is detailed in the next chapter.

Is it possible that crossed afferent pathways do not have a role to play in man? This may be so, but unlikely to be plausible. Crossed pathways are histologically detectable in species that bear a close relationship to man, such as the apes (Culberson *et al*, 1979). These decussating fibres are not related to any existing neurophysiological framework although appear to have a physiological role (Fitzgerald, 1982 a and b). Contralateral responses are ablated following disruption of the peripheral or central nervous system, but not of the circulatory system (see Chapter 2). The circumstantial evidence for crossed afferent pathways to have a

meaningful role in species related to man is considerable and there would be no reason for thinking that these pathways would not be active in man.

6.5.2 Discussion of age and regional differences in skin blood flow

Skin blood flow is known to reduce as people grow older. Tsuchida *et al* (1991) examined the skin blood flow in the deltoid region of 55 volunteers ranging from 20-72 years old and found significant decreases in the clearance of radioactive Xenon from the skin correlated with increasing age. In a related study Tsuchida (1990) noted that this decrease was about 30-40%. This study supports both the quality and quantity of that observation (Figure 6.4, top graph).

The relationship with age, region, immunisation and skin blood flow is interesting. Significant differences were seen in the skin blood flow responses in the control regions following immunisation that was not seen in the contralateral region opposite to the immunisation (Figures 6.4-6). These significant differences in the older age group arise due to the increase in skin blood flow in the control lower arm regions following immunisation (Table 6.6). There is no increase in skin blood flow in the topographically precise contralateral region following immunisation. Therefore, although there are significant differences between the control and experimental groups in this post-hoc analysis there were no significant differences between the skin blood flow in this region following immunisation when compared to 2 months later using a Wilcoxon signed-rank test. This does not invalidate the null hypothesis and further investigation is required to test this association before any firm conclusions can be drawn. Furthermore, the numbers were small in the over 50 years age group (n=9) compared to the younger age group and this could have skewed the slope at this point.

The relationship between the skin blood flow in the upper arms when compared to the lower arms is also interesting. It is possible that proximal body regions will have relatively higher vascular pressures, relatively larger blood vessels and hence relatively higher blood flows. There is some evidence in support of this from Helme and McKernan (1985) who investigated the skin flare following the application of a defined amount of topical capsaicin in various regions of the body. They found that the more proximal sites generated larger flare reactions. Similarly, Tsuchida (1979)

examined the skin blood flow using a $^{[133]}$Xenon clearance method and found that the anterior chest wall and face had higher blood flow than the deltoid region which consequently had higher blood flow than posterior cervical, lateral thoracic, lateral abdominal, and gluteal sites. He did not use sites on the forearms as comparators.

6.5.3 Developing this model further

Further work to detect contralateral responses might include changing the protocol to address all of the above factors discussed in section 6.5.1. For example, the timing of the recruitment could be extended to ensure that in all cases the increased blood flow caused by the immunisation had been captured. A different stimulus could be included. Some of these have been considered in Chapter 5 (Table 6.1). Most of these stimuli suffer from the same perceived problem as an immunisation. Larger stimuli would not ethically be permissible but could be recruited from patients with appropriate local inflammatory lesions. Such examples might be abscesses, unilateral trauma and local tumours. Recruitment would be limited however and it would be difficult to compare cases due to the uncontrolled variability of the different insults.

It was thought that a different method for detecting changes in a given outcome could be considered. Radio-isotopic labelling and clearance methods, high resolution Doppler ultrasound, and microangiography were thought not to be sufficient to provide enough sensitivity to detect small changes. More sophisticated scanning techniques such as functional Magnetic Resonance Imaging or Positron Emission Topography might have the ability to detect small changes in skin blood flow in the deeper tissues, but these were not available. A different line of investigation was therefore chosen to attempt to capture contralateral changes. This was immunohistochemical in nature and this will now be discussed in Chapter 7.

Chapter 7. Dilutional immunohistochemistry to semi-quantify E-selectin staining density contralateral to MMR immunisation

Summary

In this chapter, the hypothesis that topographically precise contralateral inflammatory changes occur following an immunisation is tested at the microscopic level. Skin biopsies were taken from the upper (experimental) and lower (control) arm contralateral to an MMR immunisation. An immunohistochemical technique, using supraoptimal dilutions of the primary antibody, was used to semi-quantify the amounts of the protein E-selectin expressed on the dermal endothelium. No differences between the experimental and control groups were found in any of the outcome measures. The null hypothesis is again supported.

7.1.1 Hypothesis

The hypothesis is that there is greater expression of endothelial E-selectin in skin biopsies taken from the exact contralateral area to an MMR immunisation (given one to three days prior) when compared to the control contralateral skin biopsy taken from a different dermatomal area.

The **null** *hypothesis is that there is* **no** *difference in the expression of endothelial E-selectin in skin biopsies taken from the exact contralateral area to an MMR immunisation (given one to three days prior) when compared to the control contralateral skin biopsy taken from a different dermatomal area.*

7.2.1 Rationale for using an immunisation as the stimulus

It was decided to use the same stimulus (active immunisation) as had previously been used as this was still felt to be the best available stimulus to induce contralateral responses due to its immuno-inflammatory properties and longevity (see Chapters 2 & 5). As previously discussed this stimulus also allowed adequate recruitment of volunteers. It is unknown however whether an immunisation induces inflammation in distant tissues even though there are short-lived systemic effects (see Chapter 5).

7.3.1 E-selectin in normal human skin

E-selectin is not expressed in large quantities in normal human skin. Some studies have indicated the presence of small amounts (Groves *et al*, 1991 and 1992; Smith *et al*, 1993; Terajima *et al*, 1998; Chong *et al*, 2004), whereas others have not detected any presence of E-selectin (Cotran *et al*, 1986; Sepp *et al*, 1994; Sais *et al*, 1997; Strickland *et al*, 1997; Sigurdsson *et al*, 2000; van der Laan, 2001) in normal skin from healthy human volunteers.

For example, Chong *et al* (2004) readily demonstrated the presence of E-selectin in all 12 skin biopsies taken from non-inflamed skin. This skin had been removed in cosmetic plastic surgery to the face, breast and abdomen in patients with no known inflammatory condition. They used a monoclonal antibody and the ABC method (see below) stained with the NovaRed substrate kit. The distribution of E-selectin was patchy in these samples. Some biopsies were positive in one section and negative in an adjacent section and, even within one vessel, E-selectin expression could be seen to vary from one area of the lumen to another.

For another example, Van der Laan (2001) obtained 6 skin biopsies from patients (average age 60 years old) about to undergo elective surgery and could not demonstrate the presence of E-selectin protein. Again a monoclonal antibody (H18/7) was used, this time with a peroxidase conjugated secondary antibody visualised with amino-ethylcarbazole. This is a relatively insensitive method compared with the ABC method. Interestingly, human endothelial cells studied from these biopsies under electron microscopy showed a variety of different stages of 'activation', possibly corroborating Chong *et al*'s (2004) findings.

The patchy expression of E-selectin and different staining protocols may explain the different results seen between studies that examine the dermal endothelia of healthy human volunteers.

7.3.2 E-selectin expression is induced following inflammatory stimulation

E-selectin is upregulated rapidly following inflammatory stimuli and this process is linked to transcriptional up-regulation via the NF-κB pathway (Barnes and Karin, 1997). Although some studies have induced E-selectin using the pro-inflammatory

cytokines TNFα and IL-1, some other inflammatory stimuli may be quite mild. For example, E-selectin mRNA is demonstrable 4 hours after human forearm skin has been rubbed with an eraser for two minutes (Takeuchi *et al*, 2003).

E-selectin protein expression is detectable following neuropeptide release after 24 hours, either through capsaicin (Egan *et al*, 1998), or direct injection of substance P (Smith *et al*, 1993). Egan *et al* (1998) explored the histological relationship between unmyelinated nerves and mast cells in the skin of mice and applied topical capsaicin to the skin of human volunteers. They found an intimate relationship between the nerves and mast cells in mice and an upregulation of E-selectin from immunohistochemical techniques in the volunteers. Smith *et al* (1993) injected SP, CGRP and VIP into the skin of volunteers and compared the numbers of neutrophils, eosinophils and E-selectin expression over the following 24 hours. There were significant increases in both types of cell and E-selectin expression between 1-8 hours following injection of each of these neuropeptides.

7.4.1 Rationale for immunohistochemistry

There are many laboratory investigational techniques to detect inflammatory responses. Immunohistochemistry is used to demonstrate the presence of an antigen within tissue. First described by Albert H Coons and colleagues in 1941 (Polak and van Noorden, 1997), there are now many different techniques available. Its advantages are that it is relatively cheap, reliable and quick to use compared to other techniques such as *in situ* hybridisation or the polymerase chain reaction. A disadvantage of immunohistochemistry compared to these other techniques is that it can not be used to gain absolutely quantitative measurements. However it can be used qualitatively and semi-quantitatively in a comparative manner, using techniques such as the supra-optimal dilution method.

For the purposes of this study, the immunohistochemical technique used is the avidin-biotin-peroxidase complex (ABC) method (Hsu *et al*, 1981). This three-layer technique exploits the strong and specific attraction of avidin and biotin. Avidin has four binding sites per molecule for the low molecular weight vitamin, biotin. Biotin

has just one binding site for avidin and can be conjugated to many other macromolecules, such as fluorophores or enzymes.

First, the primary antibody is added to the section, after the standard preparation and blocking techniques. The second layer is the biotinylated secondary antibody which binds specifically to the primary antibody. The third layer is a suspension of avidin and biotinylated peroxidase. This complex can be visualised under light microscopy after adding diaminobenzidine tetrahydrochloride which is oxidised by the peroxidase. The following reaction product is intensified with copper to give a dark-brown stain.

7.4.2 Supraoptimal dilution

First described in 1985 by Vacca-Galloway, this technique is useful in semi-quantifying the amount of antigen in one sample relative to another, or one structure relative to another within the same sample. This technique has been used by several groups in order to semi-quantify tissue antigens (Springall *et al*, 1988; Bhatia *et al*, 1998; Arantes and Nogueira, 2001).

The principle is dependent upon the varying interaction between the fixed concentration of antigen in the section with the different antibody concentrations. The antibody is first titrated in a series of dilutions to find the optimal dilution that gives strong staining and a low background as well as the 'supra-optimal' dilution at which staining is weak but still reliably demonstrates all the positive structures. The end-point occurs at the dilution where no reliable staining of the antigen occurs. 'Titration' curves can then be drawn from the semi-quantified staining that occurs at each antibody dilution. There are three relevant outcome measures that have been used with this technique to compare the amount of tissue antigen between two samples. These are the end-point dilution, the slope of the titration curve, and the amount of staining at a supra-optimal dilution compared to the optimal dilution (Vacca-Galloway, 1985; Arantes and Nogueira, 2001).

The constraints to this technique are that a rigid protocol must be adhered for all samples to be compared. For example, tissue on separate slides must be as contiguous as possible to allow reliable counts. Traditionally, the relatively

insensitive peroxidase-anti-peroxidase (PAP) method has been used for supraoptimal dilution methods because of the difficulty in identifying high and low amounts of antigen using the more sensitive ABC method (Sternberger and Sternberger, 1986). As will be seen, this has not proved to be a problem in the following protocols, presumably due to the very low concentrations of primary antibody that were used. Finally, good image analysis techniques should be available with adequate reproducibility measures.

The following sections describe the establishment of the immunohistochemical techniques: the protocol; the image analysis; and the reproducibility of this technique.

7.5.1 Detecting E-selectin in the laboratory using immunohistochemistry

To determine whether E-selectin could be detected using standard ABC immunohistochemical techniques (see section 7.6.3), and to assess the effects of an inflammatory stimulus on its expression, three skin biopsies (see section 7.6.2) were taken from one subject. The sites were: a control site that had not been exposed to any stimulus; an immunisation site that had been injected with an influenza immunisation 24 hours prior; and a capsaicin site that had been injected with 0.1% capsaicin solution 8 hours prior. The intradermal capsaicin site was used as a positive control for the technique as capsaicin is known to induce E-selectin expression (Egan *et al*, 1998).

The results are shown in Image 7.1 with negative controls from the protocol shown in Image 7.2. Consecutive sections were stained with either human E-selectin antibodies or human CD31 antibodies (endothelial marker) so that co-localised staining patterns could be ascertained. As can be seen, the distribution of the E-selectin staining pattern co-localises with that of the CD31 pattern, suggesting that this positive stain is very likely to represent true E-selectin staining. There is very little E-selectin in the control section although normal amounts of endothelial CD31 are seen. E-selectin is heavily expressed in the capsaicin exposed skin. The skin exposed to immunisation also demonstrates the up-regulation of E-selectin.

The stimulus (immunisation) and detection technique (immunohistochemistry) are therefore adequate for detecting an inflammatory response and would be appropriate to use in a model to test the hypothesis.

7.5.2 Supraoptimal dilution technique in the three samples

Supraoptimal dilutions were then carried out using these samples and the following fold dilutions of the primary antibody: 20 50 100 200 800 1,600 5,000 15,000 50,000 and 150,000. Images were captured at low power using Zeiss KS300 microscope and Image Capture software. Images were then processed using interactive software that identified regions of interest and automatically calculated a pixel count. By simultaneously using high power microscopy, a consecutive section stained for the endothelial marker CD31, and the image analysis, non-specific staining could be identified. Hence areas of true endothelial staining representative of E-selectin staining were more likely to be counted. The amount of staining correlates with the distribution of the antigen and, at low doses of primary antibody, its concentration in the tissues. As can be seen in Image 7.3 the staining of endothelium with the E-selectin antibody vanishes at a dilution of 150,000.

Image 7.1 E-selectin and CD31 staining in consecutive sections from skin biopsies obtained from a single individual from control, capsaicin and immunisation sites

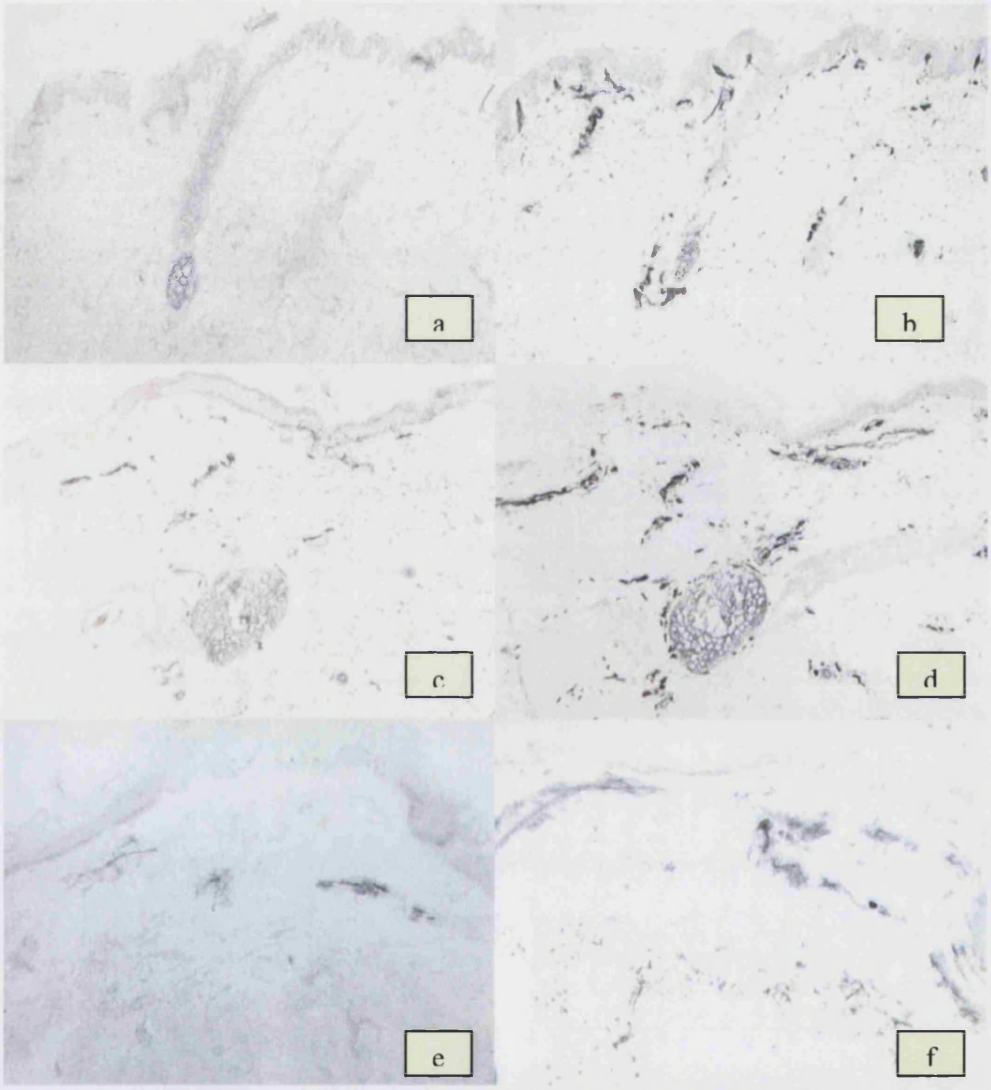

Images **a**, **c**, **e** stained for E-selectin at 1:50 dilution for one hour. Images **b**, **d**, **f** stained for CD-31 at 1:400 dilution for one hour (endothelial stain). All images are x10 magnification. All skin biopsies were taken from the same individual.

Images **a** and **b** were taken from a control site and demonstrate little or no E-selectin staining. Images **c** and **d** were taken 8 hours following a capsaicin injection and demonstrate a large amount of E-selectin staining co-localised with CD-31 staining. Images **e** and **f** were taken 24 hours following an influenza immunisation and demonstrate E-selectin staining co-localised with CD-31 staining.

Image7.2 Negative control sections for E-selectin immunohistochemistry

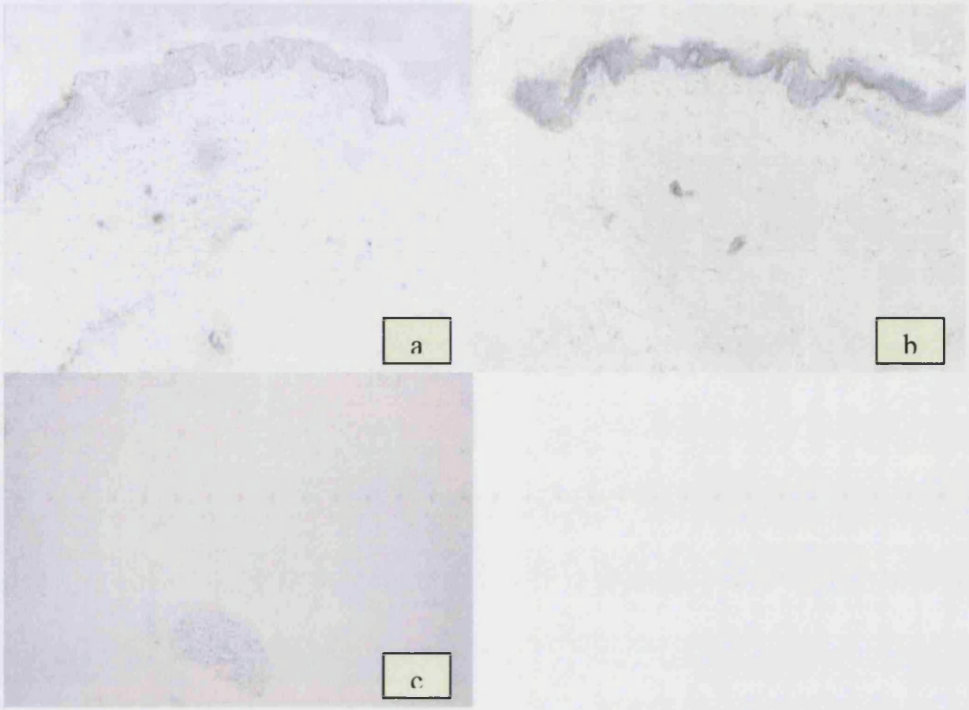

Image **a** obtained after primary antibody had been omitted. Image **b** obtained after secondary antibody had been omitted. Image **c** was obtained after mouse IgG1 antibody had been added instead of primary antibody. In all of these sections, there is no significant staining of endothelium. There is some background staining of the epithelium and some sweat glands.

Image 7.3 Effects of diluting the primary antibody on the staining pattern

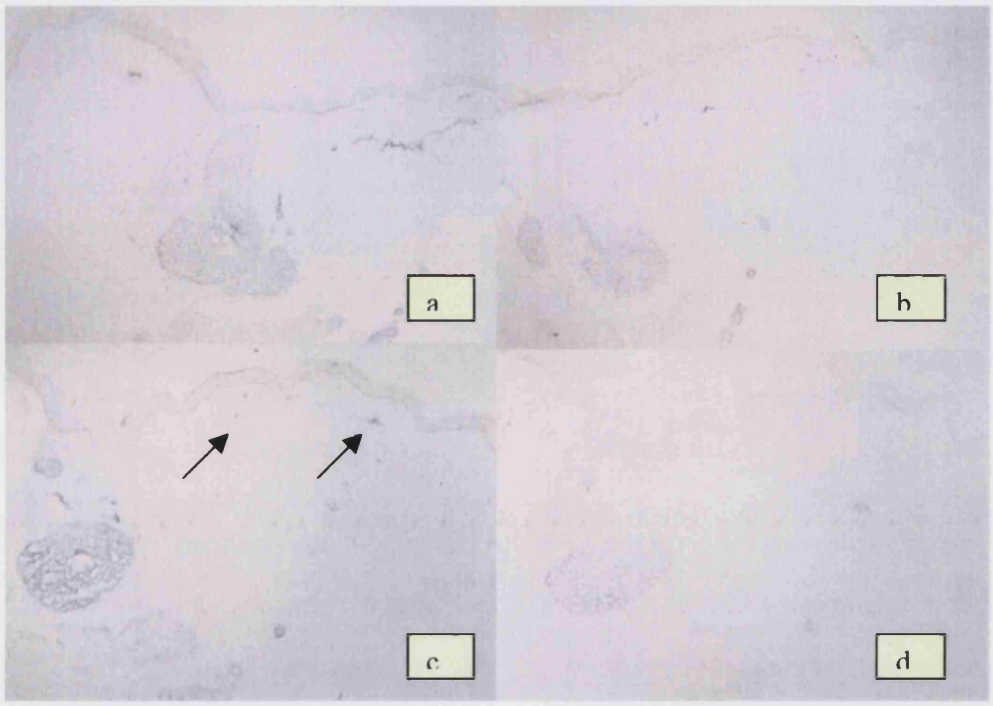

All images have been obtained from sections of skin following intradermal capsaicin injection. ABC immunohistochemistry was performed using human e-selectin as the primary antibody. Images **a**, **b**, **c**, and **d** use a fold dilution of 50, 800, 50,000 and 150,000 respectively. Faint staining can be seen in image **c** (arrowed), but not in image **d**. The 'end point' of this reaction would therefore be 150,000. Not all of the dilutions that were performed have been shown here to save space.

Two separate analyses were made, one of E-selectin, and the other of CD31 in adjacent sections. First, the total area of E-selectin stained tissue (in pixels) was calculated and corrected for the total area of the tissue (Image 7.4). Second, in order to compare the E-selectin staining in two tissue samples meaningfully, a correction for endothelial density (anti-CD31 staining density on the adjacent section) was made.

Image 7.4 Highlighted regions of interest using Zeiss Image Analysis

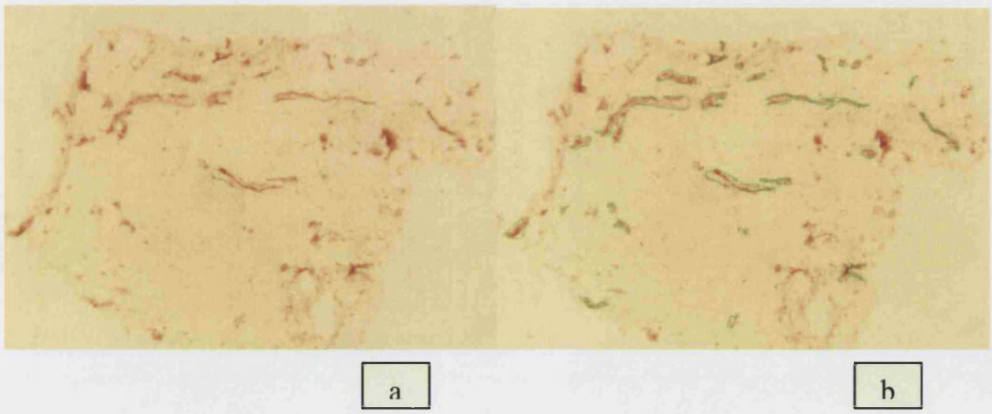

a b

Image **a** is analysed using the 'Interactive' function in the Zeiss Image Analysis 3.01 software program. This allows each region of interest to be identified manually (in green). Note that in image **b**, not all of the staining regions have been identified. This is because these regions were thought to have irrelevant staining when viewed at high power magnification. This degree of subjectivity highlights the need for repeated observations using independent observers when using this form of analysis.

Intra- and inter-observer counts were therefore obtained. Both observers were blinded to the original results and evaluated 10 slides, a mix of both E-selectin and CD31 stains. Figures 7.1 and 7.2 detail the results of the intra- and inter-observer differences respectively.

Figure 7.1 Bland-Altman plot of *intraobserver* readings for staining percentages from 10 samples with a mixture of E-selectin and CD31 stained sections

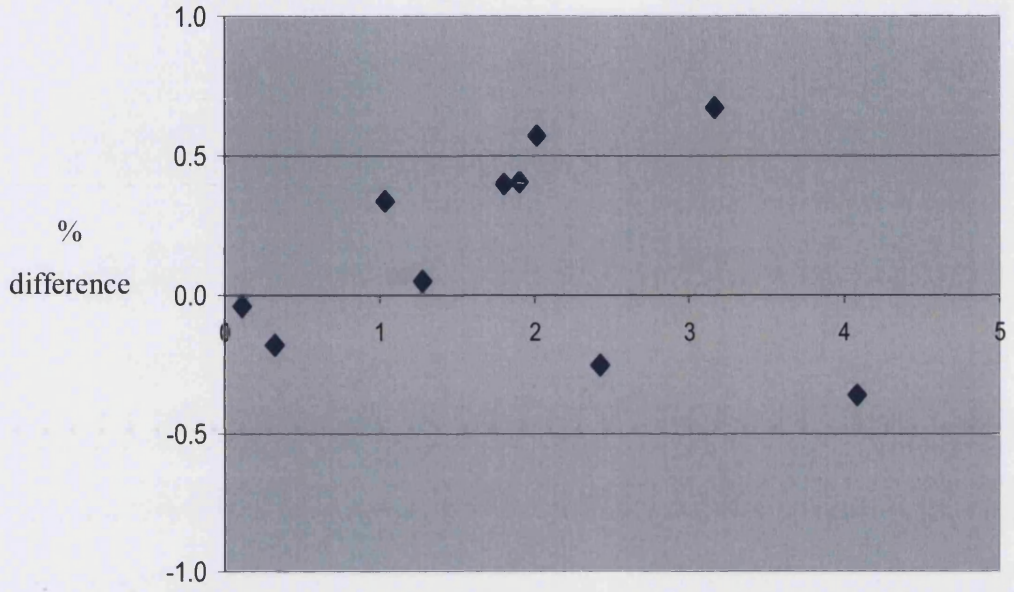

Figure 7.2 Bland-Altman plot of *interobserver* readings for staining percentages from 10 samples with a mixture of E-selectin and CD31 stained sections

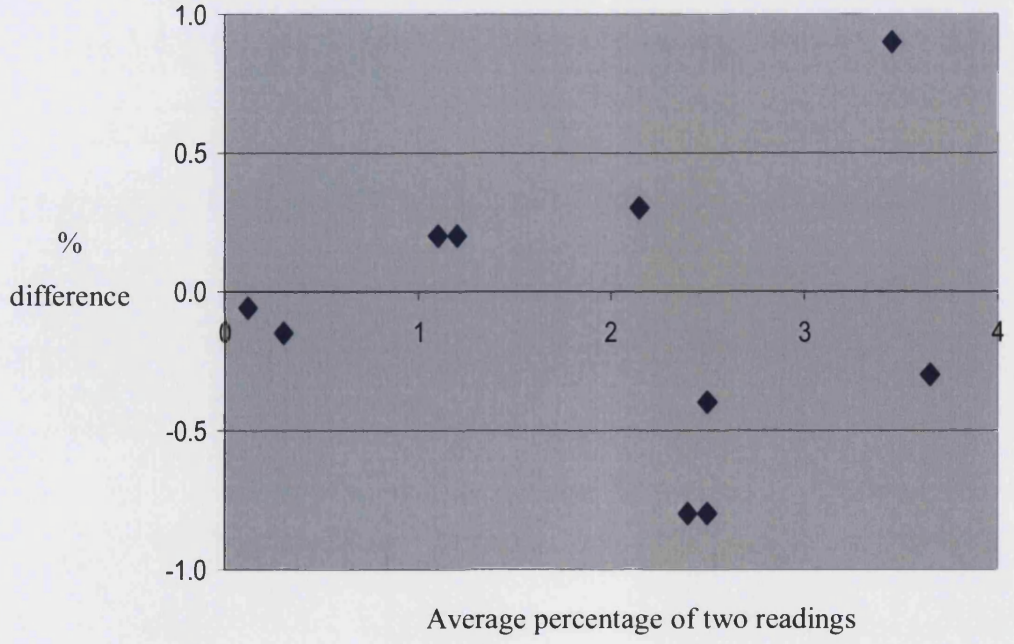

Intraobserver values gave a variability of 8.8% (95% confidence interval (CI): 39.8%) from the original reading, with an absolute minimum detectable difference of 0.72% from the original reading. Interobserver values for the same data set gave similar values. There was an average of 4.7% deviation between the two readings with a 95% CI of 53.6%. This translated into an absolute minimum detectable difference of 1.0% from the original reading in the density of staining for either E-selectin or CD31.

The immunohistochemical technique and subsequent image analysis demonstrated staining densities of between 0.5–4% in the tissue. The minimum detectable differences that could not be attributable to observer variability to a level of 95% chance is therefore between 0.7–1%. This technique would be useful for detecting large differences in the staining densities between two tissue samples.

7.6.1 Subject recruitment

All subjects were students recruited within 3 days of having a Mumps, Measles and Rubella triple immunisation booster at the University of Bath. Each student was given a £100 stipend to compensate for time and inconvenience. This study had received the approval of the Bath LREC (BA 172).

7.6.2 Skin biopsy protocol

Two areas of skin were identified. The experimental (upper) site was identified on the exact area contralateral to the immunisation (dermatome C5/C6). The control (lower) site was identified on the forearm of the contralateral arm (dermatome C7/C8).

The site was sterilised with liberal amounts of chlorhexidine, air-dried and injected with 1ml of 1% lidocaine. A 4mm punch biopsy was obtained, placed into Optimum Cutting Compound (OCT) and then plunged into isopentane before being placed into liquid nitrogen. Specimens were then stored in a –70°C freezer and used within 6 months. Standard aftercare was offered to all students. There were no complications. No volunteer for this protocol had been included in any previous protocol.

15 students volunteered, 10 males and 5 females. Their average age was 20.3 years (range 18-23 years). 13 had been immunised in the left arm, 2 in the right. All were fit and well with no illnesses and were taking no medication.

7.6.3 Immunohistochemistry protocol (ABC method)

Consecutive Sections were cut 7-10 μm thick using a cryostat (Brights, UK) at –20°C. Some of the sections were manipulated so that the interposing surfaces were face-up on two successive slides. These 'flip-flop' sections allow more reliable staining for the purposes of comparative semi-quantitative analysis and were used when the supraoptimal staining compared to optimal staining was analysed.

Sections were then thawed at room temperature for 30 minutes before being placed into acetone for 5 minutes and rehydrated in phosphate buffered saline (PBS) for 5 minutes. Sections were then washed in 0.3% hydrogen peroxide twice, each for 3 minutes, and then placed in PBS for 5 minutes. An Elite ABC kit (VectaStain, PK-6102) was used. Blocking peptide (horse serum) was added for 20 minutes and shaken off before 50μm of the primary antibody was added for one hour. Sections were washed twice in PBS, each for 5 minutes. Secondary antibody (ABC kit) was added for 30 minutes. Sections were washed twice in PBS, each for 5 minutes. Avidin-Biotin-peroxidase complex (made up 30 minutes previously) was then added to the sections for 30 minutes. Sections were washed twice in PBS, each for 5 minutes. Copper-enriched diaminobenzidine was prepared from a kit (Vector Laboratories, SK-4100) and added for 5 minutes before being stopped in tap water. Sections were then dehydrated in industrial methylated spirit for 2 minutes and then xylene for 2 minutes, mounted in DPX and left overnight before analysis.

All reagents were made fresh for each experiment. Primary antibodies were all from the same lot number. The ABC kit was sufficient for all experiments.

The primary monoclonal antibodies were human E-selectin raised in mouse (R&D Systems, IgG1 isotype from clone BBIG-E4 (5D11), lot AQE02); and human CD-31 raised in mouse (BD Pharmingen, IgG1 isotype from clone WM59, lot G74641E).

Negative controls omitting primary or secondary antibody steps were obtained for each biopsy. Neither of these controls produced any significant staining. Irrelevant mouse IgG1 antibodies (DAKO, X0931) were also used instead of primary antibody for each biopsy as a control.

7.6.4 Analysis

The outcomes to be semi-quantitatively analysed are

A the end-point dilution

B the percentage supra-optimal staining compared to optimal dilution.

C the slope of the titration curve

These outcomes are all defined on non-linear or non-parametric scales and to be analysed comparatively between the experimental and control groups. The Wilcoxon signed rank test was used.

7.7.1 Results: End-point dilutions

Alternate sections were stained with either anti-CD31 or E-selectin. Only sections stained for E-selectin that co-localised with anti-CD31 were counted as having E-selectin positivity. Serial dilutions of the E-selectin monoclonal antibody were made from 1:20 to 1:150,000 (see 6.5.2). The end-point was defined as the dilutional level where no staining was detected (Table 7.1). The median end-point for the upper arm was a dilution of 5000 and this was the same value for the median in the lower arm. There were no significant differences when these results were analysed with the Wilcoxon signed-rank test.

7.7.2 Results: Supraoptimal compared to optimal staining

Using Zeiss Image Analysis 3.0, the density of E-selectin staining in both the optimal and supra-optimal sections was first determined (Table 7.2). The density of CD31 staining in adjacent sections was then determined (Table 7.3). The E-selectin staining was then expressed as a percentage of endothelial density (Table 7.4) to give a density of E-selectin staining corrected for endothelial density. Finally, the expression of supraoptimal staining expressed as a percentage of optimal staining was calculated (Figure 7.3). There were no significant differences between the experimental and control groups using the Wilcoxon signed-rank test.

Table 7.1 Dilutional end-points

Volunteer	Upper	Lower
1	1600	5000
2	15000	15000
3	1600	5000
4	50000	150000
5	15000	1600
6	800	200
7	1600	1600
8	1600	800
9	5000	5000
10	50000	50000
11	15000	15000
12	1600	1600
13	15000	5000
14	50000	5000
15	800	800

The E-selectin end-dilution for each volunteer's skin biopsy (upper contralateral to the immunisation site, lower acting as control) was calculated as described in section 7.7.1.

Table 7.2 Density percentage of E-selectin staining in both upper (experimental) and lower (control) samples for both optimal and supraoptimal dilutions

Volunteer	Upper (optimal)	Upper (supraoptimal)	Lower (optimal)	Lower (supraoptimal)
1	0.23	0.09	0.40	0.22
2	1.11	1.28	0.32	0.20
3	0.36	0.17	3.04	1.95
4	1.24	0.50	1.54	0.24
5	0.50	0.28	1.86	1.45
6	1.31	0.24	2.37	0.69
7	0.31	0.20	0.53	0.15
8	1.65	0.90	0.33	0.33
9	1.20	1.05	1.01	0.46
10	0.81	0.54	2.21	0.63
11	1.41	0.76	0.43	0.21
12	0.82	0.31	2.77	1.41
13	0.25	0.16	0.32	0.27
14	1.79	0.38	0.90	0.40
15	1.09	0.35	0.55	0.27

The density of E-selectin postitive staining was expressed as a percentage of total area of each skin biopsy. This was calculated for each volunteer's skin biopsy (upper contralateral to the immunisation site, lower acting as control) at the supraoptimal dilution as well as the optimal.

Table 7.3 Density percentage of CD31 staining in both upper (experimental) and lower (control) samples

	Upper	Lower
1	2.3	2.0
2	2.3	3.9
3	1.3	1.2
4	4.8	7.6
5	4.0	2.5
6	2.1	3.5
7	7.1	8.8
8	2.3	1.6
9	2.3	3.2
10	3.7	2.8
11	2.7	1.6
12	3.3	2.0
13	1.1	2.1
14	2.1	2.7
15	1.3	1.7

The density of CD31 positive staining was expressed as a total percentage of the skin biopsy's surface area. This was calculated separately for both upper and lower regions.

Table 7.4 E-selectin density expressed as a percentage of CD31 staining in both upper (experimental) and lower (control) samples for both optimal and supraoptimal dilutions

	Upper (Optimal)	Upper (Supraoptimal)	Lower (Optimal)	Lower (Supraoptimal)
1	10.0	3.9	20.0	11.0
2	48.3	55.7	8.2	5.1
3	27.7	13.1	84.4	54.2
4	25.8	10.4	20.3	3.2
5	12.5	7.0	74.4	58.0
6	62.4	11.4	67.7	19.7
7	4.4	2.8	6.0	1.7
8	71.7	39.1	20.6	20.6
9	52.2	45.7	31.6	14.4
10	21.9	14.6	78.9	22.5
11	52.2	28.2	26.9	13.
12	24.9	9.4	89.4	45.5
13	22.7	14.6	15.2	12.9
14	85.2	18.0	33.3	14.8
15	83.9	26.9	32.4	15.9

The E-selectin density is expressed as a percentage of the CD31 staining for each sample (upper and lower) for each volunteer. This is done at both supraoptimal and optimal dilutions.

Figure 7.3 Supraoptimal:optimal dilution for e-selectin immunohistochemistry

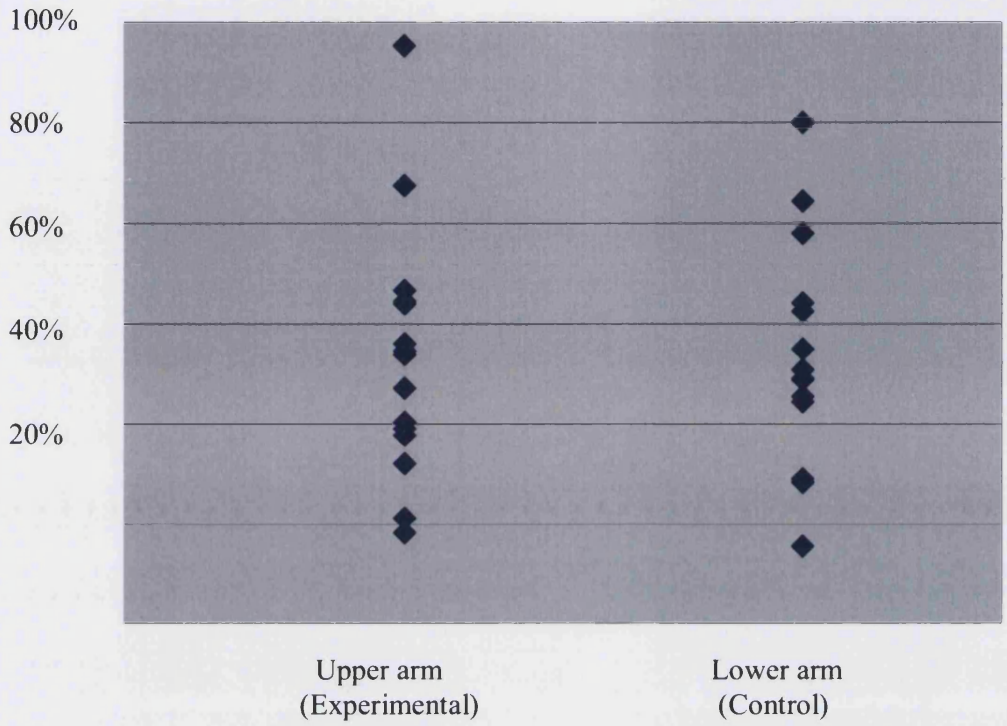

7.7.3 Titration curve slope

The titration curve of the primary antibody dilution was plotted against the staining percentage. There were no significant differences between these groups when these results were analysed (figure 7.4).

7.8.1 Discussion

A reliable, semi-quantitative, immunohistochemical method to investigate differences in the E-selectin staining density, corrected for endothelial density, has been demonstrated. However no differences in E-selectin staining density were found between experimental and control skin biopsies taken from the arm contralateral to an MMR immunisation in 15 human volunteers in any of the outcome measures. The following discussion explores possible weaknesses in the experimental technique used to test this hypothesis.

Figure 7.4 The percentage of E-selectin staining as a proportion of CD31 (endothelial) staining at different concentrations of primary antibody (optimal (50); supraoptimal (200) and end-point (15000)

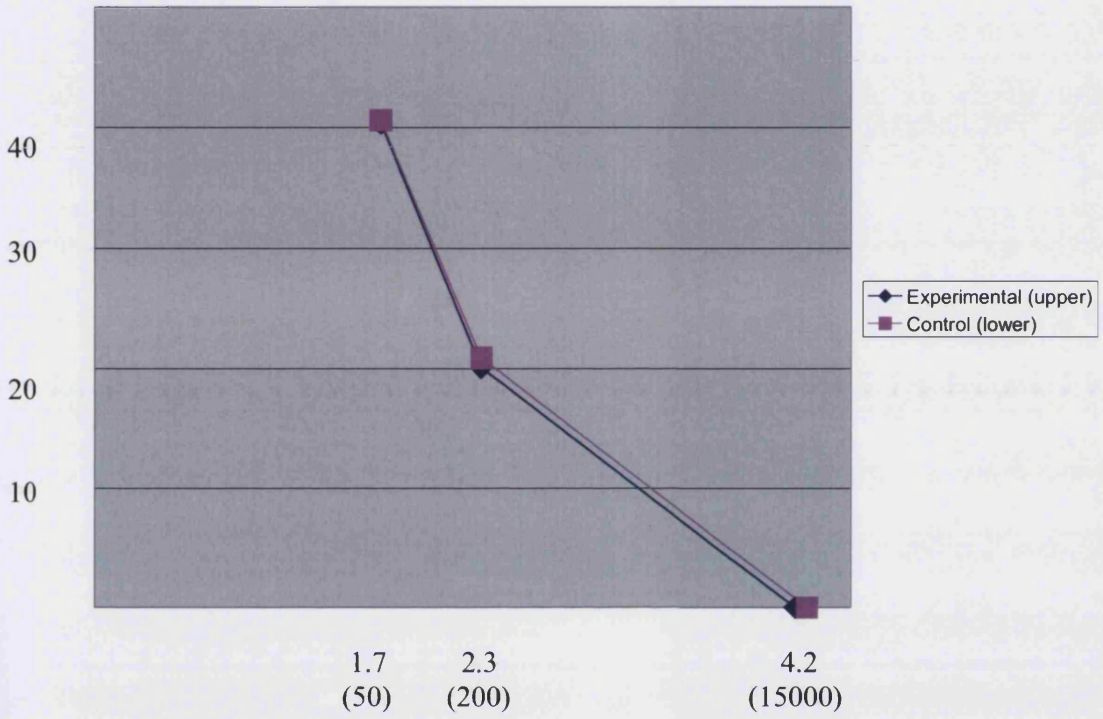

As discussed in Chapters 2 and 5, the contralateral response is small in magnitude. Sensitive methods are required to detect such responses. Immunohistochemical techniques are not as sensitive as other methods, such as *in situ* hybridisation or the polymerase chain reaction (PCR). Similarly, the immunisation may not have introduced a sufficiently large enough stimulus to generate the contralateral response or the timing of the experiment may have missed the contralateral response.

Recently, Roberts (2006), in our laboratory, has investigated contralateral responses in a rat model using the unilateral injection of latex spheres into a hindpaw to introduce a mainly macrophage response. PCR was used to quantify E-selectin mRNA at several time points using the forepaws as control. The contralateral hindpaw was seen to demonstrate E-selectin mRNA expression at 6 hours following

the stimulus, but not at baseline, 1 hour nor 24 hours. Similarly, control forepaws in the same rats did not demonstrate any E-selectin mRNA (unpublished data, Roberts (2006)). This more sensitive technique, coupled with a more inflammatory stimulus, was able to demonstrate a topographically precise contralateral response.

The control region was selected because it was located within a different dermatome. However anatomical studies demonstrate that afferent neuropeptide-containing neurons enter the spinal cord and travel rostro-caudally for up to two adjacent dermatomes before synapsing. The small number of neurons that are seen to do this may have a significant role in changing spinal responses and initiating contralateral responses. Perhaps a more appropriate control region would therefore have been from a different limb. This was proposed to and rejected by the Local Research Ethics Committee on the grounds that it was an unnecessary intervention. However, as can be seen in Roberts' albeit more aggressive rat model, differences are apparent when controls are taken from a different limb.

E-selectin levels may have returned to baseline before the biopsy was taken. A retrospective subanalysis with a linear regression model was performed using time since biopsy (range 1-3 days) (SPSS 12.0). This did not indicate any significant influence of this variable. It is possible that any E-selectin response could have peaked and subsided during this time, although it was felt that this was unlikely.

It is possible that E-selectin levels may not have been activated by any contralateral response. This was again thought to be unlikely as contralateral responses are thought to be neuropeptide-induced and, as outlined above, substance P and CGRP are both known to induce dermal E-selectin expression in humans.

7.9.1 Conclusion

No differences between experimental and control skin biopsies were found with respect to E-selectin expression. Although this result supports the null hypothesis, there was sufficient experimental doubt with regards to stimulus magnitude and investigational techniques as to warrant further investigation, such as with PCR methods.

Chapter 8. Summary and conclusions

8.1.1 Background

Some diseases are inexplicably symmetrical in phenotype. These diseases are generally best described as immune-mediated inflammatory diseases (IMIDs), although there are exceptions such as osteoarthritis. Such examples of IMIDs include rheumatoid arthritis and skin psoriasis. In chapter 1, three different hypotheses are suggested as to what may cause the symmetry in these conditions. These are neurogenic, biomechanical and genetic hypotheses. The evidence for each of these is evaluated and a neurogenic hypothesis is thought to be the most important to evaluate for two reasons. There is good evidence that it is likely to account for this symmetry and there is unexplored therapeutic potential should the hypothesis be supported.

The evidence for a neurogenic hypothesis via crossed afferent pathways at both a spinal and a supraspinal level is reviewed in chapter 2. It is seen that afferent fibres decussate through the dorsal commissure to synapse in the contralateral dorsal horn and deeper spinal laminae (Szentagothai (1964), Light and Perl (1979), Culberson *et al* (1979)). These fibres are seen throughout the spinal cord and in all species studied. Spinal reflex arcs affect the resting state of neurons in the contralateral dorsal horn following local stimuli. Although these are mainly inhibitory in otherwise healthy rats, this can change dependent upon previous stimuli, such as capsaicin (Fitzgerald 1982a and b). Contralateral responses seen in the spinal cord include metabolic activation and the expression of immediate-early genes (see 2.6.4). This implies that the contralateral dorsal horn has a physiological role in the response to a unilateral stimulus. Contralateral responses effecting a motor reflex have been well described, but the anatomical position and functional nature of the areas affected in the dorsal horn suggest a sensory function for these contralateral effects.

The literature demonstrates that central sensory changes in response to a unilateral stimulus occur in rats following hindpaw inflammation (Shenker *et al* (2003)). Furthermore, in several animal models peripheral changes are also seen to occur in the structure contralateral to the local inflammation (Shenker *et al* (2003)). This

allows a pathway to be hypothesised connecting bilateral regions through spinal conduits (Levine *et al* (1985). In a chronic setting established bilateral inflammation would feedback positively in a reciprocal pattern and propagate the disease process (Kidd *et al* (1989)).

Neuropeptides contained in the thinly myelinated or unmyelinated neurons can contribute markedly to important processes of classical inflammation (see 3.3.1-7). These include vasodilatation, plasma exudation, recruitment of leukocytes, activation of leukocytes, and the secondary recruitment of immunological elements (Garrett *et al* (1992)).

The influence of neurogenic inflammation on chronic inflammatory processes has not been elucidated and no targets have been successfully therapeutically translated. Laboratory work and animal models suggest that some neuropeptides and nerves are important in the propagation of chronic inflammation (see 3.3.1-7). The identification of an autoregulatory neural feedback loop that links bilateral anatomical structures would not only provide evidence that the nervous system is important in IMIDs, but highlight the unexplored potential for beneficially influencing these processes.

8.1.2 Distribution of erosions over time in a group of patients with early RA

The distribution and evolution of erosions over 18 months were studied using macroradiographs from a cohort of 42 patients who had had 6 months of symptoms of rheumatoid arthritis in chapter 4. The erosions were very symmetrical at baseline (odds ratio of 6) and were more likely to become symmetrical over time (odds ratio of 11). Some of this symmetry was accounted for by correcting for an individual site's predisposition to developing an erosion and the number of erosions that an individual developed. The remaining symmetry appeared to derive from the patients who had few erosions who were far more likely to have their erosions distributed in a symmetrical pattern.

This apparently contradictory finding can be explained by suggesting the presence of two underlying mechanisms in the development of erosions. Process S might define a small number of highly symmetrical erosions. This could later be masked by a more general process (P) that affects the predisposed areas. Process P appears symmetrical

due to its predilection towards a restricted number of sites and as this process progresses the overall rate of symmetry increases. It is unclear from the data whether a neurogenic or biomechanical process is supported more strongly.

8.2.1 Previous work in man

Although the thesis that one side of the body can influence processes in the exact contralateral region was published in the 1980s (Levine *et al* (1985) and Kidd *et al* (1989), and several animal models have demonstrated that this is likely to have a physiological role in distant inflammatory responses (Shenker *et al* (2003), little work has been performed in man.

Our group has previously studied sensory changes occurring on the contralateral forearm within 30 minutes following a capsaicin injection (see 2.10.1-6). Hyperalgesia and allodynia occurred in about 50% of volunteers, either patients with rheumatoid arthritis or healthy volunteers, and were topographically precise and transient in nature suggesting that they were not an artefact. Furthermore, these contralateral changes were not seen in the control group.

This study was not designed to detect peripheral responses. Observations at the time suggested that an increase flare-wheal response occurred following Semmes-Weinstein monofilament stimulation in some individuals in the exact contralateral area to the capsaicin injection when compared to other areas of skin not contralateral to the capsaicin injection. Do peripheral changes occur in the exact contralateral area to a local stimulus in man?

8.3.1 Skin blood flow responses contralateral to an active immunisation

Chapter 5 details how a clinical model to test contralateral changes to a local inflammatory stimulus was established using the outcome measure of a change in skin blood flow over time. The skin blood flow response to topical capsaicin as a surrogate outcome for the neuropeptide concentration in the skin was not found to be useful as no differences were detectable over time in the small number of healthy volunteers studied. Skin blood flow was seen to increase in the region following the introduction of an active immunisation and possibly in the contralateral region.

Chapter 6 details the clinical study of 59 healthy volunteers who had received an active immunisation. The contralateral region was compared with control regions and skin blood flow was evaluated 1-4 days following immunisation and 2 months later as a control time. No change in skin blood flow when compared to the control regions was seen.

8.3.2 E-selectin expression contralateral to an MMR immunisation

15 healthy volunteers who had received an MMR immunisation 1-3 days prior donated two skin biopsies from the contralateral arm (Chapter 7). One region was exactly opposite the immunisation site, whereas the other was from the lower arm in a different region. E-selectin was semi-quantified by a supraoptimal dilutional method. No differences were found in any of the three outcomes between the amount e-selectin between the experimental and control groups

8.4.1 Further work

The null hypothesis was supported by the experiments that were performed. This could mean that there are no functional crossed afferent pathways in man, but could also mean that these pathways were not operational in a detectable fashion following the first four days after an active immunisation.

Further experiments to test the hypothesis in man should focus on delivering a stimulus more likely to overcome the threshold required to generate a contralateral response. A longer time course may be need to detect contralateral responses and perhaps a more sensitive technique would be helpful.

8.5.1 Conclusion

This thesis provides preliminary data investigating the hypothesis that a local inflammatory stimulus can induce topographically precise contralateral changes in man. Radiographic analysis of hands of patients with very early rheumatoid arthritis showed that a subpopulation of these patients demonstrated mirror-imaging of their erosions to a remarkable degree. Changes in skin blood flow contralateral to an active immunisation were seen in a small number of individuals but this did not reach statistically significance. No clear evidence for a contralateral response was achieved

immunohistochemically in terms of E-selectin expression following an active immunisation. The hypothesis therefore remains open.

Now that preliminary studies have been completed further work should address the questions of stimulus and timing of contralateral responses in man as it is clear that these may differ extensively from those observed in model systems.

Bibliography

Dequeker J and Dieppe P. Disorders of Bone and Cartilage. In "Rheumatology" 2nd Ed. Klippel and Dieppe. 1997. Mosby, London. Sections 8.2 – 8.4.

Daly LE and Bourke GJ. Interpretation and Uses of Medical Statistics 5th Edition, Blackwell Science Ltd, 2000, Oxford. pp136.

Dixon A. Hemiplegia, hand dominance and asymmetry of expression of arthritis in relation to intra-articular pressure. In "Raised intra-articular pressure – clinical consequences". Edited by Dixon A and Hawkins C. Bath Institute for Rheumatic Diseases, Bath, 1989. pp 65.

Gordon DA and Hastings DE. Rheumatoid arthritis: clinical features and systemic involvement. In "Rheumatology" 2nd Ed. Klippel and Dieppe. 1997. Mosby, London. Section 5.3.1-14.

Hokfelt T, Xu ZD, Broberger C, Shi TS and Zhang X. General Overview of Neuropeptdes. "Psychopharmacology, Fourth Generation of Progress" American College of Neuropsychopharmacology, 2004.

Lotz M. Neuropeptides and free radicals in RA. In "Rheumatology" 2nd Ed. Klippel and Dieppe. 1997. Mosby, London. Section 5.11.1-5.

Polak JM and Van Noorden S. "Introduction to Immunocytochemistry". 2nd Edition. BIOS Scientific Publishers, Oxford, 1997. pp52 & pp99-100.

Thompson DW "On Growth and Form" Ed Bonner JT. Cambridge University Press, London, 1965.

Roberts E, PhD Thesis, University of Bath, 2006.

Stewart I and Golubitsky M. "Fearful symmetry: is God a geometer". Penguin, 1992.

Van der Laan N. Acute inflammation after blunt trauma. Univ of Groningen, PhD dissertation, 2001.

References

Al'Abadie MS, Senior HJ, Bleehen SS and Gawkrodger DJ. Neuropeptides and general neuronal marker in psoriasis – an immunohistochemical study. Clin Exp Dermatol, 1995; 20: 384-389.

Alexander CM and Harrison PJ. The bilateral control of the trapezius muscle in humans. Exp Brain Res, 2002; 142: 418.

Allsup SJ, Gosney M, Regan M, Haycox A, Fear S and Johnstone FC. Side effects of influenza vaccination in healthy older people: a randomised single-blind placebo-controlled trial. Gerontology, 2001; 47: 311-314.

Aloisi AM, Porro CA, Cavazzuti M, Baraldi P and Carli G. 'Mirror pain' in the formalin test: behavioural and 2-deoxyglucose studies. Pain, 1993; 55: 267-273.

Amann R, Sirinathsinghji DJ, Donnerer J, Liebmann I and Schuligoi R. Stimulation by nerve growth factor of neuropeptide synthesis in the adult rat in vivo: bilateral response to unilateral intraplantar injections. Neurosci Lett, 1996; 203: 171-4.

Andersson SE, Lexmuller K and Ekstrom GM. Physiological characterization of mBSA antigen induced arthritis in the rat. I. Vascular leakiness and pannus growth. J Rheum, 1998; 25: 1772-1777.

Arantes RME and Nogueira AMMF. Increased intracellular content of enteroglucagon in proximal colon is related to intestinal adaptation to germ-free status. Cell Tissue Res, 2001; 303: 447-450.

Arnett FC, Edworthy SM, Bloch DA *et al.* The American Rheumatism Association 1987 revised criteria for the classification of rheumatoid arthritis. Arth Rheum, 1988; 31: 315-324.

Asai R, Taguchi E, Kume Y, Saito M and Kondo S. Zebrafish leopard gene as a component of the putative reaction-diffusion system. Mech Dev, 1999. 89: 87-92.

Badavi M, Khoshbaten A and Hajizadeh S. Decreased response of rat knee joint blood vessels to phenylephrine in chronic inflammation: involvement of nitric oxide. Exp Physiol, 2000; 85: 49-55.

Barnes, PJ and Karin M. Nuclear factor-kappaB: a pivotal transcription factor in chronic inflammatory diseases. NEJM, 1997; 336: 1066.

Bedoui S, Kawamura N, Straub RH, Pabst R, Yamamura T and von Horsten S. J Neuroimmunol, 2003; 134: 1-11.

Benjamin M and McGonagle D. The anatomical basis for disease localisation in seronegative spondyloarthropathy at entheses and related sites. J Anat, 2001; 903-926.

Betoin F, Ardid D, Herbet A, Aumaitre O, Kemeny JL, Duchene-Marullaz P, Lavarenne J and Eschalier A. Evidence for a central long-lasting antinociceptive effect of vapreotide, an analog of somatostatin, involving an opioidergic mechanism. J Pharmacol Exp Ther, 1994; 269: 7-14.

Bevan SJ and Szolcsanyi J. Sensory neuron-specific actions of capsaicin: mechanisms and applications. Trends Pharmacol Sci, 1990; 11: 330-333.

Bhatia AJ, Blades S, Cambridge G and Edwards J. Differential distribution of FcγRIIIa in normal human tissues and co-localization with DAF and fibrillin-1: implications for immunological microenvironments. Immunology, 1998; 94: 56-63.

Bhattacharya SK, Das N and Rao PJ. Effect of pre-existing inflammation on carrageenan-induced paw oedema in rats. J Pharm Pharmacol, 1987; 39: 854-6.

Bileviciute I, Lundeberg T, Ekblom A and Theodorsson E. Bilateral changes of substance P, neurokinin A, calcitonin gene-related peptide and neuropeptide Y-like immunoreactivity in rat knee joint synovial fluid during acute monoarthritis. Neurosci Lett, 1993; 153: 37-40.

Bileviciute I, Stenfors C, Theodorsson E and Lundeberg T. Unilateral injection of calcitonin gene-realted peptide (CGRP) induces bilateral oedema formation and release of CGRP-like immunoreactivity in the rat hindpaw. Br J Pharmacol, 1998; 125: 1304-1312.

Bileviciute-Ljungar I and Lundeberg T. Contralateral but not systemic administration of bupivacaine reduces acute inflammation in the rat hindpaw. Somatosens Mot Res, 2000; 17: 285-293.

Bileviciute-Ljungar I and Spetea M. Contralateral but not systemic administration of the k-opioid agonist U-50,488H induces anti-nociception in acute hindpaw inflammation. British Journal of Pharmacology, 2001; 132: 252-258.

Bird HA, Ring EJF and Bacon PA. A thermographic and clinical comparison of three intra-articlar steroid preparations in rheumatoid arthritis. Ann Rheum Dis, 1979; 38: 36-39.

Bland JH and Eddy WM. Hemiplegia and rheumatoid hemiarthritis. Arth Rheum, 1968; 11: 72-80.

Boonsaner K, Louthrenoo W, Meyer S and Schumacher HR. Effect of dominancy on severity in rheumatoid arthritis. Br J Rheum, 1992; 31: 77-80.

Borum S, Nielsen K, Bisgaard H and Mygind N. Experimentally induced nasal hypersecretion does not reduce the efficacy of intranasal levocabastine. Rhinology, 1998; 36: 153-155.

Boyle DL, Nguyen KH, Zhuang S, Shi Y, McCormack JE, Chada S and Firestein GS. Intra-articular IL-4 gene therapy in arthritis: anti-inflammatory effect and enhanced th2 activity. Gene Ther, 1999; 6: 1911-8.

Brain SD, Williams TJ, Tippins JR, Morris HR and MacIntyre I. Calcitonin gene-related peptide is a potent vasodilator. Nature, 1985; 313: 54-56.

Brennum J, Kjeldsen M, Jensen K and Jensen TS. Measurements of human pressure-pain thresholds on fingers and toes. Pain, 1989; 38: 211-217.

Brizzolara AL and Burnstock G. Endothelium-dependent and endothelium-independent vasodilatation of the hepatic artery of the rabbit. Br J Pharmacol, 1991; 103: 1206-1212.

Brook A and Corbett M. Radiographic changes in early rheumatoid disease. Ann Rheum Dis, 1977; 36: 71-73.

Buckland-Wright JC. Microfocal radiographic examination of erosions in the wrists and hands of patients with rheumatoid arthritis. Ann Rheum Dis, 1984; 43: 160-171.

Buckland-Wright JC, Carmichael I and Walker SR. Quantitative microfocal radiography accurately detects joint changes in rheumatoid arthritis. Ann Rheum Dis, 1986; 45: 379-383.

Buckland-Wright JC and Walker SR. Incidence and size of erosions in the wrist and hand of rheumatoid arthritis: a quantitative microfocal radiographic study. Ann Rheum Dis, 1987; 46: 463-467.

Buckland-Wright JC and Bradshaw CR. Clinical applications of high-definition microfocal radiography. Br J Rad, 1989a; 62: 209-217.

Buckland-Wright JC, Clarke GS and Walker SR. Erosion number and area progression in the wrists and hands of rheumatoid patients: a quantitative microfocal radiographic study. Ann Rheum Dis, 1989b; 48: 25-29.

Buckland-Wright JC, Clarke GS, Chikanza IC and Grahame R. Quantitative microfocal radiography detects changes in erosion area in patients with early rheumatoid arthritis treated with myocrisine. J Rheumatol, 1993; 20: 243-247.

Bukhari M, Lunt M, Harrison BJ, Scott DG, Symmons DJ and Silman A. Erosions in inflammatory polyarthritis are symmetrical regardless of rheumatoid factor status: results from a primary care-based inception cohort of patients. Rheumatology (Oxford), 2002; 41: 246-252.

Carrasquillo Y and Gereau RW. Rodent models clarify the role of cells expressing the substance P receptor in pain. Drug Discovery Today, 2004; 1: 107-113.

Caterina MJ, Schumacher MA, Tominaga M, Rosen TA, Levine JD, and Julius D. The capsaicin receptor: a heat-activated ion channel in the pain pathway. Nature, 1997; 389: 816–824.

Ceccherelli F, Gagliardi G, Faggian L, Loprete F and Giron G. Analgesic effect of subcutaneous administration of oxygen-ozone. A blind study in the rat on the modulation of the capsaicin-induced edema. Acupunct Electrother Res, 1998; 23: 171-184.

Chaisson CE, Zhang Y, Sharma L, Kannel W and Felson DT. Grip strength and the risk of developing radiographic hand osteoarthritis: results from the Framingham study. Arth Rheum, 1999; 42: 33-38.

Chan J, Smoller BR, Raychauduri SP, Jiang WY and Farber EM. Intraepidermal nerve fiber expression of calcitonin gene-related peptide, vasoactive intestinal peptide and substance P in psoriasis. Arch Dermatol Res, 1997; 289: 611-616.

Chandrasekhar S, Harvey AK, Hrubey PS and Bendele AM. Arthritis induced by interleukin-1 is dependent on the site and frequency of intraarticular injection. Clin Immunol Immunopathol, 1990; 55: 382-400.

Charkoudian N. Skin blood flow in adult human thermoregulation: how it works, when it does not, and why. Mayo Clin Proc, 2003; 78: 603-12.

Chen J, Luo C, Li H and Chen H. Primary hyperalgesia to mechanical and heat stimuli following subcutaneous bee venom injection into the plantar surface of hindpaw in the conscious rat: a comparative study with the formalin test. Pain, 1999; 83: 67-76.

Chong BF, Murphy J, Kupper TS and Fuhlbrigge R. E-selectin, thymus- and activation-regulated chemokine/CCL17, and intercellular adhesion molecule-1 are constitutively coexpressed in dermal microvessels: a foundation for a cutaneous immunosurveillance system. J Immunology, 2004; 172: 1575-1581.

Clapp BR, Hingorani AD, Kharbanda RK, Mohamed-Ali V, Stephens JW, Vallance P and MacAllister RJ. Inflammation-induced endothelial dysfunction involves reduced nitric oxide bioavailability and increased oxidant stress. Cardiovasc Res, 2004; 64: 172-178.

Clarke GS, Buckland-Wright JC and Grahame R. Symmetry of radiological features in the wrist and hands of patients with early to moderate rheumatoid arthritis: a quantitative microfocal radiographic study. Br J Rheum, 1994; 33: 249-254.

Clarke JA, Hollinger FB, Lewis E, Russell LA, Miller CH, Huntley A and Flynn NM. Intradermal inoculation with Heptavax-B. Immune response and histological evaluation of injection sites. JAMA, 1989; 262: 2567-2571.

Clough GF, Boutsiouki P and Church MK. Comparison of the effects of levocetirizine and loratadine on histamine-induced wheal, flare, and itch in human skin. Allergy, 2001; 56: 985-988.

Coderre TJ and Melzack R. Cutaneous hyperalgesia: contributions of the peripheral and central nervous system to increase in the pain sensitivity after injury. Brain Res, 1987; 404: 95-106.

Coderre TJ and Melzack R. Increased pain sensitivity following heat injury involves a central mechanism. Behav Brain Res, 1985; 15: 259-262.

Coghill RC, Price DD, Hayes RL and Mayer DJ. Spatial distribution of nociceptive processing in the rat spinal cord. J Neurophysiol, 1991; 65: 133-140.

Corna S, Galante M, Grasso M, Nardone A and Schieppati M. Unilateral displacement of lower limb evokes bilateral EMG responses in leg and foot muscles in standing humans. Exp Brain Res, 1996; 109: 83-91.

Coste F and Forestier J. Hemiplegie et nodosites d'Heberden contralaterales. Bull Mem Soc Med Hopitaux Paris, 1935; 5: 772.

Cotran RS, Gimbrone MA, Bevilacqua MP, Mendrick DL and Pober JS. Induction and detection of a human endothelial activation antigen in vivo. J Exp Med, 1986; 164: 661-666.

Courtwright LJ and Kuzell WC. Sparing effect of neurological deficit and trauma on the course of adjuvant arthritis in the rat. Ann Rheum Dis, 1965; 24: 360-368.

Culberson JL, Haines DE, Kimmel DL and Brown PB. Contralateral projection of primary afferent fibres to mammalian spinal cord. Expl Neurol, 1979; 64: 83-97.

Da Silva P and Carmo-Fonseca M. Peptide containing nerves in human synovium: immunohistochemical evidence for decreased innervation in rheumatoid arthritis. J Rheum, 1990; 17: 1592-1599.

Day RM, Harbord M, Forbes A and Segal AW. Cantharidin blisters: a technique for investigating leukocyte trafficking and cytokine production at sites of inflammation in humans. J Immunol Methods, 2001; 257: 213-220.

De Ceballos ML, Jenner P and Marsden CD. Increased [Met]enkephalin and decreased substance P in spinal cord following thermal injury to one limb. Neuroscience, 1990; 36: 731-736.

De Stefano N, Narayanan S, Matthews PM, Francis GS, Antel JP and Arnold DL. *In vivo* evidence for axonal dysfunction remote from focal cerebral demyelination of the type seen in multiple sclerosis. Brain, 1999; 122: 1933-1939.

Decaris E, Guingamp C, Chat M, Philippe L, Grillasca J-P, Abid A, Minn A, Gillet P, Netter P and Terlain B. Evidence for neurogenic transmission inducing degenerative cartilage damage distant from local inflammation. Arth Rheum, 1999; 42: 1951-1960.

Delgado M, Abad C, Martinez C, Lecta J and Gomariz RP. Vasoactive intestinal peptide prevents experimental arthritis by downregulating both autoimmune and inflammatory components of the disease. Nat Med, 2001; 7: 563-568.

Delgado, M, Pozo D and Ganea D. The significance of vasoactive intestinal peptide in immunomodulation. Pharmacol Rev, 2004; 56: 249-290.

Denko CW and Petricevic M. Sympathetic or reflex footpad swelling due to crystal induced inflammation in the opposite foot. Inflammation, 1978; 3: 81-86.

Devlin J, Gough A, Huissoon A, Perkins P, Jubb R and Emery P. The outcome of knee synovitis in early arthritis provides guidelines for management. Clin Rheumatol, 2000; 19: 82-85.

Donaldson LF, McQueen DS and Seckl JR. Neuropeptide gene expression and capsaicin-sensitive primary afferents: maintenance and spread of adjuvant arthritis in the rat. J Physiol, 1995; 486: 473-482.

Donaldson LF, Seckl JR and McQueen DS. A discrete adjuvant-induced monoarthritis in the rat; effects of adjuvant dose. Journal of Neurosci Meth, 1993; 49: 5-10.

Dye SF, Vaupel and Dye CC. Conscious neurosensory mapping of the internal structures of the human knee without intraarticular anesthesia. Am J Sports Med, 1998; 26: 773-777.

Eccles JC and Sherrington CS. Studies on the flexor reflex. VI. Inhibition. Proc Roy Soc B, 1931; 109: 91-113.

Egan CL, Viglione-Schneck MJ, Walsh LJ, Green B, Trojanowski JQ, Whitaker-Menezes D and Murphy GF. Characterization of unmyelinated axons uniting epidermal and dermal immune cells in primate and murine skin. J Cutan Pathol, 1998; 25: 20-29.

Esselinckx W, Bacon PA, Ring EFJ, Crooke D, Collins AJ and Demottaz D. A thermographic assessment of three intra-articular prednisolone analogues given in rheumatoid synovitis. British J Clin Pharm, 1978; 5: 447-451.

Essex TJ and Byrne PO. A laser Doppler scanner for imaging blood flow in skin. J Biomed Eng, 1991; 13: 189-194.

Falcini F, Matucci Cerinic M, Lombardi A, Generini S, Pignone A, Tirassa P, Ermini M, Lepore L, Partsch G and Aloe L. Increased circulating nerve growth factor is directly correlated with disease activity in juvenile chronic arthritis. Ann Rheum Dis, 1996; 555: 745-748.

Fang J-Y, Tsai M-J, Huang Y-B, Wu P-C and Tsai Y-H. Percutaneous absorption and skin erythema: Quantification of capsaicin and its synthetic derivatives from gels incorporated with benzalkonium chloride by using non-invasive bioengineering methods. Drug Development Research, 1997; 40: 56-67.

Farber EM, Nickoloff BJ, Recht B and Fraki JE. Stress, symmetry and psoriasis: possible role of neuropeptides. J Am Acad Dermatol, 1986; 14: 305-311.

Feige U, Karbowski A, Rordorf-Adam C and Pataki A. Arthritis induced by continuous infusion of hr-interleukin-1α into the rabbit knee joint. Int J Tiss React, 1989; 11: 225-238.

Finnerup NB, Johannesen IL, Fuglsang-Frederiksen A, Bach FW and Jensen TS. Sensory function in spinal cord injury patients with and without central pain. Brain, 2003; 126: 57-70.

Fitzgerald M. The contralateral input to the dorsal horn of the spinal cord in the decerebrate rat. Brain Res, 1982a; 236: 275-287.

Fitzgerald M. Alterations in the ipsi- and contralateral afferent inputs of dorsal horn cells produced by capsaicin treatment of one sciatic nerve in the rat. Brain Res, 1982b; 248: 97-107.

Flemming A, Crown JM and Corbett M. Early rheumatoid disease. Patterns of joint involvement. Ann Rheum Dis, 1976; 35: 361-364.

Forestier MJ. Rheumatism d'Heberden chez un hemilplegique. Lesions articulaires limitees au cote sain. Rev Neurol (Paris), 1935; 63: 442-452.

Fraser SE and Harland RM. The molecular metamorphosis of experimental embryology. Cell, 2000; 100: 41-55.

Fuchs EA, Callahan LF, Kay JJ, Brooks RH, Nance EP and Pincus T. Radiographic and joint count findings of the hand in rheumatoid arthritis: related and unrelated findings. Arth Rheum, 1988; 31: 44-51.

Galeazza MT, Stucky CL and Seybold VS. Changes in [125I]hCGRP binding in rat spinal cord in an experimental model of acute, peripheral inflammation. Brain Res, 1992; 591: 198-208.

Gallagher P, Blake DR and Lever J. Audit of closed synovial biopsy in the diagnosis of inflammatory joint disease. Scand J Rheum, 1985; 14: 307-314.

Ganju P, Davis A, Patel S, Nunez X and Fox A. p38 stress-activated protein kinase inhibitor reverses bradykinin B(1) receptor-mediated component of inflammatory hyperalgesia. Eur J Pharmacol, 2001; 421: 191-199.

Garrett NE, Mapp PI, Cruwys SC, Kidd BL and Blake DR. Role of substance P in inflammatory arthritis. Ann Rheum Dis, 1992; 51: 1014-1018.

Gault SJ and Spyker MJ. Beneficial effect of immobilization of joints in rheumatoid and related arthrtitides: a splint study using sequential analysis. Arth Rheum, 1969; 12: 34-44.

Glick EN. Asymmetrical rheumatoid arthritis after poliomyelitis. BMJ, 1967; 3: 26-28.

Glyn JH, Sutherland I, Walker GF and Young AC. Low incidence of osteoarthritis in hip and knee after anterior poliomyelitis: a late review. BMJ, 1966; 2: 739-742.

Goldberger AL, Amaral LAN, Glass L, Hausdorff JM, Ivanov PCh, Mark RG, Mietus JE, Moody GB, Peng C-K and Stanley HE. PhysioBank, PhysioToolkit, and PhysioNet: Components of a New Research Resource for Complex Physiologic Signals. Circulation, 2000; 101: 215-220.

Gothefors L, Bergstrom E and Backman M. Immunogenicity and reactogenicity of a new measles, mumps and rubella vaccine when administered as a second dose at 12 years of age. Scand J Infect Dis, 2001; 33: 545-549.

Gronblad M, Konttinen YT, Korkala O, Liesi P, Hukkanen M and Polak J. Neuropeptides in the synovium of patients with rheumatoid arthritis and osteoarthritis. J Rheum, 1988; 15: 1807-1810.

Grossman M, Jamieson MJ, Kellogg DL, Kosiba WA, Pergola PE, Crandall CG and Shepherd AMM. The effect of iontophoresis on the cutaneous vasculature: evidence for current-induced hyperemia. Microvascular Research, 1995; 50: 444-452.

Groves RW, Allen MH, Barker J, Haskard DO and MacDonald DM. Endothelial leucocyte adhesion molecule-1 (ELAM-1) expression in cutaneous inflammation. Br J Dermatol, 1991; 124: 117-123.

Groves, RW, Ross E, Barker J, Ross JS, Camp RDR and MacDonald DM. Effect of in vivo interleukin-1 on adhesion molecule expression in normal human skin. J Invest Dermatol, 1992; 98: 384.

Grubb BD, Stiller RU and Schaible HG. Dynamic changes in the receptive field properties of spinal cord neurons with ankle input in rats with chronic unilateral inflammation in the ankle region. Exp Brain Res, 1993; 92: 441-452.

Halla JT, Fallahi S and Hardin JG. Small joint involvement: a systematic roentgenographic study in rheumatoid arthritis. Ann Rheum Dis, 1986; 45: 327-330.

Halliday DA, Zettler C, Rush RA, Scicchitano R and McNeil JD. Elevated nerve growth factor levels in the synovial fluid of patients with inflammatory joint disease. Neurochem Res, 1998; 23: 919-922.

Harding LM, Murphy A, Kinnman E and Baranowski AP. Characterization of secondary hyperalgesia produced by topical capsaicin jelly- a new experimental tool for pain research. Eur J Pain, 2001; 5: 363-71.

Harris R and Copp EP. Immobilisation of the knee joint in rheumatoid arthritis. Ann Rheum Dis, 1962; 21: 353-359.

Helliwell PS, Hetthen J, Sokoll K, Green M, Marchesoni A, Lubrano E, Veale D and Emery P. Joint symmetry in early and late rheumatoid and psoriatic arthritis. Arth Rheum, 2000; 43: 865–871.

Helme RD and McKernan S. Neurogenic flare responses following topical application of capsaicin in humans. Ann Neurol, 1985; 18: 505-509.

Helyes Z, Szabo A, Nemeth J, Jakab B, Pinter E, Banvolgyi A, Kereskai L, Keri G and Szolcsanyi J. Antiinflammatory and analgesic effects of somatostatin released from capsaicin-sensitive nerve terminals in a Freund's adjuvant-induced chronic arthritis model in the rat. Arth Rheum, 2004; 50: 1677-1685.

Herdegen T, Walker T, Leah JD, Bravo R and Zimmerman M. The Krox-24 protein, a new transcription regulating factor: expression in the rat central nervous system following afferent somatosensory stimulation. Neurosci Lett, 1990; 120: 21-24.

Herdegen T, Tolle TR, Bravo R, Zieglgansberger W and Zimmerman M. Sequential expression of Jun B, Jun D and Fos B proteins in rat spinal neurons: cascade of transcriptional operations during nociception. Neurosci Lett, 1991a; 129: 221-224.

Herdegen T, Leah JD, Manisali A, Bravo R and Zimmermann M. c-JUN-like immunoreactivity in the CNS of the adult rat: basal and transsynaptically induced expression of an immediate-early gene. Neuroscience, 1991b; 41: 643-654.

Hingorani AD, Cross J, Kharbanda RK, Mullen MJ, Bhagat K, Taylor M, Donald AE, Palacios M, Griffin GE, Deanfield JE, MacAllister RJ and Vallance P. Acute systemic inflammation impairs endothelium-dependent dilatation in humans. Circulation, 2000; 102: 994-999.

Holzer P. Local effector function of capsaicin-sensitive sensory nerve endings: involvement of tachykinins, calcitonin gene-related peptide and other neuropeptides. Neurosci, 1988; 24: 739-768.

Hood VC, Cruwys SC, Urban L and Kidd BL. The neurogenic contribution to synovial leucocyte infiltration and other outcome measures in a guinea pig model of arthritis. Neurosci Lett, 2001; 299: 201-204.

Hsu SM, Raine L and Fanger H. Use of avidin-biotin-peroxidase complex (ABC) in immunoperoxidase techniques: a comparison between ABC and unlabeled antibody (PAP) procedures. J Histochem Cytochem, 1981; 29: 577-580.

Ianaro A, Cicala C, Calignano A, Koteliansky V, Gotwals P, Bucci M, Gerli R, Santucci L, Fiorucci S and Cirino G. Anti-very late antigen-1 monoclonal antibody modulates the development of secondary lesion and T-cell response in experimental arthritis. Lab Invest, 2000; 80: 73-80.

Jacqueline F. Un cas de polyarthrite evolutive a localisations contralaterales d'une hemiplegie. Rev Rhum Malad Osteoartic, 1953; 20: 323.

Jayson MI, Rubenstein D and Dixon AS. Intra-articular pressure and rheumatoid geodes (bone 'cysts'). Ann Rheum Dis, 1970; 29: 496-502.

Johansson O, Han SW and Enhamre A. Altered cutaneous innervation in psoriatic skin as revealed by PGP 9.5 immunohistochemistry. Arch Dermatol Res, 1991; 283: 519-523.

Jolliffe VA, Anand P and Kidd BL. Assessment of cutaneous sensory and autonomic axon reflexes in rheumatoid arthritis. Ann Rheum Dis, 1995; 54: 251-255.

Kamermann JS. Protective effect of traumatic lesions on rheumatoid arthritis. Ann Rheum Dis, 1966; 25: 361-363.

Kane D, Lockhart JC, Balint PV, Mann C, Ferrell WR and McInnes IB. Protective effect of sensory denervation in inflammatory arthritis (evidence of regulatory neuroimmune pathways in the arthritic joint). Ann Rheum Dis, 2005; 64: 325-327.

Kantner RM, Kirby ML and Goldstein BD. Increase in substance P levels in the dorsal horn of rat spinal cord during a chemogenic nociceptive stimulus. Brain Res, 1985; 338: 196-199.

Kayser V and Guilbaud G. Local and remote modifications of nociceptive sensitivity during carrageenan-induced inflammation in the rat. Pain, 1987; 28: 99-107.

Kayser V, Benoist JM, Neil A, Gautron M and Guilbaud G. Behavioural and electrophysiological studies on the paradoxical antinociceptive effects of an extremely low dose of naloxone in an animal model of acute and localized inflammation. Exp Brain Res, 1988; 73: 402-10.

Kellgren JH and Samuel EP. The sensitivity and innervation of the articular capsule. J Bone Joint Surg, 1950; 32B: 84-92.

Kharbanda RK, Walton B, Allen M, Klein N, Hingorani AD, MacAllister RJ and Vallance P. Prevention of inflammation-induced endothelial dysfunction: a novel vasculo-protective action of aspirin. Circulation, 2002; 105: 2600-2604.

Kidd BL, Cruwys SC, Garrett NE, Mapp PI, Jolliffe VA and Blake DR. Neurogenic influences on contralateral responses during experimental rat monoarthritis. Brain Research, 1995; 688: 72-76.

Kidd BL, Mapp PI, Gibson SJ, Polak JM, O'Higgins F, Buckland-Wright JC and Blake DR. A neurogenic mechanism for symmetrical arthritis. Lancet, 1989; 1128-1129.

Kissin I, Lee SS and Bradley EL Jr. Effect of prolonged nerve block on inflammatory hyperalgesia in rats: prevention of late hyperalgesia. Anesthesiology, 1998; 88: 224-232.

Koch AE, Szekanecz Z, Friedman J, Haines GK, Langman CB and Bouck NP. Effects of thrombospondin-1 on disease course and angiogenesis in rat adjuvant-induced arthritis. Clin Immunol Immunopathol, 1998; 86: 199-208.

Koepp H, Eger W, Muehleman C, Valdellon A, Buckwalter JA, Kuettner KE and Cole AA. Prevalence of articular cartilage degeneration in the ankle and knee joints of human organ donors. J Orthop Sci, 1999; 4: 407-412.

Koltzenburg M, Wall PD and McMahon SB. Does the right side know what the left side is doing? TINS, 1999; 22: 122-127.

Laberge G, Mailloux CM, Gowan K, Holland P, Bennett DC, Fain PR and Spritz RA. Early disease onset and increased risk of other autoimmune diseases in familial generalized vitiligo. Pigment Cell Res, 2005; 18: 300-5.

Lam FY and Ferrell WR. Capsaicin suppresses substance P-induced joint inflammation in the rat. Ann Rheum Dis, 1989; 48: 928-932.

Lambrecht BN. Immunologists getting nervous: neuropeptides, dendritic cells and T cell activation. Resp Res, 2001; 2: 133-138.

LaMotte RH, Lundberg LE and Torebjork HE. Pain, hyperalgesia and activity in nociceptive C units in humans after intradermal injection of capsaicin. J Physiol, 1992; 448: 749-764.

Landis JR and Koch GG. The measurement of observer agreement for categorical data. Biometrics, 1977; 33: 159-174.

Langley RG, Krueger GG and Griffiths CE. Psoriasis: epidemiology, clinical features and quality of life. Ann Rheum Dis, 2005; Suppl 2: 18-25.

Lassere M, Boers M, van der Heijde D, Boonen A, Edmonds J, Saudan and Verhoeven AC. Smallest detectable difference in radiological progression. J Rheumatol, 1999; 26: 731-739.

Leah JD, Porter J, de-Pommery J, Menetrey D and Weil-Fuguzza J. Effect of acute stimulation on Fos statement in spinal neurons in the presence of persisting C-fiber activity. Brain Res, 1996; 719: 104-111.

Leak RS, Rayan GM and Arthur RE. Longitudinal radiographic analysis of rheumatoid arthritis in the hand and wrist. J Hand Surg, 2003; 28: 427-434.

Lechman ER, Jaffurs D, Ghivizzani SC, Gambotto A, Kovesdi I, Mi Z, Evans CH and Robbins PD. Direct adenoviral gene transfer of viral IL-10 to rabbit knees with experimental arthritis ameliorates disease in both injected and contralateral control knees. J Immunol, 1999; 163: 2202-8.

Levine JD, Clark R, Devor M, Helms C, Moskowitz MA and Basbaum AI. Intraneuronal substance P contributes to the severity of experimental arthritis. Science, 1984; 226: 547-549.

Levine JD, Collier D H, Basbaum AI, Moskowitz MA and Helms CA. Hypothesis. The nervous system may contribute to the pathophysiology of rheumatoid arthritis. J Rheum, 1985a; 12: 406-411.

Levine JD, Dardick SJ, Basbaum AI and Scipio E. Reflex neurogenic inflammation. I. Contribution of the peripheral nervous system to spatially remote inflammatory responses that follow injury. J Neurosci, 1985b; 5: 1380-1386.

Levine JD, Dardick SJ, Roizen MF, Helms CA and Basbaum AI. Contribution of sensory afferents and sympathetic efferents to joint injury in experimental arthritis. J. Neuroscience, 1986; 6: 3423-3429.

Levite M. Neuropeptides, by direct interaction with T cells, induce cytokine secretion and break the commitment to a distinct T helper phenotype. Proc Natl Acad Sci USA, 1998; 95: 12544-12554.

Light AR and Perl ER. Reexamination of the dorsal root projection to the spinal dorsal horn including observation of the differential termination of coarse and fine fibres. J Comp Neurol, 1979; 186: 117-132.

Lippe IT and Holzer P. Participation of endothelium-derived nitric oxide but not prostacyclin in the gastric mucosal hyperemia due to acid back-diffusion. Br J Pharmacol, 1992; 105: 708-714.

Li-Tsang CW, Hung LK and Mak AF The effect of corrective splinting on flexion contracture of rheumatoid fingers. J Hand Ther, 2002; 15: 185-191.

Liu JB, Li M, Yang S, Gui JP, Wang HY, Du WH, Zhao XY, Ren YQ, Zhu YG and Zhang XJ. Clinical profiles of vitiligo in China: an analysis of 3742 patients. Clin Exp Dermatol, 2005; 3: 327-331.

Lorton D, Lubahn C, Engan C, Schaller J, Felten DL and Bellinger DL. Local application of capsaicin into the draining lymph nodes attenuates expression of adjuvant-induced arthritis. Neuroimmunomodulation, 2000; 7: 115-125.

Manal K, Lu X, Nieuwenhuis MK, Helders PJ and Buchanan TS. Force transmission through the juvenile idiopathic arthritis wrist: a novel approach using a sliding rigid body spring model. J Biomech, 2002; 35: 125-133.

Manni L, Lundeberg T, Fiorito S, Bonini S, Vigneti E and Aloe L. Nerve growth factor release by human synovial fibroblasts prior to and following exposure to tumour necrosis factor-alpha, interleukin-1 beta and cholecystokinin-8: the possible role of NGF in the inflammatory response. Clin Exp Rheum, 2003; 21: 617-614.

Manni L, Lundeberg T, Tirassa P and Aloe L. Role of cholecystokinin-8 in nerve growth factor and nerve growth factor mRNA expression in carrageenan-induced joint inflammation in adult rats. Rheumatology (Oxford), 2002; 41: 787-792.

Mapp PI, Terenghi G, Walsh DA, Chen ST, Cruwys SC, Garrett N, Kidd BL, Polak JM and Blake DR. Monoarthritis in the rat knee induces bilateral and time-dependent changes in substance P and calcitonin gene-related peptide immunoreactivity in the spinal cord. Neuroscience, 1993; 57: 1091-1096.

Mapp PI. Innervation of the synovium. Ann Rheum Dis, 1995; 54: 398-403.

Martel W, Hayes JT and Duff IF. The pattern of bone erosion in the hand and wrist in rheumatoid arthritis. Radiology, 1965; 84: 204-214.

Masters BR. Fractal analysis of the vascular tree in the human retina. Ann Rev Biomed Eng, 2004; 6: 427-452.

Mattingley PC, Matheson JA and Dickson RA. The distribution of radiological joint damage in the rheumatoid hand. Rheum Rehab, 1979; 18: 142-147.

Menetrey D, Gannon A, Levine JD and Basbaum AI. Expression of c-fos protein in interneurons and projection neurons of the rat spinal cord in response to noxious somatic, articular and visceral stimulation. J Comp Neurol, 1989; 285: 177-195.

Mentzel K and Brauer R. Matrix metalloproteinases, IL-6, and nitric oxide in rat antigen-induced arthritis. Clin & Exp Rheum, 1998; 16: 269-276.

Merighi, A, Polak, JM, Gibson, SJ, Gulbenkian, S, Valentino, KL and Peirone, SM. Ultrastructural studies on calcitonin gene-related peptide-, tachykinins- and somatostatin-immunoreactive neurones in rat dorsal root ganglia: evidence for the colocalization of different peptides in single secretory granules. Cell Tissue Res, 1988; 254: 101–109.

Meyer P, Burkhardt H, Palombo-Kirme E, Grunder W, Brauer R, Stiller KJ, Kalden JR, Becker W and Kinne RW. 123-I-antileukoproteinase scintigraphy reveals microscopic cartilage alterations in the contralateral knee joint of rats with 'monoarticular' antigen-induced arthritis. Arth Rheum, 2000; 43: 279-284.

Miagkov AV, Kovalenko DV, Brown CE, Didsbury JR, Cogswell JP, Stimpson SA, Baldwin AS and Makarov SS. NF-kappaB activation provides the potential link between inflammation and hyperplasia in the arthritic joint. Proc Natl Acad Sci U S A 1998; 95: 13859-13864.

Millan MJ and Colpaert FC. The influence of sustained opioid receptor blockade in a model of long-term, localized inflammatory pain in rats. Neurosci Lett, 1990; 113: 50-55.

Millan MJ and Colpaert FC. Opioid systems in the response to inflammatory pain: sustained blockade suggests role of kappa- but not mu-opioid receptors in the modulation of nociception, behaviour and pathology. Neuroscience, 1991; 42: 541-553.

Mine T, Kimura M, Sakka A and Kawai S. Innervation of nociceptors in the menisci of the knee joint: an immunohistochemical study. Arch Orth Traum Surg, 2000; 120: 201-204.

Mohammadian P, Andersen OK and Arendt-Nielsen L. Correlation between local vascular and sensory changes following tissue inflammation induced by repetitive application of topical capsaicin. Brain Res, 1998; 792: 1-9.

Morris GC, Gibson, SJ and Helme RD. Capsaicin-induced flare and vasodilation in patients with post-herpetic neuralgia. Pain, 1995; 63: 93-101.

Morris S and Shore A. Skin blood flow responses to the iontophoresis of acetylcholine and sodium nitroprusside in man: possible mechanisms. J Physiol, 1996; 496; 531-542.

Möttönen TT, Hannonen P, Toivanen J, Rekonen A and Oka M. Value of joint scintigraphy in the prediction of erosiveness in early rheumatoid arthritis. Ann Rheum Dis, 1988; 47: 183-189.

Mulherin D, Bresnihan B and Fitzgerald O. Digital denervation is associated with absence of nail and distal interphalangeal joint involvement in psoriatic arthritis. J Rheumatol, 1995; 22: 1211-1212.

Murray CD. The physiological principle of minimum work. I. The vascular system and the cost of blood volume. PNAS, 1926a; 12: 295-299.

Murray CD. The physiological principle of minimum work. II. Oxygen exchange in capillaries. PNAS, 1926b; 12: 299-304.

Naukkarinen A, Harvima I , Paukkonen K, Aolto ML and Horsmanheimo M. Immunohistochemical analysis of sensory nerves and neuropeptides, and their contacts with mast cells in developing and mature psoriatic lesions. Arch Dermatol Res, 1993; 285: 341-346.

Nava P. Atrite reumatoide antiga. Icte cerebral surto exolutive agude nas articulacoes doentes do lado hemiplegico. Brasil-med, 1953; 67: 318.

Neugebauer V and Schaible HG. Evidence for a central component in the sensitization of spinal neurons with joint input during development of acute arthritis in cat's knee. J Neurophysiol, 1990; 64: 299-311.

Newton DJ, Khan F and Belch JF. Assessment of microvascular endothelial function in human skin. Clinical Science 2001; 101: 567-572.

Niu J, Zhang Y, LaValley M, Chaisson CE, Aliabadi P and Felson DT. Symmetry and clustering of symptomatic hand osteoarthritis in elderly men and women: the Framingham study. Rheumatology (Oxford), 2003. 42: 343-348.

Njoo MD, Westerhof W. Vitiligo. Pathogenesis and treatment. Am J Clin Dermatol 2001; 2: 167-181.

Noguchi K, Kowalski K, Traub R, Solodkin A, Iadarola MJ and Ruda MA. Dynorphin expression and Fos-like immunoreactivity following inflammation induced hyperalgesia are colocalised in spinal cord neurons. Mol Brain Res, 1991; 10: 227-233.

Oh U, Hwang SW and Kim D. Capsaicin activates a non-selective cation channel in cultured rat dorsal root ganglion neurons. J Neurosci, 1996; 16: 659-667.

Owsianik WD, Kundi A, Whitehead JN, Kraag GR and Goldsmith C. Radiological articular involvement in the dominant hand in rheumatoid arthritis. Ann Rheum Dis, 1980; 39: 508-510.

Panchanathan V, Kumar S, Yeap W, Devi S, Ismail R, Sarijan S, Sam SM, Jusoh Z, Nordin S, Leboulleux D and Pang T. Comparison of safety and immunogenicity of a Vi polysaccharide typhoid vaccine with a whole-cell killed vaccine in Malaysian Air Force recruits. Bull World Health Organ, 2001; 79: 811-817.

Partridge REH and Duthie JJR. Controlled trial of the effects of complete immobilization of the joint in rheumatoid arthritis. Ann Rheum Dis, 1963; 22: 91-99.

Pedersen JL and Kehlet H. Secondary hyperalgesia to heat stimuli after burn injury in man. Pain, 1998; 76: 377-84.

Pedersen JL. Inflammatory pain in experimental burns in man. Dan Med Bull, 2000; 47: 168-95.

Pergolizzi S, Vaccaro M, Magaudda L, Mondello MR, Arco A, Bramanti P, Cannavo SP and Guaneri B. Immunohistochemical study of epidermal nerve fibres in involved and uninvolved psoriatic skin using confocal laser scanning microscopy. Arch Dermatol Res, 1998; 290: 483-489.

Pierre-Jerome C, Bekkelund SI, Mellgren SI, Torbergsen T, Husby G and Nordstrom R. The rheumatoid wrist MR analysis of the distribution of rheumatoid lesions in axial plan in a female population. Clin Rheumatol, 1997; 16: 80-86.

Pincelli C. Nerve growth factor and keratinocytes: a role in psoriasis. Eur J Derm, 2000; 10: 85-90.

Pinter E and Szolcsanyi J. Inflammatory and antiinflammatory effects of antidromic stimulation of dorsal roots in the rat. Agents Actions, 1988; 25: 240-242.

Pitzalis C, Cauli A, Pipitone N, Smith C, Barker J, Marchesoni A, Yanni G and Panayi GS. Cutaneous lymphocyte antigen-positive T lymphocytes preferentially migrate to the skin but not to the joint in psoriatic arthritis. Arthritis Rheum, 1996; 39: 137-145.

Plassman P and Jones TD. MAVIS: a non-invasive instrument to measure area and volume of wounds. Med Eng Phys, 1998; 20: 332-338.

Porro CA, Cavazzuti M, Galetti A, Sassatelli L and Barbier GC. Functional activity of the rat spinal cord during formalin-induced noxious stimulation. Neuroscience, 1991; 41: 655-665.

Rachaudhuri SP, Sanyal M, Weltman H and Kundu-Raychaudhuri S. K252a, a high-affinity nerve growth factor receptor blocker, improves psoriasis: an in vivo study using the sever combined immunodeficient mouse-human skin model. J Inv Derm, 2004; 122: 812-819.

Raines SA and Cox NH. 'Minerva' BMJ, 2002; 324: 434.

Ramsay JE, Simms RJ, Ferrell WR, Crawford L, Greer IA, Lumsden MA and Sattar N. Enhancement of endothelial function by pregnancy: inadequate response in women with type 1 diabetes. Diabetes Care 2003; 26: 475-9.

Ranson SW, Davenport HK and Doles EA. Intramedullary course of the dorsal root fibres of the first three cervical nerves. J Comp Neurol, 1932; 54: 1-12.

Rotshenker S and Tal M. The transneuronal induction of sprouting and synapse formation in intact mouse muscles. J Physiol, 1985; 360: 387-396.

Ruckman A, Ehle B and Trampisch H. How to evaluate measuring methods in the case of non-defined external validity. J Rheumatology, 1995; 22: 1998-2000.

Sabitha P, Prabha Adhikari MR, Chowdary A, Prabhu M, Soofi M, Shetty M, Kamath A, Lokaranjan SS and Bangera SS. Comparison of the immunogenicity and safety of two different brands of *salmonella typhi* VI capsular polysaccharide vaccine. Indian J Med Sci. 2004; 58: 141-149.

Sais G, Vidaller A, Jucgla A, Condom E and Peyri J. Adhesion molecule expression and endothelial cell activation in cutaneous leukocytoclastic vasculitis: an immunohistologic an clinical study in 42 patients. Arch Dermatol, 1997; 133: 443-450.

Schade Willis TM, Hopp RJ, Romero JR and Larsen PD. The protective effect of brachial plexus palsy in purpura fulminans. Pediatr Neurol, 2001; 24: 379-381.

Schadrack J, Neto FL, Ableitner A, Castro-Lopes JM, Willoch F, Bartenstein P, Zieglgansberger W and Tolle TR. Metabolic activity changes in the rat spinal cord during adjuvant monoarthritis. Neuroscience, 1999; 94: 595-605.

Segal R, Avrahami E, Lebdinski E, Habut B, Leibovitz A, Gil I, Yaron M and Caspi D. The impact of hemiparalysis on the expression of osteoarthritis. Arth Rheum, 1998; 41: 2249-2256.

Sepp NT, Gille J, Li JL, Caughman SW, Lawley TJ and Swerlick RA. A factor in human plasma permits persistent expression of E-selectin by human endothelial cells. Journal of Inv Derm, 1994; 102: 445-450.

Shenker N, Haigh R, Roberts E, Mapp P, Harris N and Blake D. A review of contralateral responses to a unilateral inflammatory lesion. Rheumatology, 2003; 42: 1279-1286.

Sigurdsson V, de Vries IJ, Toonstra J, Bihari IC, Thepen T, Bruijnzeel-Koomen CA and van Vloten WA. Expression of VCAM-1, ICAM-1, E-selectin, and P-selectin on endothelium in situ in patients with erythroderma, mycosis fungoides and atopic dermatitis. J Cutan Pathol, 2000; 27: 436-440.

Simone DA, Baumann TK and LaMotte RH. Dose-dependent pain and mechanical hyperalgesia in humans after intradermal injection of capsaicin. Pain, 1989; 38: 99-107.

Skaare AB, Kjaerheim V, Barkvoll P and Rolla G. Does the nature of the solvent affect the anti-inflammatory capacity of triclosan? An experimental study. J Clin Periodontol, 1997; 24: 124-128.

Smith CH, Barker JN, Morris RW, MacDonald DM and Lee TH. Neuropeptides induce rapid expression of endothelial cell adhesion molecules and elicit granulocytic infiltration in human skin. J Immunol, 1993; 151: 3274-3282.

Soila P. A roentgenological study of asymmetry in rheumatoid arthritis. A preliminary communication. Acta Rheum Scand, 1963; 9: 264-268.

Sotgui ML, Brambilla M, Valente M and Biella GEM. Contralateral input modulates the excitability of dorsal horn neurons involved in noxious signal processed. Potential role in neuronal sensitization. Somat Mot Res, 2004; 21: 211-215.

Springall DR, Collina G, Barer G, Suggett AJ, Bee D and Polak JM Increased intracellular levels of calcitonin gene-related peptide-like immunoreactivity in pulmonary endocrine cells of hypoxic rats. J Pathol, 1988; 155: 259-267.

Squarcione S, Sgricia S, Biasio LR, Perinetti E. Comparison of the reactogenicity and immunogenicity of a split and a subunit-adjuvanted influenza vaccine in elderly subjects. Vaccine, 2003; 21: 1268-1274.

Stecher RM and Karnosh LJ. Heberden's nodes. VI. The effect of nerve injury upon the formation of degenerative joint disease of the fingers. Am J Med Sci, 1947; 213: 181.

Sternberger NH and Sternberger LA. The unlabeled antibody method. Comparison of the sensitivity of peroxidase-antiperoxidase with avidin-biotin complex method by a new mode of quantitative immunocytochemistry. J Histochem Cytochem, 1986; 34: 599-605.

Strickland I, Rhodes LE, Flanagan BF and Friedmann PS. TNF-alpha and IL-8 are upregulated in the epidermis of normal human skin after UVB exposure: correlation with neutrophil accumulation and E-selectin expression. J Invest Dermatol, 1997; 108: 763-768.

Stucker M, Heese A, Hoffmann K, Rochling A and Altmeyer P. Precision of laser Doppler scanning in clinical use. Clin Exp Dermatol, 1995; 20: 371-376.

Stucker M, Reuther T, Hoffmann K, Aicher B and Altmeyer P. Quantification of cutaneous pharmacological reactions - comparison of Laser Doppler Scanning, colorimetry, planimetry and skin temperature measurement. Skin Research and Technology, 1996; 2: 18-22.

Stucky CL, Galeazza MT and Seybold VS. Time dependent changes in Bolton-Hunter-labelled 125-I-substance P in rat spinal cord following unilateral adjuvant-induced peripheral inflammation. Neuroscience, 1993; 57: 397-409.

Szentagothai J. Neuronal and synaptic arrangement in the substantia gelatinosa rolandi. J Comp Neurol, 1964; 122: 219-239.

Takeuchi F, Streilein RD and Hall RP. Increased E-selectin, IL-8 and IL-10 gene expression in human skin after minimal trauma. ExpDerm, 2003; 12: 777.

Tarkowski E, Naver H, Wallin BG, Blomstrand C, Grimby G and Tarkowski A. Lateralization of cutaneous inflammatory responses in patients with unilateral paresis after poliomyelitis. J Neuroimmunol, 1996; 67: 1-6.

Taub A. Local, segmental and supraspinal interactions with a dorsolateral spinal cutaneous afferent system. Exp Neurol, 1964; 10: 357-364.

Terajima, SM, Higaki, Y. Igarashi T, Nogita M and Kawashima M. An important role of tumor necrosis factor-alpha in the induction of adhesion molecules in psoriasis. Arch Dermatol Res, 1998; 290: 246-252.

Thompson M and Bywaters EGL. Unilateral rheumatoid arthritis following hemiplegia. Ann Rheum Dis, 1962; 21: 370-377.

Tsuchida Y. Rate of skin blood flow in various regions of the body. Plast Reconstr Surg, 1979; 64: 505-508.

Tsuchida Y. Age-related changes in skin blood flow at four anatomic sites of the body in males studied by xenon-133. Plast Reconstr Surg, 1990; 85: 556-561.

Tsuchida Y, Fukuda O and Kamata S. The correlation of skin blood flow with age, total cholesterol, hematocrit, blood pressure and haemoglobin. Plast Reconstr Surg, 1991; 88: 844-850.

Turing, AM. The chemical basis of morphogenesis. Phil Trans R Soc London B, 1952. 237: 37-72.

Turner PJ, Dear JW and Foreman JC. Involvement of kinins in hyperresponsiveness induced by platelet activating factor in the human nasal airway. Br J Pharmacol, 2000; 129: 525-523.

Vacca-Galloway LL. Differential immunostaining for substance P in Hungtington's diseased and normal spinal cord: significance of serial (optimal, supra-optimal and end-point) dilutions of primary anti-serum in comparing biological specimens. Histochemistry, 1985; 83: 561-569.

Veale D, Farrell and Fitzgerald O. Mechanism of joint sparing in a patient with unilateral psoriatic arthritis and a longstanding hemiplegia. Br J Rheum, 1993; 32: 413-416.

Von Banchet SG, Petrow P, Brauer PK and Schaible HG. Monoarticular antigen-induced arthritis leads to pronounced bilateral up-regulation of the expression of neurokinin 1 and bradykinin 2 receptors in dorsal root ganglion neurons of rats. Arthritis Research, 2000; 2: 424-427.

Von Euler US and Gaddum JH. An unidentified depressor substance in certain tissue extracts. J Physiol, 1931; 72: 577-583.

Wagman IH and Price DD. Responses of dorsal horn cells of *M. mulatta* to cutaneous and sural nerve A and C fibre stimulation. J Neurophys, 1969; 32: 803-817.

Wardell K, Jakobsson A and Nilsson GE. Laser Doppler perfusion imaging by dynamic light scattering. IEEE Trans Biomed Eng, 1993; 40: 309-16.

Werring DJ, Brassat D, Droogan AG, Clark CA, Symms MR, Barker GJ, MacManus DG, Thompson AJ and Miller DH. The pathogenesis of lesions and normal-appearing white matter changes in multiple sclerosis: a serial diffusion MRI study. Brain, 2000; 123: 1667-1676.

Williams S, Evan GI and Hunt SP. Changing patterns of c-fos induction in spinal neurons following thermal cutaneous stimulation in the rat. Neuroscience, 1990; 36: 73-81.

Winter S. Unilateral Heberden's nodes in a case of hemiplegia. New York J Med, 1952; 52: 349-350.

Wongsurakiat P, Maranetra KN, Gulprasutdilog P, Aksornint M, Srilum W, Ruengjam C and Sated W. Adverse effects associated with influenza vaccination in patients with COPD: a randomized controlled study. Respirology, 2004; 9: 550-556.

Woolf CJ, Allchorne A, Safieh-Garabedian B and Poole S. Cytokines, nerve growth factor and inflammatory hyperalgesia: the contribution of tumour necrosis factor alpha. Br J Pharmacol, 1997; 121: 417-424.

Woolf CJ. Evidence for a central component of post-injury pain hypersensitivity. Nature, 1983; 306: 686-688.

Yaighmai I, Rooholamini SM and Faunce HF. Unilateral rheumatoid arthritis: protective effect of neurologic deficits. Am J Roentgenol, 1977; 128: 199-201.

Yu LC, Hansson P, Brodda-Jansen G, Theodorsson E and Lundeberg T. Intrathecal CGRP8-37-induced bilateral increase in hindpaw withdrawal latency in rats with unilateral inflammation. Br J Pharmacol, 1996; 117: 43-50.

Zamir M. Arterial branching with the confines of fractal L-system formalism. J Gen Phys, 2001; 118: 267-276.

Zangger P, Kachura JR, Bombardier C, Redelmeier DA, Badley EM and Bogoch ER. Assessing damage in individual joints in rheumatoid arthritis: a new method based on the Larsen system. Joint Bone Spine, 2004; 71: 389-396.

Zangger P, Keystone EC and Bogoch ER. Asymmetry of small joint involvement in rheumatoid arthritis: prevalence and tendency towards symmetry over time. Joint Bone Surgery, 2005; 72: 241-247.

Zhelev Z and Bakalova R. Laser-Doppler imaging of activation-flow coupling in the somatosensory cortex: normalization of signal when the baseline changes significantly. Methods Find Exp Clin Pharmacol, 2002; 24: 559-64.

Zhong J, Seifalian AM, Salerud GE and Nilsson GE. A mathematical analysis on the biological zero problem in laser Doppler flowmetry. IEEE Trans Biomed Eng, 1998; 45: 354-364.

Ziljstra TR, Heijnsdijk-Rouwenhorst L and Rasker JJ. Silver ring splints improve dexterity in patients with rheumatoid arthritis. Arth Rheum, 2004; 51: 947-951.